Vol. 8, no. 4, 2024
eISSN 2541-9129
PEER-REVIEWED SCIENTIFIC AND PRACTICAL JOURNAL

Safety of Technogenic and Natural Systems

Technosphere Safety

Machine Building

Chemical Technologies, Materials Sciences, Metallurgy

www.bps-journal.ru
DOI 10.23947/2541-9129

Safety of Technogenic and Natural Systems

Bezopasnost' Tekhnogennyh i Prirodnyh Sistem

Peer-Reviewed Scientific and Practical Journal

eISSN 2541-9129

Published Since 2017

Periodicity – 4 issues per year

DOI: 10.23947/2541-9129

Founder and Publisher — Don State Technical University (DSTU), Rostov-on-Don, Russian Federation

The journal is created in order to highlight the results of research and real achievements on topical issues of Mechanical Engineering, Technosphere Safety, Modern Metallurgy and Materials Science. The journal highlights the problems of the development of fundamental research and engineering developments in a number of important areas of technical sciences. One of the main activities of the journal is integration into the international information space.

The Journal Publishes Articles in the Following Fields of Science:

Ground Transport and Technological Means and Complexes
Machines, Aggregates and Technological Processes
Metallurgical Science and Heat Treatment of Metals and Alloys
Powder Metallurgy and Composite Materials
Materials Science
Fire Safety
Environmental Safety
Occupational Safety

Registration:	Mass Media Registration Certificate ЭЛ № ФС 77 – 66531 Dated Jule, 21, 2016, Issued by the Federal Service for Supervision of Communications, Information Technology and Mass Media
Indexing and Archiving:	RISC, CyberLeninka, CrossRef, DOAJ, Index Copernicus, Internet Archive
Website:	https://bps-journal.ru
Address of the Editorial Office:	1, Gagarin Sq. Rostov-on-Don, 344003, Russian Federation
E-mail:	vestnik@donstu.ru
Telephone:	+7 (863) 2–738–372
Date of Publication No.4,2024:	29.11.2024

Безопасность техногенных и природных систем

Safety of Technogenic and Natural Systems

Рецензируемый научно-практический журнал

eISSN 2541-9129

Издается с 2017 года

Периодичность – 4 выпуска в год

DOI: 10.23947/2541-9129

Учредитель и издатель — Федеральное государственное бюджетное образовательное учреждение высшего образования «Донской государственный технический университет» (ДГТУ), г. Ростов-на-Дону

Создан в целях освещения результатов исследований и реальных достижений по актуальным вопросам машиностроения, техносферной безопасности, современной металлургии и материаловедения. В журнале освещаются проблемы развития фундаментальных исследований и инженерных разработок в ряде важнейших областей технических наук. Одним из главных направлений деятельности журнала является интеграция в международное информационное пространство.

Журнал включен в перечень рецензируемых научных изданий, в котором должны быть опубликованы основные научные результаты диссертаций на соискание ученой степени кандидата наук, на соискание ученой степени доктора наук (Перечень ВАК) по следующим научным специальностям:

2.5.11 – Наземные транспортно-технологические средства и комплексы (технические науки)
2.5.21 – Машины, агрегаты и технологические процессы (технические науки)
2.6.1 – Металловедение и термическая обработка металлов и сплавов (технические науки)
2.6.5 – Порошковая металлургия и композиционные материалы (технические науки)
2.6.17 – Материаловедение (технические науки)
2.10.1 – Пожарная безопасность (технические науки)
2.10.2 – Экологическая безопасность (технические науки)
2.10.3 – Безопасность труда (технические науки)

Регистрация:	Свидетельство о регистрации средства массовой информации ЭЛ № ФС 77 – 66531 от 21 июля 2016 г., выдано Федеральной службой по надзору в сфере связи, информационных технологий и массовых коммуникаций
Индексация и архивация:	РИНЦ, CyberLeninka, CrossRef, DOAJ, Index Copernicus, Internet Archive
Сайт:	https://bps-journal.ru
Адрес редакции:	344003, Российская Федерация, г. Ростов-на-Дону, пл. Гагарина, 1
E-mail:	vestnik@donstu.ru
Телефон:	+7 (863) 2–738–372
Дата выхода №4,2024 в свет:	29.11.2024

Editorial Board

Contents

Содержание

TECHNOSPHERE SAFETY
ТЕХНОСФЕРНАЯ БЕЗОПАСНОСТЬ

UDC 504.064.45
https://doi.org/10.23947/2541-9129-2024-8-4-7-15

Original Theoretical Research

Method for Recycling Lithium-Ion Batteries with the Extraction of Valuable Components

Anna S. Melnikova ✉, **Natalya V. Kostryukova**
Ufa University of Science and Technology, Ufa, Russian Federation
✉ annamel7@mail.ru

EDN: WMZISP

Abstract

Introduction. Due to the increasing demand for lithium-ion batteries, it has become a pressing issue to find an environmentally friendly and safe way to dispose of old batteries. The life cycle of these batteries is shorter than that of the equipment they power, which leads to a growing amount of waste. This waste poses a serious problem for disposal and can have harmful effects on the environment. At the same time, recycling spent lithium-ion batteries offers a solution. By extracting valuable components we can return these components to the production process and create a closed-loop system. In this regard, the aim of this study is to investigate the methods of recycling lithium-ion batteries and to analyze the proposed method for their disposal, which involves extracting valuable components such as Li2CO3, while introducing the principles of a closed-loop economy into the production process.

Materials and Methods. The methods of systematizing scientific literature on lithium-ion battery recycling were used. The “Mpr_Dipl” software was used to select the most promising method, which includes direct decision-making, paired comparison, and weighted sum methods. A technological process for lithium-ion batteries processing was developed using the COMPASS-3D software.

Results. As a result of the analysis, the advantages and disadvantages of each lithium-ion recycling method were highlighted. A hydrochemical method was selected using the multi-criteria decision-making method. A five-stage process for lithium ion battery processing with lithium carbonate extraction was developed, including grinding, separation, filtration, precipitation, and wet Li2CO3 capture. The material balance for the developed method was calculated.

Discussion and Conclusion. The developed recycling system ensures safe recycling of used lithium-ion batteries with minimal negative environmental impact and maximum recovery of valuable components. These results can be used to optimize the recycling process and maximize the extraction of valuable materials from spent lithium-ion batteries for further sale as lithium carbonate, thereby generating additional revenue.

Keywords: lithium-ion battery, recycling, disposal, circular economy, hydrometallurgy

Acknowledgements. The authors would like to thank Elvira Valerikovna Nafikova, the mentor of the “Green Project” environmental club at Ufa University of Science and Technology, for her assistance in preparing this paper. They also extend their gratitude to the Editorial team and reviewers for their attention and valuable recommendations, which made it possible to improve the quality of the paper.

For citation. Melnikova AS, Kostryukova NV. Method for Recycling Lithium-Ion Batteries with the Extraction of Valuable Components. *Safety of Technogenic and Natural Systems.* 2024;8(4):7–15. https://doi.org/10.23947/2541-9129-2024-8-4-7-15

Оригинальное теоретическое исследование

Способ утилизации литий-ионных аккумуляторов с извлечением ценных компонентов

А.С. Мельникова ✉, **Н.В. Кострюкова**
Уфимский университет науки и технологий, г. Уфа, Российская Федерация
✉ annamel7@mail.ru

Аннотация
Введение. В связи с постоянно растущей потребностью в литий-ионных аккумуляторах (ЛИА) и увеличением количества уже используемых накопительных устройств актуальной темой на сегодняшний день является создание экологичного, безопасного и дешевого способа их утилизации. Жизненный цикл литий-ионных аккумуляторов меньше, чем оборудования, где они применяются, поэтому возрастает риск образования большого количества отходов, которые могут привести к серьезным проблемам с утилизацией и пагубному воздействию на окружающую среду. В то же время отработанные литий-ионные аккумуляторы можно использовать вторично, извлекая из них ценные компоненты для возвращения в производственный цикл. В связи с этим целью данной работы является исследование методов утилизации литий-ионных аккумуляторов и анализ предложенного авторами способа их утилизации с извлечением ценных компонентов (Li_2CO_3) при внедрении принципов экономики замкнутого цикла в производство.
Материалы и методы. Авторами использовались методы систематизации научной литературы по проблематике утилизации литий-ионных аккумуляторов. Для выбора наиболее перспективного из них была использована программа Mpr_Dipl. В ней заложены прямые методы принятия решений, метод парных сравнений и метод взвешенной суммы. Разработка технологической схемы процесса переработки ЛИА проводилась в программе «КОМПАС-3D».
Результаты исследования. В результате анализа были выделены достоинства и недостатки каждого метода утилизации литий-ионных аккумуляторов, а также выбран гидрохимический способ с использованием методики решения задач с многокритериальным выбором. Предложена технологическая схема процесса переработки литий-ионных аккумуляторов с извлечением карбоната лития, состоящая из пяти стадий: измельчение, разделение, фильтрация, осаждение и вылавливание влажного осадка Li_2CO_3. Рассчитан материальный баланс разработанного способа утилизации.
Обсуждение и заключение. Разработанная авторами система утилизации обеспечивает безопасную переработку отработавших литий-ионных аккумуляторов при минимальном негативном воздействии на окружающую среду и максимальном выделении ценных компонентов. Результаты исследования могут быть использованы для модернизации процесса утилизации литий-ионных аккумуляторов с целью извлечения дополнительной прибыли от продажи карбоната лития.

Ключевые слова: литий-ионный аккумулятор, переработка, утилизация, экономика замкнутого цикла, гидрометаллургия

Благодарности. Авторы выражают благодарность наставнику экологического клуба «Зеленый проект» Уфимского университета науки и технологий Эльвире Валериковне Нафиковой за помощь в подготовке исследования, а также редакции журнала и рецензентам за внимательное отношение к статье и замечания, устранение которых позволило повысить ее качество.

Для цитирования. Мельникова А.С., Кострюкова Н.В. Способ утилизации литий-ионных аккумуляторов с извлечением ценных компонентов. *Безопасность техногенных и природных систем.* 2024;8(4):7–15. https://doi.org/10.23947/2541-9129-2024-8-4-7-15

Introduction. Global energy consumption is increasing every year due to population growth, economic development, and technological progress. Scientists are currently researching the development and efficient use of renewable energy sources (RES), such as wind, solar, hydropower, and tidal power [1]. However, most of these renewable energy sources have an irregular nature, requiring the use of storage devices to ensure a consistent supply of energy from these sources [2]. One solution to this challenge is the use of lithium-ion batteries. Every year, the demand for lithium-ion batteries continues to grow and is expected to continue growing in the near future. This is due to the development of new materials and improvements in production processes. The growth in demand for LIBs is supported by expert estimates. According to Fortune business insight forecasts, the market for lithium-ion batteries will reach $193 billion in volume by 2028 (Fig. 1).

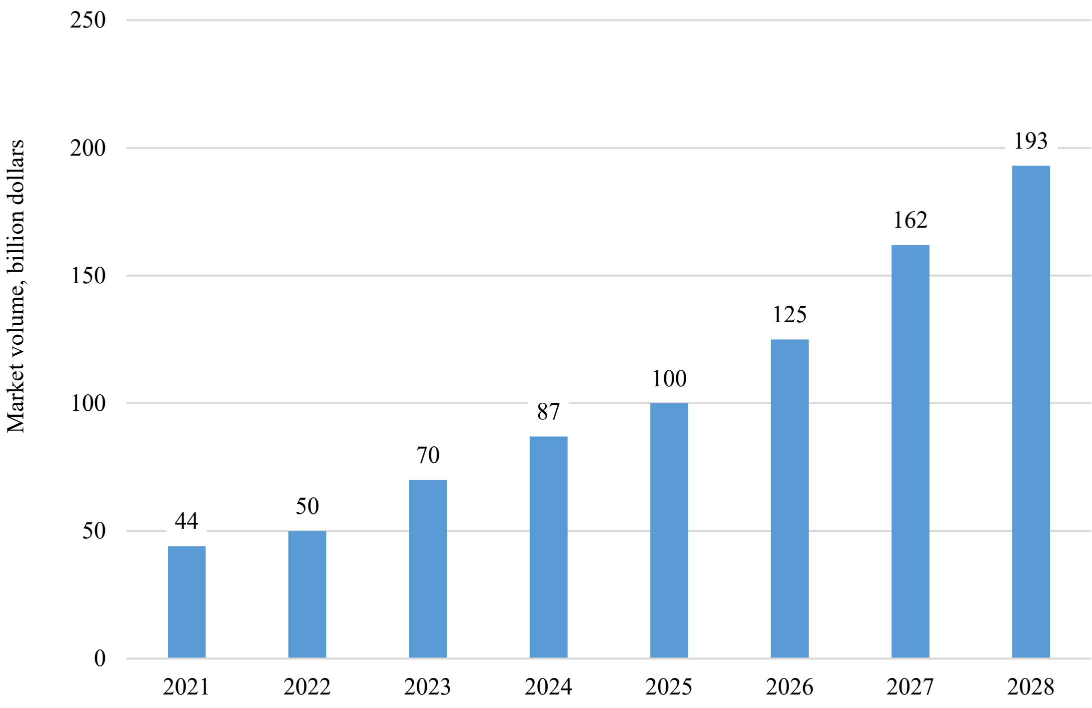

Fig. 1. Volume and forecast of the dynamics of the global lithium-ion battery market, billion US dollars

To date, there are a limited number of LIB production plants in Russia. The largest domestic enterprises producing lithium-ion batteries include:

– Aspil Energy (Pyatigorsk);

– Saturn (Krasnoyarsk);

– Uralelement (Chelyabinsk);

– Scientific Research Aeroinstitute Istochnik OAO (Saint Petersburg).

It is important to note that battery components are imported from China and Bolivia [3].

Due to the active use of LIBs, a pressing issue today is how to create an environmentally friendly, safe, and cost-effective method for disposing of used batteries. The life cycle of lithium-ion batteries depends on the linear model or linear economy in which batteries are produced, used, and then disposed of. According to predictions [4], approximately 95% of lithium-ion batteries produced worldwide remain unprocessed and end up in households, which is an inefficient approach that leads to a significant amount of waste and high material costs for disposal [5]. To address this issue, it is essential to implement closed-loop economic practices and utilize LIB with the extraction of valuable materials [6]. The aim of this research is to develop a recycling system for lithium-ion batteries that allows for the extraction of valuable components (lithium carbonate).

Materials and Methods. An analytical analysis of the methods of disposal of lithium-ion batteries has been conducted. The analysis was based on domestic and foreign research. To identify the most promising approach, we used the method of problem-solving with a multi-criteria selection using the Mpr_Dipl software.

We calculated the material balance of the system based on [7].

The process sheet was created using the COMPASS-3D program.

Research Results

1. Analysis of existing methods for LIB processing. Recycling methods are a potential solution for extending the lifespan of lithium-ion batteries in the economic cycle [8]. This is an integral part of a closed-loop economy, as it facilitates the internal circulation of materials and reduces the depletion of resources associated with primary production [9].

LIB recycling is crucial for minimizing the environmental impact of mining and waste disposal, while also conserving resources and reducing costs associated with manufacturing new batteries.

According to Figure 2, the most common recycling methods for lithium-ion batteries include physical, pyrometallurgical, and hydrochemical processes [10].

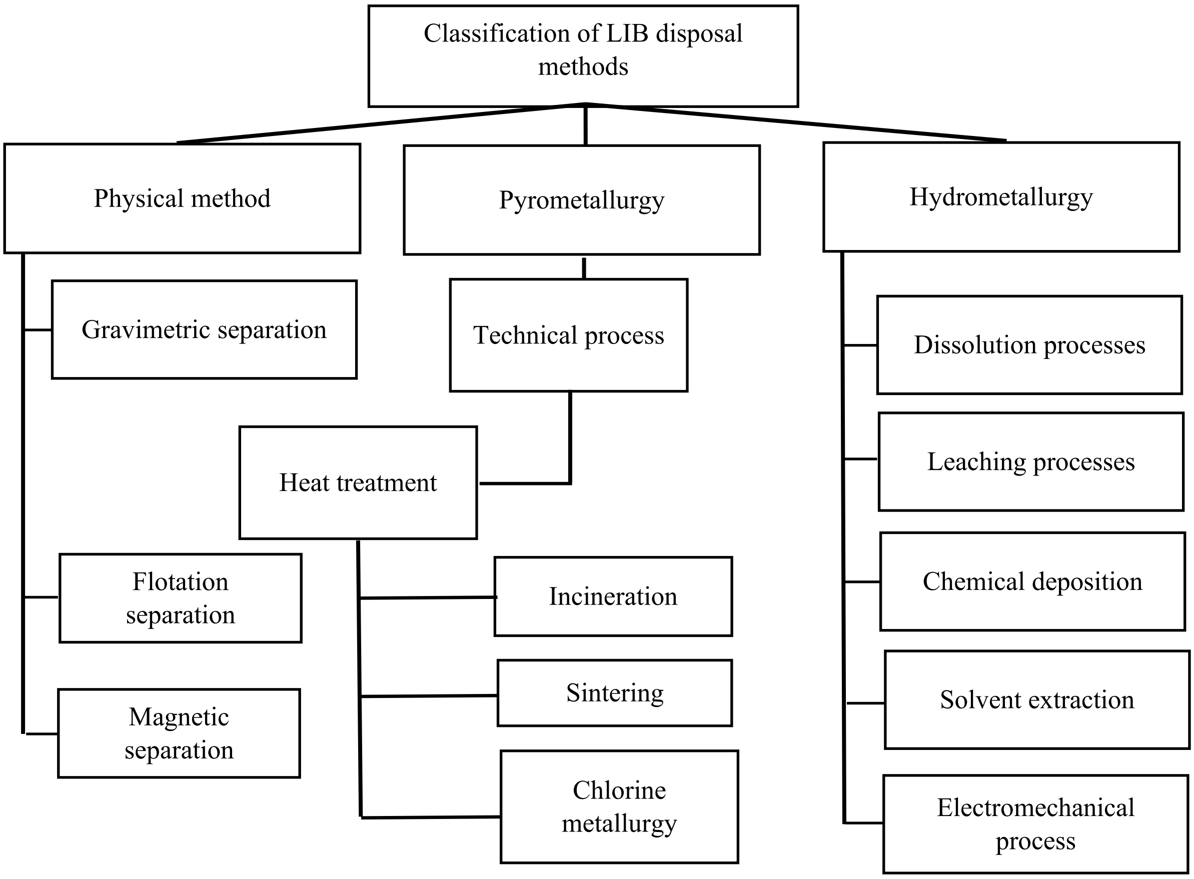

Fig. 2. Classification of LIB disposal methods

Physical method involves disassembling batteries using various techniques to separate the battery components based on their physical properties, such as density and magnetism. The main techniques used in this method include gravimetric separation, flotation separation, and magnetic separation. This method is one of the most popular ways of recycling lithium-ion batteries due to its low cost and environmentally friendly nature. However, it is important to note that physical processing techniques may not always be as effective at extracting all valuable components as other methods.

Pyrometallurgy is a well-known and reliable method that involves processing materials, often allowing for the extraction of a high percentage of valuable metals, such as cobalt and nickel, from battery waste. This process requires a significant amount of energy, but it is generally reliable and does not require specific settings for processing materials with a particular composition, which makes it suitable for materials with varying compositions, such as electronic and battery waste [11].

Pyrometallurgical process consists of three stages: metal reduction, pyrolysis, and gas combustion. During pyrolysis, the organic components of lithium-ion batteries are thermally degraded. As a result, toxic flue gases are produced, which can harm the technological process [12].

The main commercial companies involved in the pyrometallurgical processing of lithium-ion batteries are Sumitomo-Sony in Japan and Umicore AG & Co. KG in Belgium [13].

The hydrometallurgical process involves the use of aqueous solutions to extract the necessary metals from cathode material [14]. In the hydrometallurgical process, the metal extraction rate is high with lower energy costs and no toxic emissions into the atmosphere. The essence of the process is that the crushed material is treated with acid or alkali to dissolve metals. Then the resulting solution is purified and the metals are extracted. Due to the complex structure of the cells, the initial stage is grinding, followed by leaching and mechanical separation phases, which include ferromagnetism. The separation of carbon from metal oxide can also be carried out by foam flotation [15].

The main advantages of hydrometallurgy are the use of inexpensive reagents, low environmental impact, low operating costs, high occupational safety, and the possibility of industrial scale.

2. Selection of the most efficient method for LIB disposal. To select the most promising and logically sound technology for lithium-ion battery disposal, a task with a multi-criteria choice was developed. A solution was found that met the most important criteria for effective disposal using a special software program.

To solve this problem, we needed input data: alternatives — in our case, these were the disposal methods themselves. The evaluation criteria were ranked on a scale from 1 to 5: “Possibility of integration into the production process”, “Labor/energy intensity of the process”, “Level of recovery of materials”, “Process safety”, “Formation of by-products” where 1 was considered as the most favorable outcome, and 5 — the least favorable, respectively.

The main selection criterion for this task was the “Possibility of integration into the production process”, since the fundamental solution would be the use of the resources of the main production line, and assigning weight coefficients to the criteria was as follows:

“Possibility of integration into the production process” — 0.4;

“Labor/energy intensity of the process” — 0.15;

“Level of recovery of materials” — 0.2;

“Process safety” — 0.1;

“Formation of by-products” — 0.15;

Table 1 presents the ranking criteria for all three disposal methods.

Table 1

Data for the multi-criteria selection task

Criteria	Processing method		
	Physical	Pyrometallurgical	Hydrometallurgical
Labor/energy intensity of the process	2	3	4
Possibility of integration into the production process	3	5	2
Level of recovery of materials	4	5	2
Process safety	4	2	3
Formation of by-products	2	5	3

To determine the most suitable alternative, we used the Mpr_Dipl program. This program contains methods of decision-making in multi-criteria tasks: direct methods (characterized by the characteristic dependence of the usefulness of an alternative on its ratings according to some special criteria), methods of paired comparisons (criteria are ordered by importance, after which the best alternative is considered to have a higher score according to a more important criterion, regardless of the ratings according to other criteria.), the weighted sum method (methods of decision-making under conditions of certainty and under conditions of uncertainty). This program was used by the authors of article [16] to select a method for recycling sunflower husks. Figure 3 provides the calculation results.

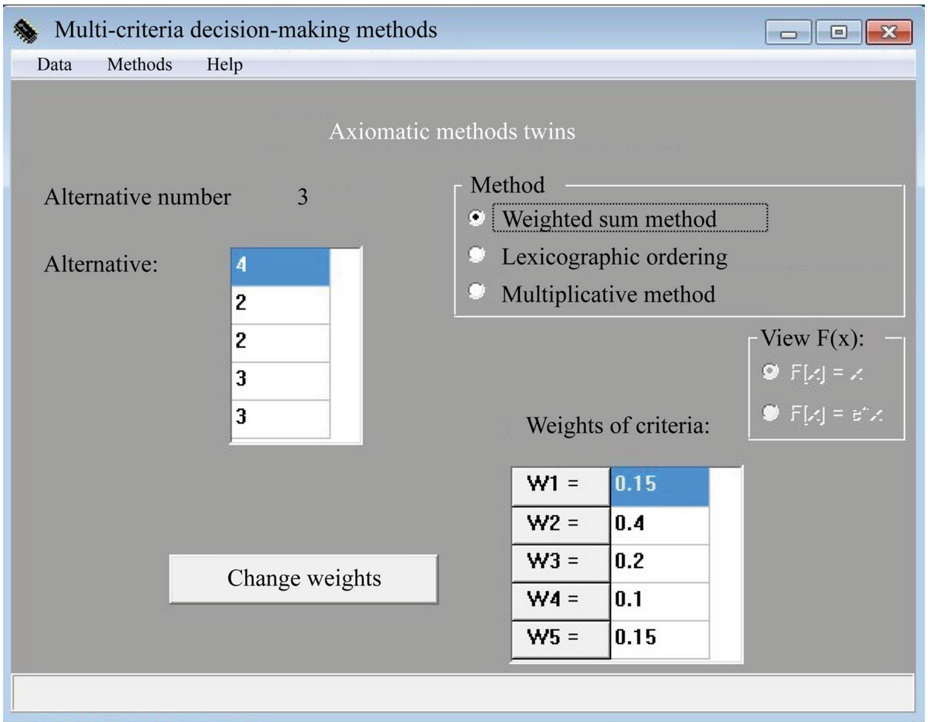

Fig. 3. Calculation results of the Mpr_Dipl program

Thus, the most suitable method of lithium-ion batteries recycling in this case was the "Hydrochemical method" (Alternative No. 3).

3. Technology for spent LIB recycling using a hydrochemical method. Based on the results of analyzing various technologies for lithium-ion battery processing, it has been decided to use a hydrochemical method involving the extraction of lithium carbonate in several stages. Lithium carbonate is a valuable product with wide application in metallurgy. It is used for steel desulfurization, as well as in pyrotechnics, the production of glasses and plastics, electrical insulating porcelain, sitals, and in agriculture as a fertilizer and feed additive. Figure 4 shows the technological scheme for the LIB processing process.

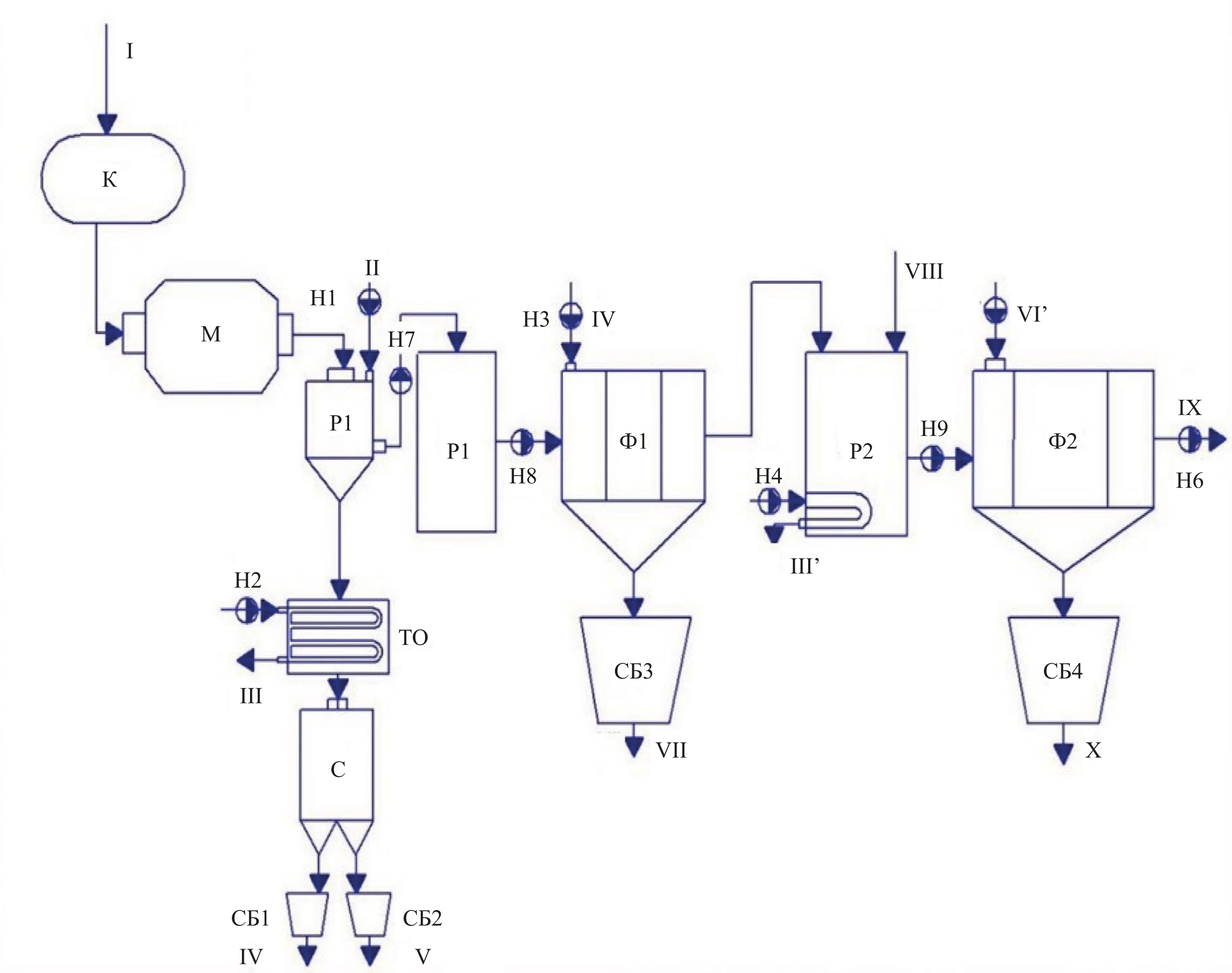

Fig. 4. Technological scheme of the LIB processing process:
I — spent LIB; II — water; III, III' — heat-carrying medium; IV — trapped plastic; V — trapped metals;
VI, VI' — water for washing the press filter; VII — trapped metal oxides, graphite; VIII — Na_2CO_3;
IX — filter for water purification; X — Li_2CO_3.

According to Figure 4, the technological scheme of the LIB processing process with the extraction of lithium carbonate consists of five stages: grinding, separation, filtration, precipitation and capture of wet Li_2CO_3 sediment. At the first stage, the equipment used is: a cryocamber, a ball mill, a vertical hammer crusher, a heat exchanger and a circulation pump. In the second stage, an electrostatic separator is used to separate metal particles and plastic. At the third stage, the main equipment used is a suspension pump and a press filter. They are necessary to capture manganese dioxide, graphite, metal particles and plastic residue. A reaction vessel is used to precipitate Li_2CO_3.

The material balance for the developed method has been calculated (Table 2). This calculation was based on a forecast that 1 ton of LIB with specific characteristics would be processed each day at the production site.

Table 2

Summary of the material balance of the recycling process

Input			
Products of processing	t/day	t/year	% wt
1. Waste in the form of lithium-ion batteries, including:	1.000	25.000	67.980
– Manganese dioxide	0.150	3.750	
– Graphite	0.060	1.500	
– Lithium compounds	0.110	2.750	
– Solvents	0.180	4.500	
– Metal particles	0.350	8.750	
– Plastic	0.150	3.750	
2. Water	0.403	10.075	27.396
Na_2CO_3	0.068	1.700	4.624
Total	1.471	36.775	100.000
Output			
Products of processing	t/day	t/year	% wt
1. Wet sediment Li_2CO_3	0.081	2.025	5.506
2. Filtrate	0.627	15.675	42.868
3. Sediment (on press filter 1)	0.254	6.350	17.267
4. Metal particles	0.349	8.725	23.725
5. Plastic	0.149	3.725	6.962
6. Water vapor released during the sludge drying process	0.011	2.750	3.672
Total	1.471	36.775	100.000

As a result of introducing the technology for LIB processing, 2.025 tons/year of wet Li_2CO_3 sludge, 6.350 tons/year of graphite, manganese dioxide, metal particles, and plastic will be produced each year from 25 tons of waste. Additionally, 8.725 tons/year of metal particles, 3.725 tons/year of plastic will be captured and separated at the primary stage. The resulting filtrate (15.675 tons/year) was proposed to be sent to the water treatment plant of the main production plant for the production of lithium-ion batteries N, where multilevel water purification takes place.

Discussion and Conclusion. As a result of the study, an analysis of various methods for recycling lithium-ion batteries has been carried out. The advantages and disadvantages of each method have been discussed. A search for the most promising method for LIB recycling has been conducted using the method of multi-criteria choice. A method for recycling lithium-ion batteries with the extraction of valuable components using a hydrochemical method has been presented. This system ensures safe recycling of used lithium-ion batteries with minimal negative impact on the environment and maximum recovery of valuable components. Calculations show that 2.025 tons/year of wet Li_2CO_3 sediment and 6.350 tons/year of graphite, manganese dioxide, metal particles and plastic sediment would be extracted from 25 tons/year of spent LIB.

Thus, the introduction of a closed-loop economy into the process of LIB processing can reduce the negative impact on the environment, as well as bring financial benefits when extracting valuable components. Recycling plays an important role in reducing waste and promoting the efficient use of energy.

References

1. Bin Huang, Zhefei Pan, Xiangyu Su, Liang An. Recycling of Lithium-Ion Batteries: Recent Advances and Perspectives. *Journal of Power Sources*. 2018;399:274–286. https://doi.org/10.1016/j.jpowsour.2018.07.116

2. Yue Yang, Emenike G Okonkwo, Guoyong Huang, Shengming Xu, Wei Sun, Yinghe He. On the Sustainability of Lithium-Ion Battery Industry – A Review and Perspective. *Energy Storage Mater*. 2021;36:186–212. https://doi.org/10.1016/j.ensm.2020.12.019

3. Arenkov IA, Ivanova DV, Zherebchikova PE. Analytical Review of the Market for Lithium-Ion Battery Manufacturers. *Journal of Economics, Entrepreneurship and Law*. 2023;13(12):5963–5980. (In Russ.) https://doi.org/10.18334/epp.13.12.119994

4. Jędrzej Piątek, Semih Afyon, Tetyana M Budnyak, Serhiy Budnyk, Sipponen MH, Adam Slabon. Sustainable Li-Ion Batteries: Chemistry and Recycling. *Advanced Energy Materials*. 2021;11(43):203456. https://doi.org/10.1002/aenm.202003456

5. Hayder Ali, Hassan A Khan, Pecht MG. Circular Economy of Li Batteries: Technologies and Trends. *Journal of Energy Storage*. 2021;40:102690. https://doi.org/10.1016/j.est.2021.102690

6. Fisher M, Apt J, Whitacre JF. Can Flow Batteries Scale in the Behind-the-Meter Commercial and Industrial Market? A Techno-Economic Comparison of Storage Technologies in California. *Journal of Power Sources*. 2019;420:1–8. https://doi.org/10.1016/j.jpowsour.2019.02.051

7. Beskov VS. *General Chemical Technology*. Moscow: IKTs Akademkniga; 2006. 452 p. (In Russ.) URL: https://library.tou.edu.kz/fulltext/buuk/b2381.pdf (accessed: 20.06.2024).

8. Velazquez-Martínez O, Valio J, Santasalo-Aarnio A, Reuter M, Serna-Guerrero R, Serna-Guerrero R. A Critical Review of Lithium-Ion Battery Recycling Processes from a Circular Economy Perspective. *Batteries*. 2019;5(4):68. https://doi.org/10.3390/batteries5040068

9. Jinqiu Xu, Thomas HR, Francis RW, Lum KR, Jingwei Wang, Bo Liang. A Review of Processes and Technologies for the Recycling of Lithium-Ion Secondary Batteries. *Journal of Power Sources*. 2008;177(2):512–527. https://doi.org/10.1016/j.jpowsour.2007.11.074

10. Melnikova AS. Methods for Disposal of Lithium-Ion Current Stones. In: *Proceedings of the International Scientific Ecological Conference "Agricultural Landscapes, Their Sustainability and Development Features"*, Krasnodar, March 24–26, 2020.Krasnodar: Kuban State Agrarian University; 2020. P. 202–204. (In Russ.)

11. Xuehu Zhong, Wei Liu, Junwei Han, Fen Jiao, Wenqing Qin, Tong Liu, et al. Pyrolysis and Physical Separation for the Recovery of Spent LiFePO4 Batteries. *Waste Management*. 2019;89:83–93. https://doi.org/10.1016/j.wasman.2019.03.068

12. Thompson DL, Hartley JM, Lambert SM, Shiref M, Harper GDJ, Kendrick E, et al. The Importance of Design in Lithium-Ion Battery Recycling — A Critical Review. *Green Chemistry*. 2020;22:7585–7603. https://doi.org/10.1039/D0GC02745F

13. Ekberg C, Petranikova M. Chapter 7 – Lithium Batteries Recycling. In book: Chagnes A, Światowska J (eds.). *Lithium Process Chemistry*. 2015. P. 233–267. https://doi.org/10.1016/B978-0-12-801417-2.00007-4

14. Juntao Hu, Jialiang Zhang, Hongxu Li, Yongqiang Chen, Chengyan Wang. A Promising Approach for the Recovery of High Value-Added Metals from Spent Lithium-Ion Batteries. *Journal of Power Sources*. 2017;351:192–199. https://doi.org/10.1016/j.jpowsour.2017.03.093

15. Pagliaro M, Meneguzzo F. Lithium Battery Reusing and Recycling: A Circular Economy Insight. *Helliyon*. 2019;5(6):e01866. https://doi.org/10.1016/j.heliyon.2019.e01866

16. Ishbulatova AI, Kusova IV. Granulation as a Way to Recycle Sunflower Husks. In: *Proceedings of the IV International Scientific and practical conference "Security Problems" (SECURITY-2022) dedicated to the 90th anniversary of USATU.* Ufa: Ufa State Aviation Technical University; 2022. P. 252–255. (In Russ.)

About the Authors:

Anna S. Melnikova, Postgraduate Student of the Industrial Safety and Industrial Ecology Department, Ufa University of Science and Technology (32, Zaki Validi Str., Ufa, 450076, Russian Federation), SPIN-code, ORCID, ScopusID, annamel7@mail.ru

Natalya V. Kostryukova, Cand. Sci. (Chem.), Associate Professor of the Industrial Safety and Industrial Ecology Department, Ufa University of Science and Technology (32, Zaki Validi Str., Ufa, 450076, Russian Federation), SPIN-code, ScopusID, kostrukova@list.ru

Claimed Contributorship:

FS Melnikova: analysis of literary data, description of the theoretical part of the research, calculation of material balance, design of a scientific article.

NV Kostryukova: creation of a technological scheme of LIB processing process.

***Conflict of Interest Statement:* the authors do not have any conflict of interest.**

All authors have read and approved the final manuscript.

Об авторах:

Анна Сергеевна Мельникова, аспирант кафедры безопасности производства и промышленной экологии Уфимского университета науки и технологий (450076, Российская Федерация, г. Уфа, ул. Заки Валиди, 32), SPIN-код, ORCID, ScopusID, annamel7@mail.ru

Наталья Викторовна Кострюкова, кандидат химических наук, доцент кафедры безопасности производства и промышленной экологии Уфимского университета науки и технологий (450076, Российская Федерация, г. Уфа, ул. Заки Валиди, 32), SPIN-код, ScopusID, kostrukova@list.ru

Заявленный вклад авторов:

А.С. Мельникова: анализ литературных данных, описание теоретической части исследования, расчет материального баланса, оформление научной статьи.

Н.В. Кострюкова: создание технологической схемы процесса переработки ЛИА.

Конфликт интересов: **авторы заявляют об отсутствии конфликта интересов.**

Все авторы прочитали и одобрили окончательный вариант рукописи.

Received / Поступила в редакцию 05.09.2024
Revised / Поступила после рецензирования 24.09.2024
Accepted / Принята к публикации 08.10.2024

TECHNOSPHERE SAFETY
ТЕХНОСФЕРНАЯ БЕЗОПАСНОСТЬ

UDC 528.9

Original Empirical Research

https://doi.org/10.23947/2541-9129-2024-8-4-16-28

Justification of Criteria and Assessment of Environmental Safety during the Operation of Metro Facilities

Sergey A. Zhukov

Mosinzhproekt AO, Moscow, Russian Federation

✉ fragrante@mail.ru

EDN: WUEXOJ

Abstract

Introduction. In today's world, with the increasing pace of urbanization, environmental safety plays a crucial role in urban planning and management. Subway operations, as an important part of urban infrastructure, contribute to population mobility, but they can also cause significant environmental problems. Such scientists as Kulikova E.Yu., Konyukhov D.S., Potapova E.V., Balovtsev S.V., Chunyuk D.Yu., etc have studied these issues. However, their research mostly ignores the fact that one of the major threats to environmental safety is the degradation of tunnel linings due to hydrogeological processes. This not only increases the risk of accidents but also increases the likelihood of negative impacts on groundwater and the environment. Therefore, the study of the nature of the development of defects in tunnel linings and their dynamics over time is of both scientific and practical interest, and is the aim of this research. To achieve this objective, it is necessary to analyze the relationship between the condition of the tunnel lining and environmental safety based on data about defects in subway tunnel structures and their impact on the environment.

Materials and Methods. For this study, we used defective sections of the subway tunnel linings from several lines of the Moscow Metro as materials. We conducted field studies of the lining's condition and geodetic surveys of the tunnels, which revealed significant changes in the indicators compared to the normative values as a result of the interaction between the human-made environment and the surrounding nature. Additionally, we employed seismoacoustic inspection methods to inspect the tunnel linings using shock excitation.

Results. Data on the dependence of defect development on changes in groundwater level has been obtained. Defects in tunnel linings contribute to the leakage of chemically active substances into soil and groundwater, which threatens biodiversity and reduces water quality used by the population.

Discussion and Conclusion. Field surveys have shown that defects in tunnel linings, such as cracks, concrete leaching, and waterproofing violations, have a direct impact on environmental safety. Therefore, maintaining the integrity of these structures is a key element in ensuring environmental safety in urban areas. The results of this research will form the basis for developing comprehensive proposals to improve monitoring techniques and ensure the structural integrity of tunnel structures.

Keywords: metro, environmental safety, sustainable development, urban transport system, environmental standards, innovative technologies

Acknowledgements. The author would like to thank the Head of the scientific project at the Scientific and Engineering Center of the Tunnel Association OOO, Cand. Sci. (Eng.), Associate Professor A.T. Ivanov, and Dr. Sci. (Eng.), Professor, Leading Researcher at the research center M.V. Sidorov, for their expert interviews together with the author of the article, as well to as the staff of Mosmetrostroy AO for their assistance in organizing the research.

For Citation. Zhukov SA. Justification of Criteria and Assessment of Environmental Safety during the Operation of Metro Facilities. *Safety of Technogenic and Natural Systems.* 2024;8(4):16–28. https://doi.org/10.23947/2541-9129-2024-8-4-16-28

Оригинальное эмпирическое исследование

Обоснование критериев и оценка экологической безопасности при эксплуатации объектов метрополитена

С.А. Жуков
АО «Мосинжпроект», г. Москва, Российская Федерация
✉ fragrante@mail.ru

Аннотация
Введение. В современном мире, где темпы урбанизации неуклонно растут, экологическая безопасность выступает в качестве критического аспекта городского планирования и управления. Эксплуатация метрополитенов, будучи важной частью городской инфраструктуры, вносит свой вклад в мобильность населения, но также может стать источником значительных экологических проблем. Данная тема исследована в трудах таких ученых, как Е.Ю. Куликова, Д.С. Конюхов, Е.В. Потапова, С.В. Баловцев, Д.Ю. Чунюк и др. Однако в их работах практически не учитывается тот факт, что одной из основных угроз экологической безопасности является ухудшение состояния тоннельной обделки под воздействием гидрогеологических процессов, которые не только усиливают риск аварийных ситуаций, но и повышают вероятность негативного воздействия на подземные воды и окружающую среду в целом. Поэтому исследование характера развития дефектов в тоннельных обделках и их динамики представляет научно-практический интерес и является целью данной работы. Для реализации поставленной цели необходимо проанализировать связи между состоянием тоннельной обделки и экологической безопасностью, основываясь на данных о дефектах конструкций тоннелей метрополитена и их влиянии на окружающую среду.
Материалы и методы. Материалами для данного исследования послужили дефектные участки обделки перегонных тоннелей некоторых линий Московского метрополитена. Проведены натурные исследования состояния обделки и геодезическая съемка туннеля, которые продемонстрировали значительные изменения показателей, по сравнению с нормативными, в результате взаимодействия техногенной среды с окружающей природой. При проведении исследования использованы также методы сейсмоакустического обследования обделки тоннеля с помощью ударного возбуждения.
Результаты исследования. Получены данные о зависимости развития дефектов от изменения уровня грунтовых вод. Дефекты тоннельной обделки способствуют утечке химически активных веществ в грунт и подземные воды, что угрожает биоразнообразию и снижает качество воды, используемой населением.
Обсуждение и заключение. Проведенные натурные изыскания показали, что дефекты тоннельной обделки, такие как трещины, выщелачивание бетона и нарушение гидроизоляции, оказывают прямое влияние на экологическую безопасность. Таким образом, поддержание целостности тоннельной обделки является ключевым элементом обеспечения экологической безопасности в городских условиях. Результаты проведенных исследований будут служить фундаментом для разработки комплексных предложений по улучшению методов мониторинга и обеспечения структурной целостности тоннельных конструкций.

Ключевые слова: метрополитен, экологическая безопасность, устойчивое развитие, городская транспортная система, экологические стандарты, инновационные технологии, риски

Благодарности. Автор благодарит руководителя научного проекта ООО «НИЦ Тоннельной ассоциации», кандидата технических наук, доцента А.Т. Иванова, доктора технических наук, профессора, ведущего научного сотрудника исследовательского центра М.В. Сидорова за проведенные ими экспертные интервью, а также коллектив АО «Мосметрострой» за помощь в организации исследования.

Для цитирования. Жуков С.А. Обоснование критериев и оценка экологической безопасности при эксплуатации объектов метрополитена. *Безопасность техногенных и природных систем.* 2024;8(4):16–28. https://doi.org/10.23947/2541-9129-2024-8-4-16-28

Introduction. The construction and operation of subways are accompanied by increased environmental risks [1] associated with geological and geochemical hazards, noise, vibration, biological influences, etc. [2]. At the same time, the main criteria that must be taken into account when managing environmental risks at metro facilities include:

– *technical criteria*, which aim to minimize potential accidents and emergency situations (minimizing the ingress of hazardous and harmful substances used in the technological process into the biosphere components);

– *economic criteria*, which are designed to minimize investment risks in the operation of a particular metro facility;

– *regulatory and legal criteria,* which aim to geo-ecological, technological, and operational safety of metro facilities;

– *resource criteria*, which regulate the intensity of natural resource use in metro operations;

– *landscape and geographical criteria,* which aim to reduce undesirable environmental impacts on geographical components of natural and technical geosteme.

Monitoring of the above criteria can only be effective with the combined use of geotechnical and geoecological monitoring.

It should be noted that one of the main factors leading to decreased environmental safety in metro tunnels [3] is geological risk [4]. Moreover, it is the hydrogeological component of the geological risk that determines the nature of the decrease in reliability and durability of underground metro facilities [5]. At the same time, defects such as leaks, fractures, ellipticity, etc., can quickly develop in tunnels due to concomitant occurrences of quicksand breakthroughs, water intrusion, and the accumulation of loose aggregate in the space between the tunnel lining and the rock [6]. The aim of this paper was to analyze the development of defects in metro tunnels, study their dynamics and assess the impact of tunnel lining conditions on the environment.

Materials and Methods. The material for this study was the results of a survey of the metro tunnel lining. It was conducted using geodetic surveying, including seismic and acoustic methods using shock excitation.

The operational regime of metro facilities is largely determined by the nature of changes in the stress-strain state of the rock mass that houses the underground facility and the hydrogeological conditions in the area where it is located. Variability in hydrogeological situation over time often leads to the development of deformation processes [7], which can cause wear of tunnel linings and reduce the operational performance of the facility [8]. This is especially important to take into account when working with unstable loose soils, as changes in their structure can lead to defects in tunnel linings, as well as the movement of loose aggregates and large volumes of water into the developed spaces [9].

Fluctuations in hydrostatic pressure in such soils can lead to the rapid development of emergencies associated with weakening of strength characteristics of the lining, changes in the structure of the overlying soils and, accordingly, subsidence of earth's surface. This can cause deformation and destruction of underground utilities, buildings, and structures on the surface. Decreased tightness of tunnel lining indicates decreased hydrostatic pressure in the rock mass, which can lead to emergencies.

Classical monitoring of hydrological situation in metro tunnels [10] is an integral part of ensuring the environmental safety of operation of its facilities [11]. Figures 1–4 show photographic materials from the monitoring of an interstation tunnel on one of the Moscow Metro lines.

Fig. 1. Leaching and wet spot in the inter-ring and inter-block joint of the lining active leakage

Fig. 2. Soil washout into the area of the contact rail

Fig. 3. Bolt malfunction

Fig. 4. Leaching and wet spot in the inter-ring and inter-block joint of the lining, active leak. A crack in the back of the tubing

The examination of defective sections formed as a result of an accident allowed us to systematize the main violations in the block, their possible causes, and consequences of their development in accordance with GOST R 57208–2016[1] (Table 1).

Table 1

Classification of defects

No.	Type of defect	Potential causes	Potential consequences
1	Concrete spalling in wall blocks and roof slabs, including areas with exposed reinforcement	Mechanical impact	Reduction in bearing capacity of the lining
2	Leaching on wall blocks and roof slabs of the running tunnel. Wet spots on wall blocks. Dripping. Active leakages	Waterproofing violations	Destruction of concrete in structures, corrosion of metal and reinforcement. Reducing the operational characteristics of facilities
3	Steps at the joints of the roof slabs in the running tunnel up to 30 mm	Manufacturing and installation errors	The degree of reduction in load-bearing capacity is determined by calculation
4	Cracks in roof slabs with an aperture width of up to 0.2 mm	Shrinkage due to the heat and moisture treatment of the concrete mix, properties of the cement, etc.	No effect on load-bearing capacity. May reduce durability
5	Disruption of joint sealing in wall blocks and roof slabs	Tunnel and metro operations (including vibrations from moving trains)	Increased water infiltration and reduced operational performance of the structure

[1] GOST R 57208–2016. *Tunnels and Subways. Rules of Inspection and Elimination of Defects and Damages under Operation*. Moscow: Standartinform; 2019. 16 p. (In Russ.)

Research Results. The study of geological sections at emergency sites revealed changes in the level of aquifers over time and structural transformations of soils [12]. Additionally, changes in the geometry of the tunnel lining structure were observed.

During geodetic surveying of the defective sections of running tunnels, measurements of the actual dimensions of the structures were carried out using a manual laser rangefinder Leica DISTO D2. Measurement accuracy: ± 1.5 mm. Significant dimensional irregularities were discovered:

– on KP0167 + 09 – KP0167 + 23 (up to 303 mm) along track I;

– on KP0166 + 73 – KP0167 + 23 (up to 355 mm) along track II.

The results of measuring the actual geometric dimensions of the structures of the existing metro facilities in the problem areas under consideration are presented in summary Tables 2 and 3. Figures 5–18 provide the values of deformations at characteristic points of the lining and a graphical representation of the dependence of deformations on kilometer posts, indicating dangerous areas along tracks I and II according to the results of geodetic survey. The position of the characteristic points along tracks I and II is shown in Figure 19.

Table 2

Values of lining deformations of track I

KP	track1					rail level	
	point 1	point 2	point 3	point 4	point 5	point 6	point 7
165+53.40	–86	47	30	76	61	–35	18
165+63.40	–38	47	31	21	–65	–24	6
165+73.30	–44	2	13	22	–4	–11	–3
165+83.30	8	12	23	0	35	1	–1
165+93.30	2	10	3	–34	32	–2	1
166+3.40	18	–1	–73	–40	–44	–9	–11
166+13.40	–19	–54	1	–41	3	–11	–15
166+23.40	18	34	32	–95	–40	–3	–1
166+33.30	86	24	–15	–50	–38	–10	–12
166+34.40	98	75	–25	–98	–103	–7	–8
166+39.40	128	69	–90	–111	–105	–6	–7
166+50.40	100	31	–86	–68	–58	–14	–15
166+56.40	70	25	–56	–53	–49	–20	–22
166+62.40	84	75	–1	–44	–42	–9	–12
166+68.40	91	45	19	–21	–69	–11	–14
166+80.40	53	89	–43	–123	–43	–11	–12
166+89.50	96	20	–67	–75	–63	–22	–23
166+97.50	150	47	–113	–109	–60	–31	–32
167+0.50	144	67	–89	–108	–77	–22	–23
167+3.50	135	51	–76	–89	–81	–28	–27
167+6.45	110	48	–76	–84	–56	–24	–25
167+7.45	99	49	–78	–78	–49	–24	–23
167+8.45	117	45	–85	–81	–51	–22	–21
167+9.45	–172	–23	–187	–182	–352	–21	–21
167+18.30	–150	–59	–303	–351	–322	–10	–9
167+23.55	–188	–137	–138	–224	–351	–4	–5

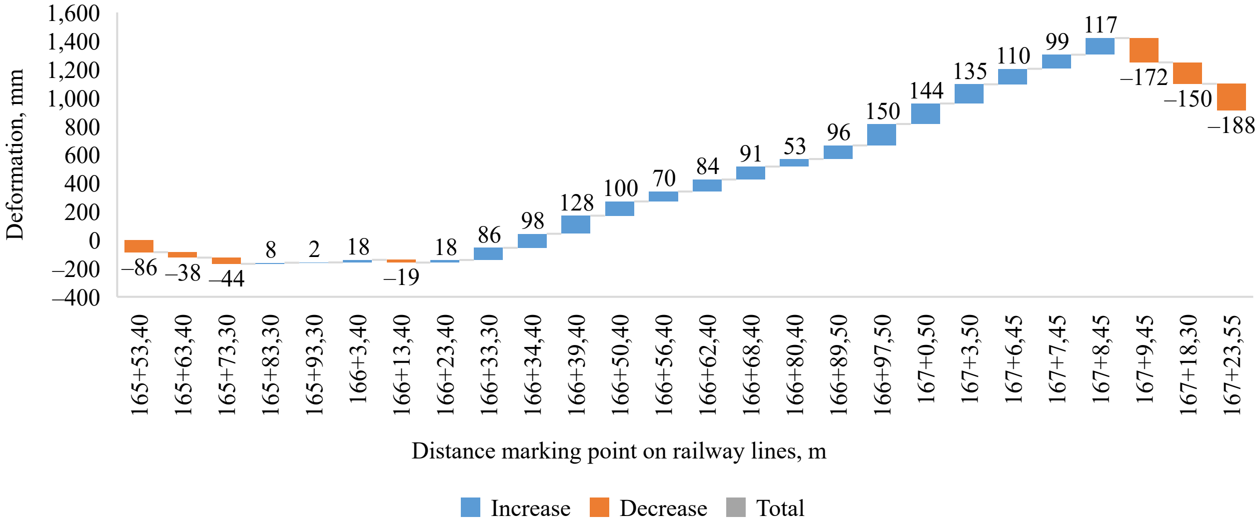

Fig. 5. Graph of lining deformation of track I point 1

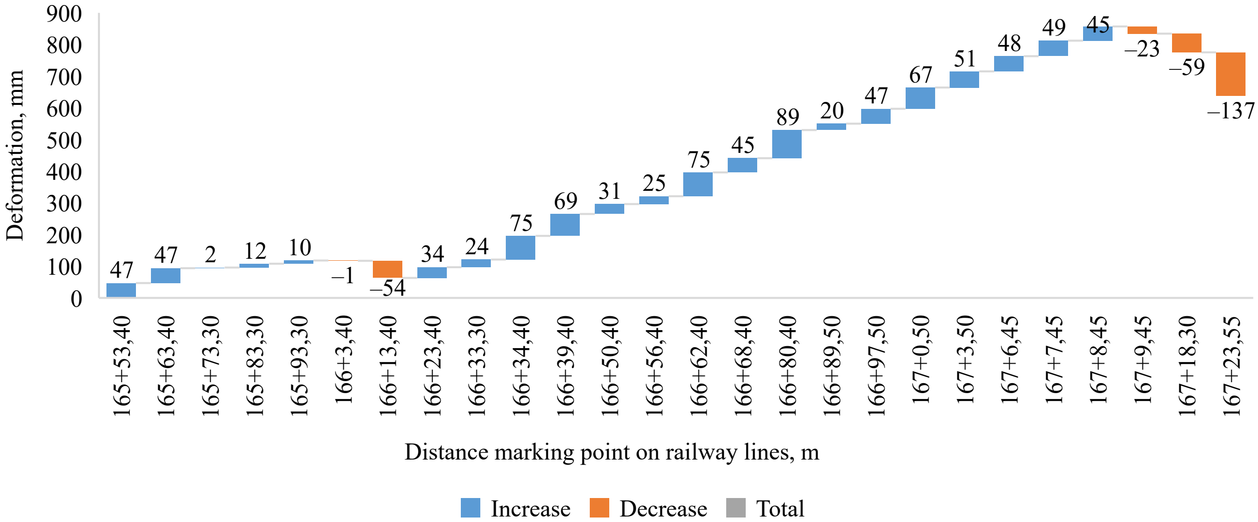

Fig. 6. Graph of lining deformation of track I point 2

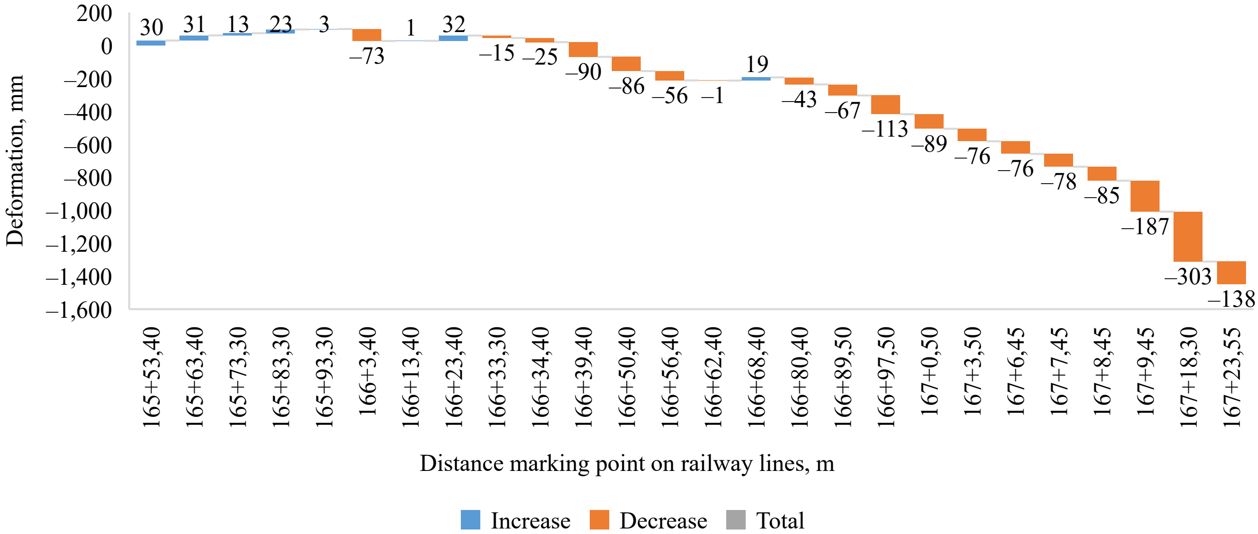

Fig. 7. Graph of lining deformation of track I point 3

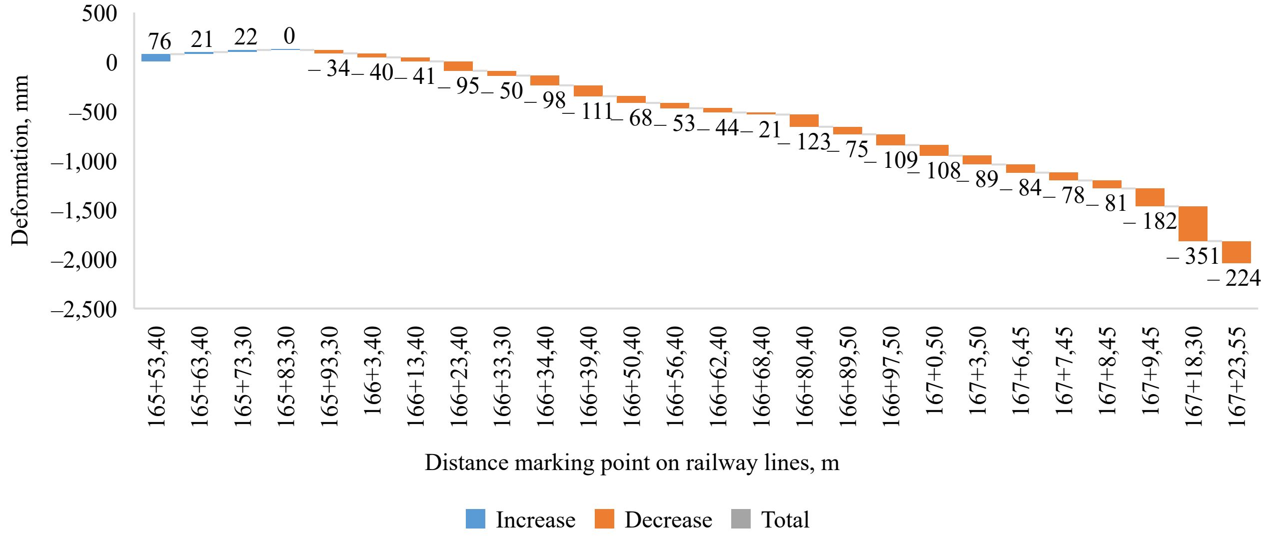

Fig. 8. Graph of lining deformation of track I point 4

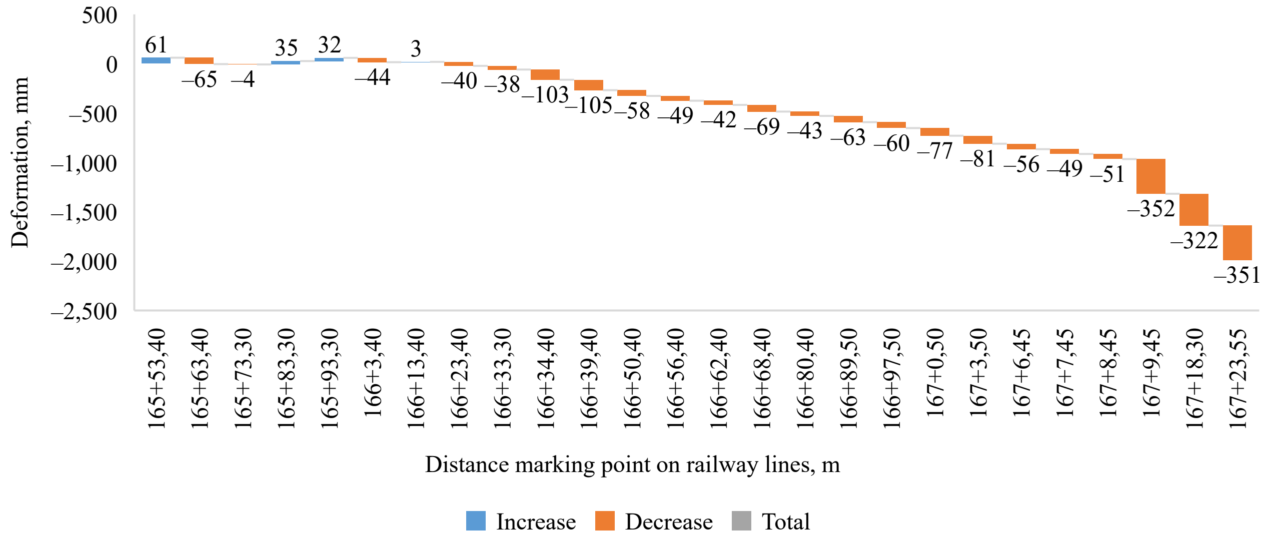

Fig. 9. Graph of lining deformation of track I point 5

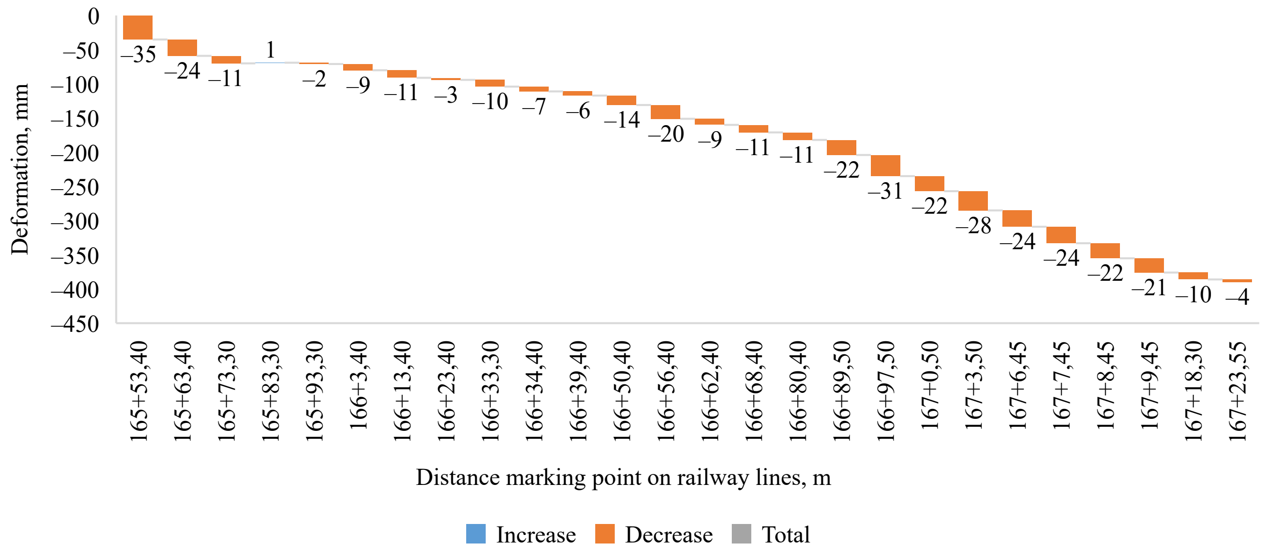

Fig. 10. Graph of lining deformation of track I point 6

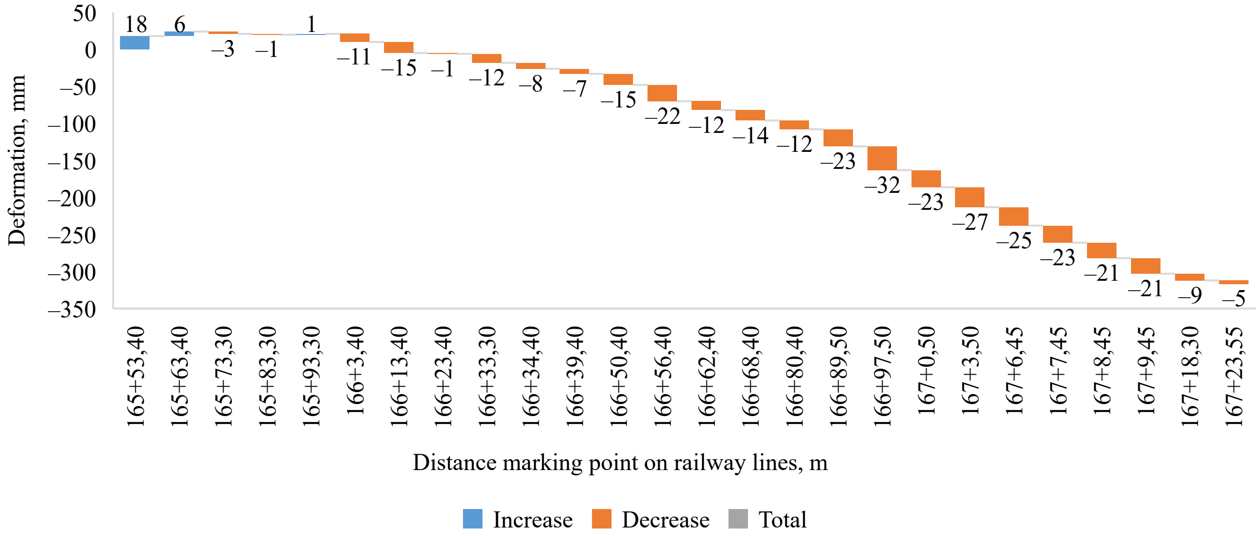

Fig. 11. Graph of lining deformation of track I point 7

Table 3

Values of lining deformations of track II

KP	track 2					rail level	
	point 1	point 2	point 3	point 4	point 5	point 6	point 7
165+69.10	–85	–71	–55	62	95	–19	–2
165+79.10	5	–8	2	17	26	–7	–5
165+89.10	–36	0	–45	–37	–30	–8	–5
165+99.20	–37	43	–32	–40	0	–6	–5
166+19.30	–38	11	58	33	0	–9	–10
166+29.30	–40	–18	16	39	38	–10	–11
166+39.30	45	14	–85	12	39	–19	–18
166+49.30	40	14	–163	–102	0	–21	–20
166+59.30	60	55	–86	–146	–80	–18	–19
166+69.30	150	47	–77	–1	–119	–5	–4
166+79.30	167	21	–129	–154	–119	–21	–19
166+99.40	194	–66	–271	–209	–95	–111	–105
167+4.40	166	–80	–268	–185	–84	–125	–127
167+7.40	261	11	–267	–284	–197	–127	–127
167+9.40	142	–66	–270	–227	–61	–131	–127
167+10.40	210	7	–273	–291	–170	–120	–120
167+13.40	231	14	–287	–301	–209	–114	–113
167+14.50	181	–92	–301	–242	–83	–77	–75
167+16.40	255	8	–332	–210	–185	–95	–93
167+17.40	210	–3	–334	–235	–181	–87	–85
167+18.40	295	–3	–355	–251	–148	–77	–75
167+19.40	214	–78	–270	–254	–55	–71	–72
167+22.40	209	37	–275	–194	–189	–44	–47
167+23.50	169	46	–261	–235	–120	–39	–42

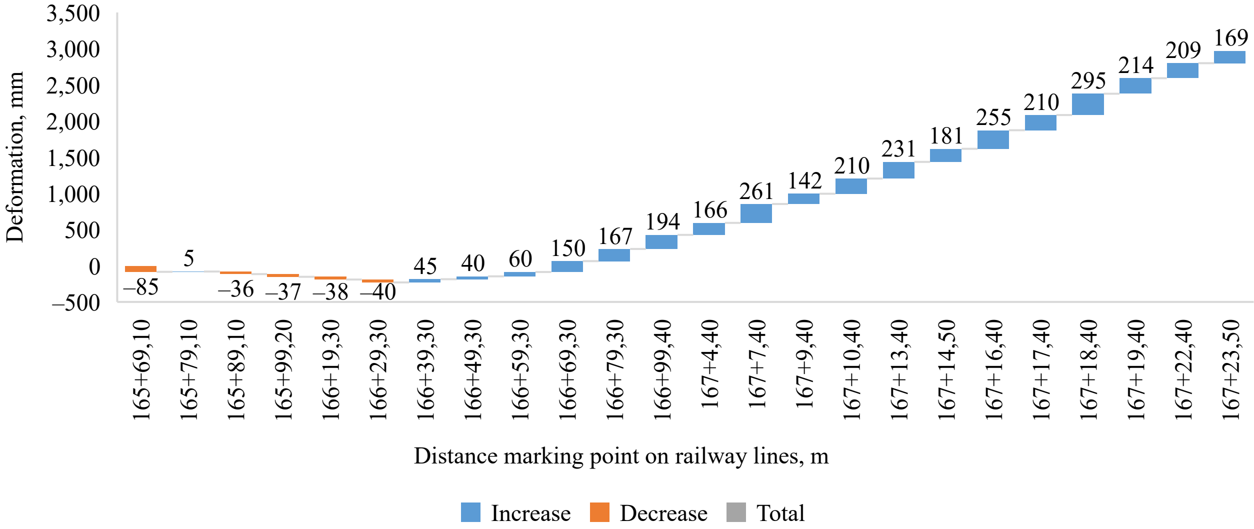

Fig. 12. Graph of lining deformation of track II point 1

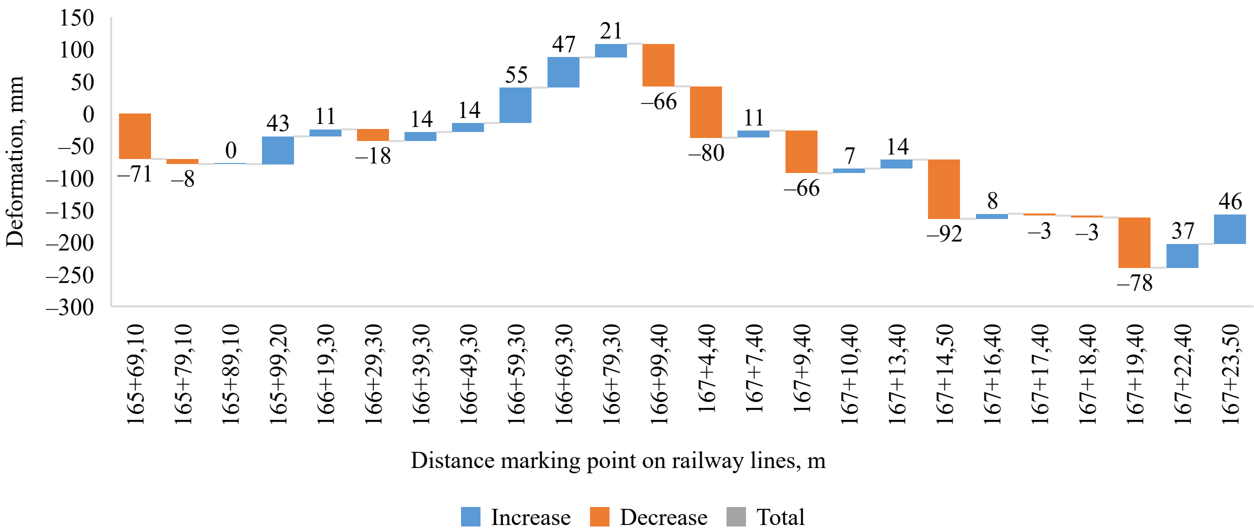

Fig. 13. Graph of lining deformation of track II point 2

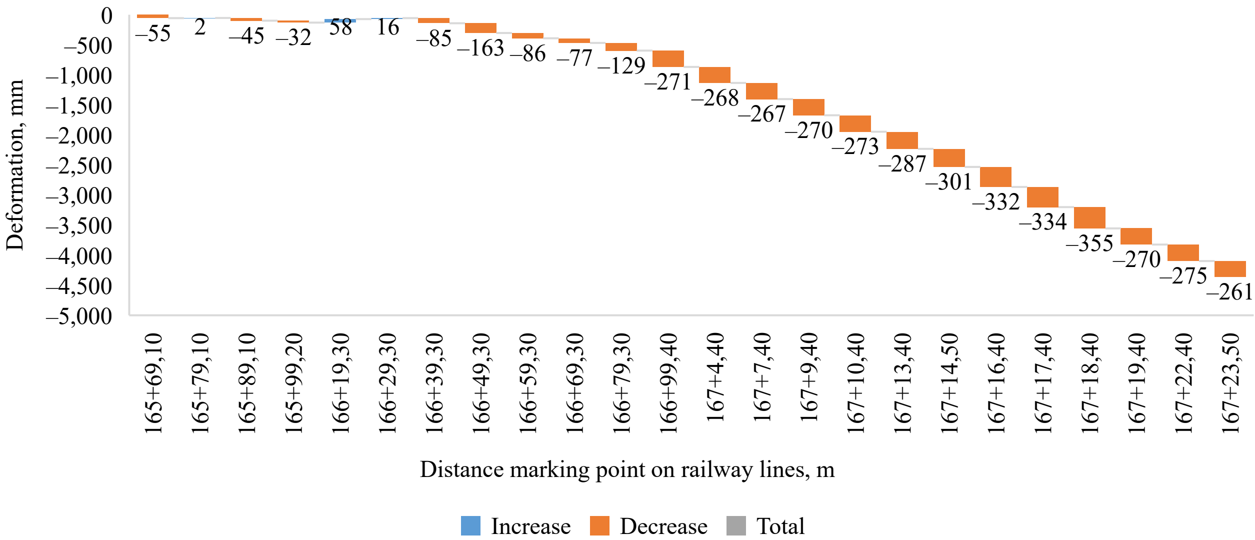

Fig. 14. Graph of lining deformation of track II point 3

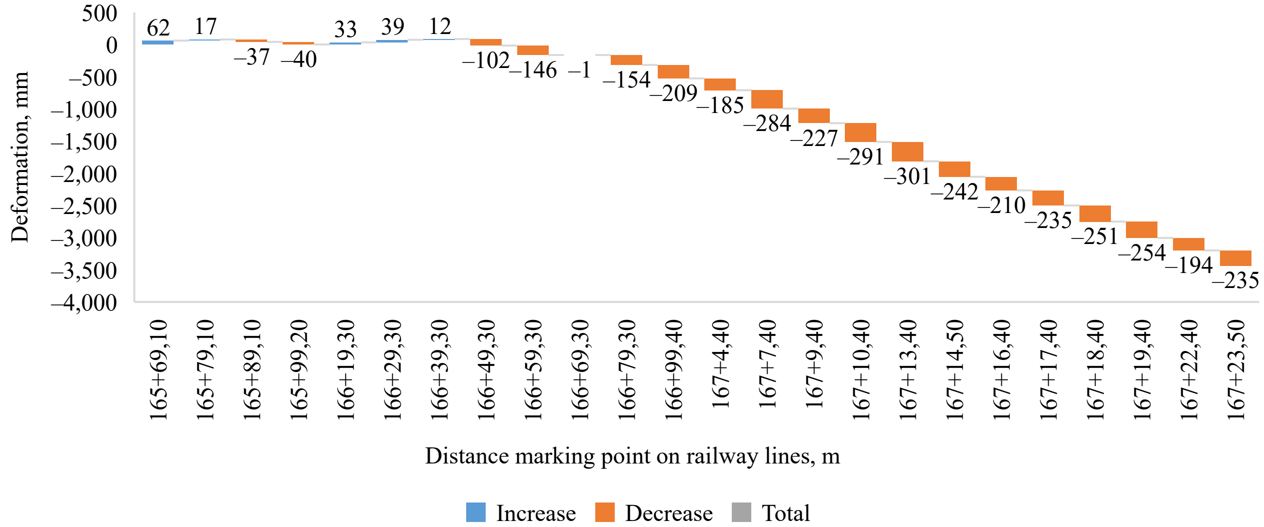

Fig. 15. Graph of lining deformation of track II point 4

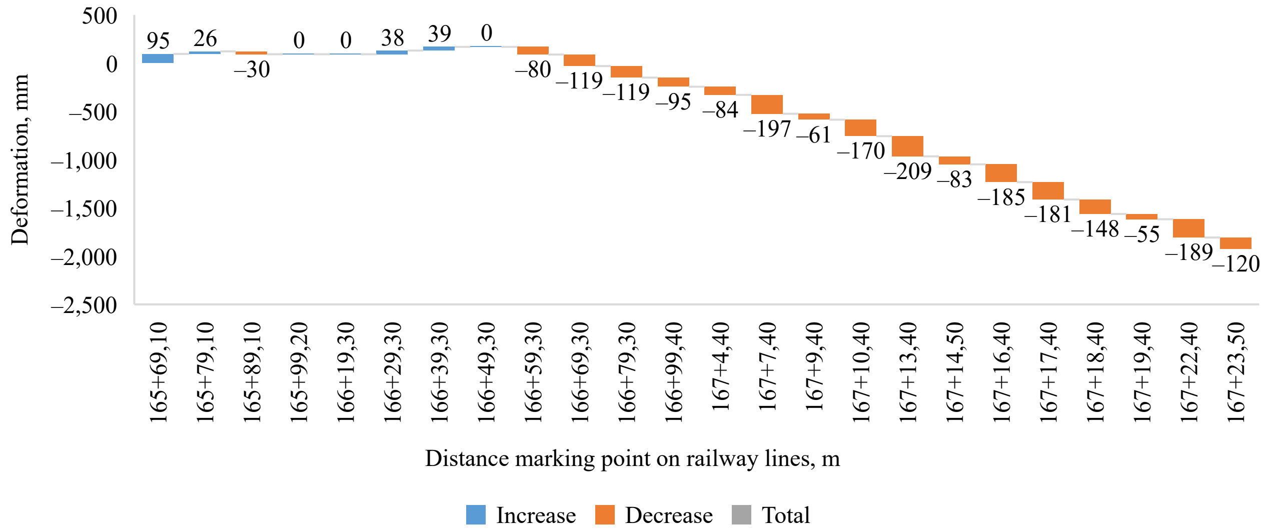

Fig. 16. Graph of lining deformation of track II point 5

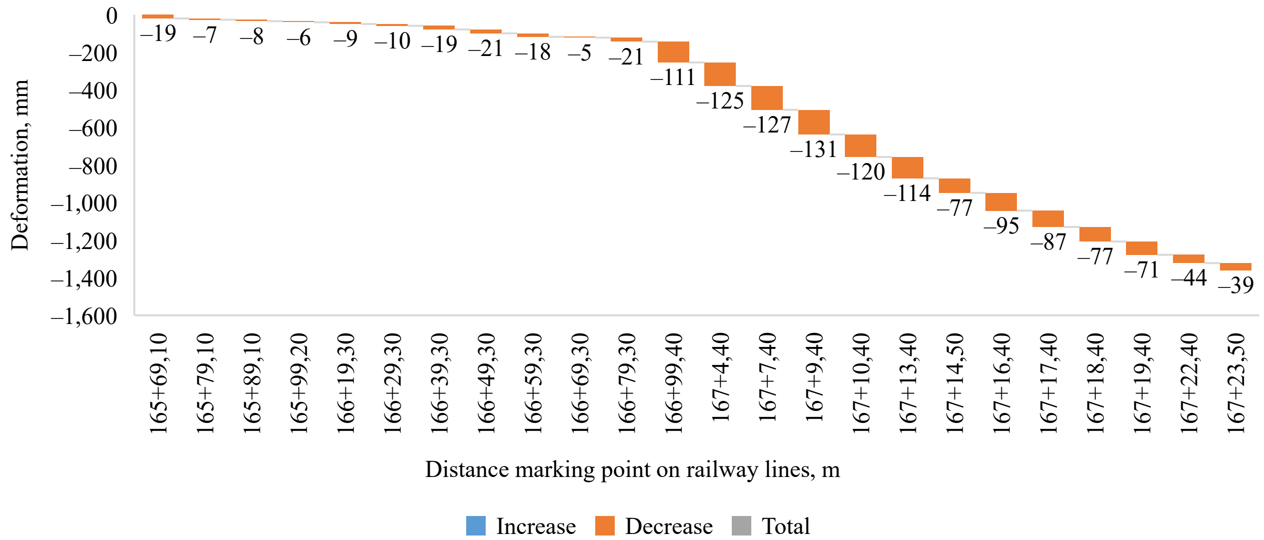

Fig. 17. Graph of lining deformation of track II point 6

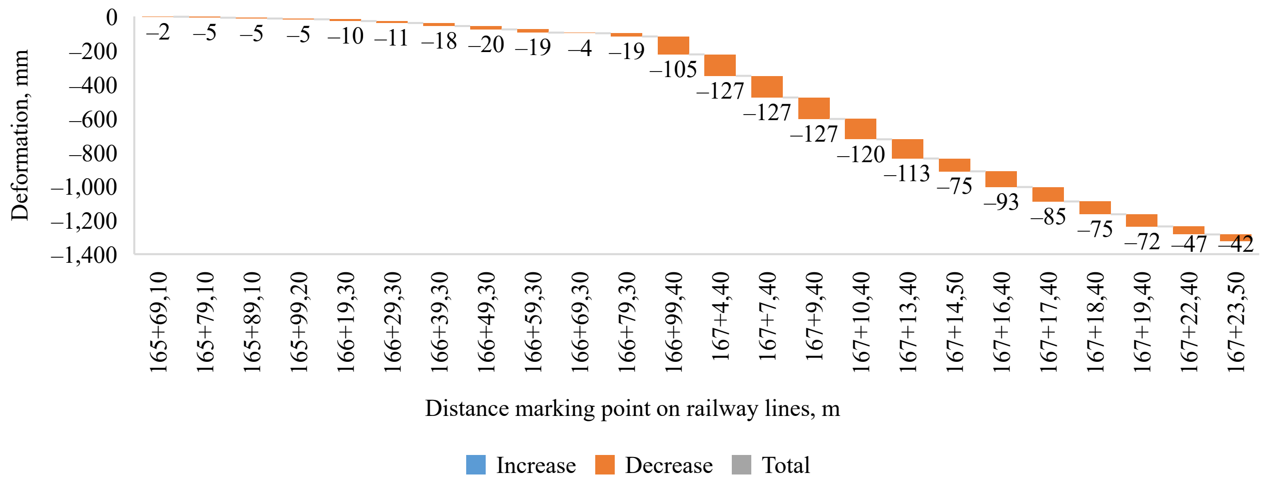

Fig. 18. Graph of lining deformation of track II point 7

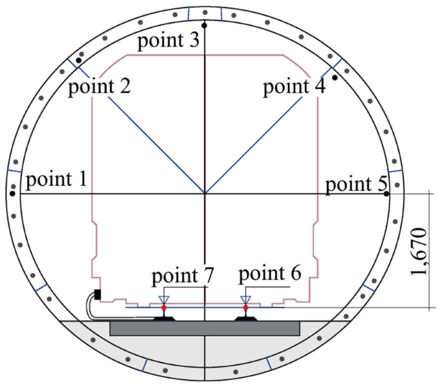

Fig. 19. Position of characteristic points

Based on Tables 2 and 3, it could be concluded that deformation processes had a negative impact on the condition of the tunnel lining, leading to its destruction [13]. An increase in groundwater inflow to the tunnel lining resulted in loss of anticorrosive and strength properties, which allowed water masses to infiltrate the space between the lining and rock through leaks and soil washout, reaching the track sections. This can be seen in the defect map created by the author (Fig. 20).

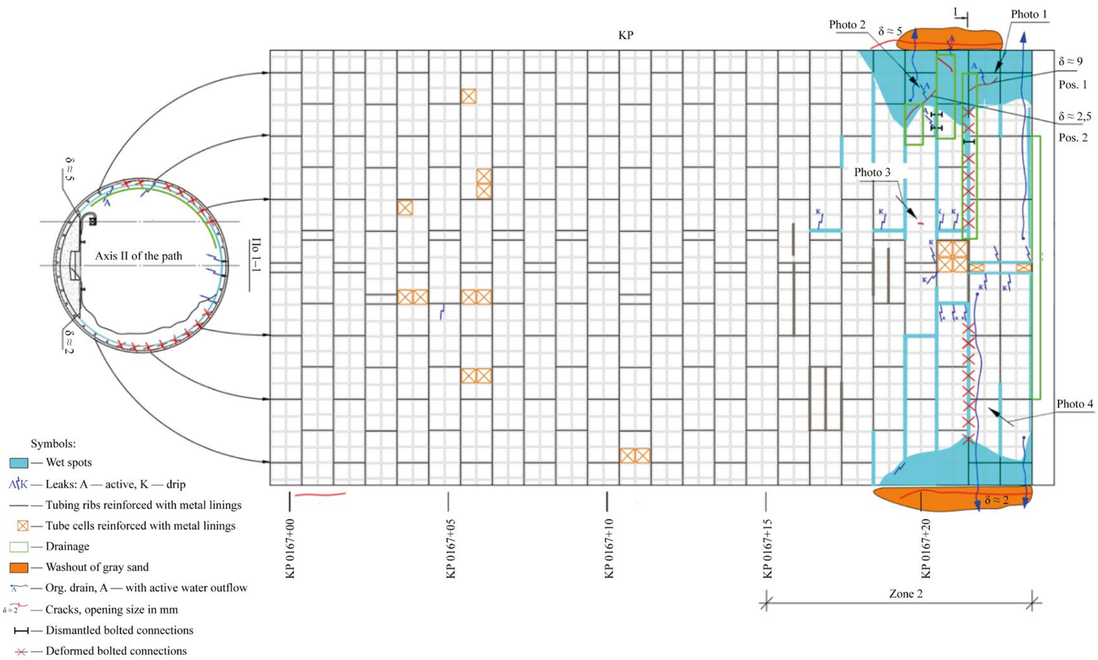

Fig. 20. Map of defects in the lining, compiled from field surveys

When using the method of seismoacoustic survey of the tunnel lining [14] using shock excitation (also called vibroacoustic, or seismoacoustic, method), zones of weakened contact “lining — soil body” were found. An electrodynamic sensor was mounted on the surface of the tubing on a special rod and pressed tightly against it. At some distance from the seismic sensor, the lining was excited using a striker mounted on another support rod. An elastic wave appeared, which was recorded when a certain threshold was exceeded. An archive of signals and responses was stored in the buffer of the device, which made it possible to record the full length of the lining response. Figure 21 provides the results of the survey.

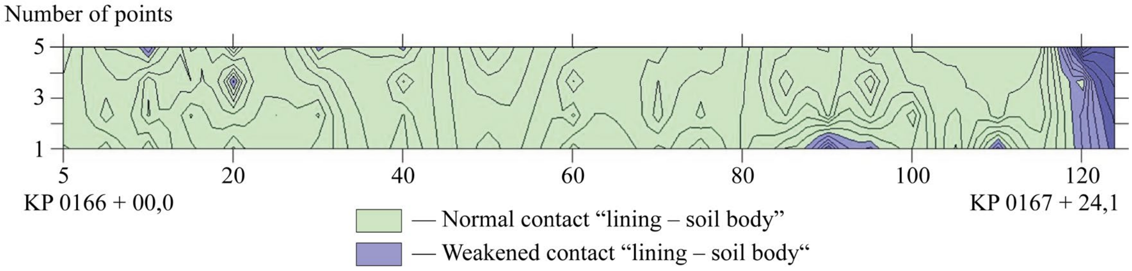

Рис. 21. Результаты сейсмоакустического контроля

A geophysical survey of the tunnels space allowed us to identify areas with weakened contact “lining — soil body”:
– on KP0166 + 10.0 in the gutter area on the left side of the running tunnel;
– on KP0166 + 20.0 at the level of the horizontal diameter on the left side of the running tunnel;
– on KP0166 + 30.0 in the gutter area on the left side of the running tunnel;
– on KP0166 + 40.0 in the gutter area on the left side of the running tunnel;
– from KP0166 + 87.0 to KP0166 + 96.0 below the horizontal diameter level in the right part of the running tunnel;
– on KP0167 + 10.0 in the gutter area on the right side of the running tunnel;
– from KP0167 + 19.0 to KP167 + 24.1 along the entire section of the tunnel.

There were less than 3% of the areas with weakened contact “lining — soil body” along track II in the space between lining and rock of the right running tunnel in the section from KP0166 + 00.0 to KP0167 + 24.1.

Discussion and Conclusion. Field surveys have shown that defects in tunnel lining (cracks, concrete leaching and waterproofing violations) have a direct impact on the level of environmental safety. These defects contribute to the leakage of polluted waters and chemically active substances into the soil, which threatens biodiversity and the quality of water used by the population. Thus, maintaining the integrity of the tunnel lining is a key element of ensuring environmental safety in urban environments.

The obtained results of this study are planned to be used as a basis for the development of proposals to improve the quality of monitoring and maintain the structural integrity of tunnel structures, which will minimize environmental risks and increase the safety level of urban underground transport.

References

1. Kulikova EYu, Balovtsev SV, Skopintseva OV. Complex Estimation of Geotechnical Risks in Mine and Underground Construction. *Sustainable development of mountain territories.* 2023;15(1):7–16. (In Russ.) http://doi.org/10.21177/1998-4502-2023-15-1-7-16

2. Kulikova EYu. Safety and Risk Management in Underground Construction as a Complex Information. *Mining informational and analytical bulletin (scientific and technical journal).* 2021;2(1):134–143. (In Russ.) http://doi.org/10.25018/0236-1493-2021-21-0-134-143

3. Xi-Cun He, Ye-Shuang Xu, Shui-Long Shen, An-Nan Zhou. Geological Environment Problems during Metro Shield Tunnelling in Shenzhen, China. *Arabian Journal of Geosciences.* 2020;13(2):87. http://doi.org/10.1007/s12517-020-5071-z

4. Ye-Shuang Xu, Jack Shuilong Shen, An-Nan Zhou, Arul Arulrajah. Geological and Hydrogeological Environment with Geohazards during Underground Construction in Hangzhou: A Review. *Arabian Journal of Geosciences.* 2018;11:544. http://doi.org/10.1007/s12517-018-3894-7

5. Xing-Tao Lin, Ren-Peng Chen, Huai-Na Wu, Hong-Zhan Cheng. Deformation Behaviors of Existing Tunnels Caused by Shield Tunneling Undercrossing with Oblique Angle. *Tunneling and Underground Space Technology.* 2019;89:78–90. http://doi.org/10.1016/j.tust.2019.03.021

6. Merisalu J, Sundell J, Rosén L. Probabilistic Cost-Benefit Analysis for Mitigating Hydrogeological Risks in Underground Construction. *Tunnelling and Underground Space Technology.* 2023;131:104815. http://doi.org/10.1016/j.tust.2022.104815

7. Konyukhov DS. Criteria Analysis of Modern Technologies of Underground Construction. *Geotechnics.* 2021;1:40–55. (In Russ.)

8. Konyukhov DS. Analysis of Mechanized Tunneling Parameters to Determine the Overcutting Characteristics. *Mining Science and Technology (Russia).* 2022;7(1):49–56 http://doi.org/10.17073/2500-0632-2022-1-49-56

9. Lebedev MO. Choosing a Calculation Method for Stress-Strain of Supports and Lining of Transport Tunnels. In: *16th World Conference of the Associated Research Centers for the Urban Underground Space (ACUUS 2018)*. Hong Kong; 2018, P. 678–687.

10. Garber VA. Non-Standard Situations in Underground Transport Facilities. *Underground Horizons*. 2018;16:20–25. (In Russ.)

11. Kulikova EYu. Methodical Principles for Improving the Ecological and Technological Reliability of Urban Underground Structures. *Mining informational and analytical bulletin (scientific and technical journal).* 2020;6(1): 176–185. (In Russ.) http://doi.org/10.25018/0236-1493-2020-61-0-176-185

12. Kulikova EYu, Balovtsev SV. Risk Control System for the Construction of Urban Underground Structures. *IOP Conference Series: Materials Science and Engineering.* 2020;962(4):042020. http://doi.org/10.1088/1757-899X/962/4/042020

13. Potapova EV. Typology of Metro Structures for the Tasks of Geotechnical Risk Classification. *Mining Science and Technology (Russia).* 2021;6(1):52–60. (In Russ.) http://doi.org/10.17073/2500-0632-2021-1-52-60

14. Kuepferle J, Röttger A, Theisen W, Alber M. Wear Prediction for Soft-Ground Tunneling Tools — A New Approach Regarding the Dominant Influencing Factors in the Tribological System of Tunneling Tools. In: *Proceeding of the World Tunnel Congress 2017 — Surface challenges — Underground solutions.* Bergen, Norway; 2017.

About the Author:

Sergey A. Zhukov, CEO, Mosinzhproekt AO (4/1, Sverchkov Lane, Moscow, 101000, Russian Federation), ORCID, fragrante@mail.ru

Conflict of interest statement: **the author does not have any conflict of interest.**

The author has read and approved the final version of manuscript.

Об авторе:

Сергей Анатольевич Жуков, генеральный директор АО «Мосинжпроект» (101000, Российская Федерация, г. Москва, пер. Сверчков, 4/1), ORCID, fragrante@mail.ru

Конфликт интересов: **автор заявляет об отсутствии конфликта интересов.**

Автор прочитал и одобрил окончательный вариант рукописи.

Received / Поступила в редакцию 06.08.2024
Revised / Поступила после рецензирования 21.08.2024
Accepted / Принята к публикации 08.09.2024

MACHINE BUILDING
МАШИНОСТРОЕНИЕ

Check for updates

UDC 620.179
https://doi.org/10.23947/2541-9129-2024-8-4-29-38

Original Empirical Research

Determination of the Optimal Volume of Elements of Building and Engineering Structures by Non-Destructive Testing of Their Strength

EDN: YIVEUL

Nikos L. Vernezi
Don State Technical University, Rostov-on-Don, Russian Federation
✉ vernezin@mail.ru

Abstract

Introduction. Before repairing or reconstructing steel structures, it is necessary to obtain information about the strength capacities of the metal. The estimated service life of metal structures is tens of years, but it is known that the mechanical properties of the original metal change over time. Additionally, many facilities operate beyond these anticipated lifespans. As some researchers have noted, the challenge of obtaining such information is due to several factors. Firstly, in most cases, it is impossible to cut samples from existing structures. Secondly, the use of non-destructive testing methods needs to ensure sufficient accuracy in assessment. Thirdly, non-destructive testing may not be physically possible due to the design features of the object. Fourthly, survey work on the operating structure can be very laborious and expensive, requiring a reduction in volume and cost. Fifthly, when assessing the mechanical characteristics of the metal, it is important to apply an approach that guarantees the accuracy of results while minimizing work by utilizing previously obtained information on similar metals. Given these challenges, the development of a methodology that combines non-destructive testing with prior information is crucial.

In non-destructive testing of structures, methods for qualitative assessment of the condition of metal or welded joints are used, such as ultrasonic, magnetic, and radiation techniques. There are also quantitative methods for evaluating mechanical characteristics, such as using portable hardness testers. However, most methods for assessing strength characteristics, such as yield strength and temporary tear resistance, are cumbersome and limited to laboratory settings.

The methods of clarifying experimental information using a priori data by experts are conventionally divided into three categories:

– according to the priority of the weight of a priori and experimental data;
– extrapolation of past data to future periods;
– based on Bayesian procedures.

This article describes a non-destructive strength testing method based on indentation developed with the author's participation and repeatedly tested in actual surveys. The aim of this article is to justify the author's methodology to minimize the amount of required samples during survey work by combining non-destructive testing methods and Bayesian accounting for experimental information.

Materials and Methods. The research plan involved analyzing experimental data on the mechanical properties of metals and developing an algorithm to minimize the number of samples of control objects. Before measuring, the metal of the structures was cleaned with a hand grinder. The method of non-destructive testing of the evaluation of mechanical characteristics according to the parameters of the impact insertion of the indenter into the surface under study was used. To minimize the amount of work, a Bayesian approach was used to reduce the variability of posterior values by utilizing additional experimental data on the mechanical characteristics of such steels. The material St3 of strength class KP 245 with yield strength of 245 MPa and tensile strength of 412 MPA was studied. Additional experimental data on this material's properties were available from a previously studied metal structure.

Results. The method of non-destructive testing of the strength of metal in pipe structures has been implemented. This method used prior information obtained from previous surveys of similar materials. Based on a Bayesian approach, experimental and previous information was combined, in particular, the values of time resistance to rupture. A method for estimating the minimum required sample size of the examined structural elements was proposed provided there was minimal risk from an estimation error. As a result of calculations, it was shown that the use of such a technique was possible with a sample size of 2–3 elements.

Discussion and Conclusion. The proposed methodology was developed based on an analysis of more than 20 surveys conducted to assess the strength of the existing metal structures. Using the non-destructive testing method, we were able to simultaneously determine the yield strength, tensile strength, elongation, and hardness. The article presents data on the values of tensile strength. It should be noted that although the duration of each measurement was 20–30 seconds, in some cases it took longer to inspect large structures, such as bridges, which could take weeks. The calculation performed using the proposed method, which combined experimental and pre-experimental information about one of the strength characteristics of steel, temporary tear resistance, showed the high efficiency and potential for further application in future surveys.

Keywords: mechanical characteristics, tensile strength, non-destructive testing, Bayesian estimation, optimal sample size during testing

Acknowledgements. The author would like to express his deepest appreciation and gratitude to A.N. Beskopylny and A.A. Veremeenko for their participation in the inspection of metal structures with the author.

For citation. Vernezi NL. Determination of the Optimal Volume of Elements of Building and Engineering Structures by Non-Destructive Testing of Their Strength. *Safety of Technogenic and Natural Systems.* 2024;8(4):29–38. https://doi.org/10.23947/2541-9129-2024-8-4-29-38

Оригинальное эмпирическое исследование

Определение оптимального объема элементов строительных и машиностроительных конструкций при неразрушающем контроле их прочности

Н.Л. Вернези

Донской государственный технический университет, г. Ростов-на-Дону, Российская Федерация

✉ vernezin@mail.ru

Аннотация

Введение. Перед ремонтом или реконструкцией стальных сооружений необходимо получить информацию о прочностных возможностях металла. Расчетные сроки службы металлоконструкций составляют десятки лет, при этом известно, что механические характеристики исходного металла за это время претерпевают изменения. Кроме того, многие объекты работают с превышением этих сроков. Как отмечают некоторые исследователи, проблема получения таких характеристик связана с тем, что, во-первых, в большинстве случаев вырезание образцов из действующих конструкций невозможно, во-вторых, применение неразрушающих методов контроля должно обеспечить достаточную точность оценки, в-третьих, неразрушающий контроль из-за конструктивных особенностей объекта физически возможен не в любой точке, в-четвертых, обследовательские работы эксплуатируемой конструкции весьма трудоёмки, дороги и требуют снижения как объёмов, так и стоимости, в-пятых, при оценке механических характеристик исследуемого металла необходимо применение подхода, позволяющего обеспечить точность результатов с минимизацией объёмов работ за счет использования ранее полученной информации о характеристиках металла подобной конструкции. Вследствие изложенного возникает задача разработки методики, объединяющей методы неразрушающего контроля и учета априорной информации.

При неразрушающем контроле конструкций на практике применяются методы качественной оценки состояния металла или сварных соединений, такие как ультразвуковой, магнитный, радиационный и др. Также имеют место количественные методы оценки механических характеристик, например, с помощью переносных твердомеров. Однако приборное обеспечение большинства методов оценки прочностных характеристик (предела текучести, временного сопротивления разрыву) громоздко или ограничено лишь лабораторными рамками.

Методы уточнения экспериментальной информации на основе использования априорных данных специалистами условно разделены на три группы:

– по приоритету весов априорной и опытной информации;

– экстраполирование прошлых данных на будущие периоды;

– основанных на байесовских процедурах.

В статье описан метод неразрушающего контроля прочности на основе индентирования, разработанный при участии автора и многократно апробированный в реальных обследованиях. Цель данной статьи заключается в обосновании предложенной автором методики минимизации объема необходимой выборки при обследовательских работах, основанной на объединении методов неразрушающего контроля и байесовского учета доопытной информации.

Материалы и методы. План исследования включал в себя анализ доопытной информации о механических характеристиках металлов и разработку алгоритма минимизации объема выборки объектов контроля. Перед измерением металл конструкций зачищался ручной шлифовальной машиной. Использовался метод неразрушающего контроля оценки механических характеристик по параметрам ударного внедрения индентора в исследуемую поверхность. Для минимизации объема работ применялся байесовский подход к сокращению дисперсии апостериорных значений за счет использования доопытной информации о механических характеристиках подобных сталей. Исследовался материал Ст3 класса прочности КП 245 с пределом текучести 245 МПа и временным сопротивлением разрыву 412 МПА, по характеристикам которого на ранее исследованной аналогичной металлоконструкции имелась доопытная информация.

Результаты исследования. Реализован метод неразрушающего контроля прочности металла трубной конструкции. При этом использована априорная информация, полученная при предыдущих обследовательских работах аналогичного материала. На основе байесовского подхода объединена опытная и доопытная информация, в частности, о значениях временного сопротивления разрыву. Предложена методика оценки минимально необходимого объема выборки обследуемых элементов конструкции при условии минимального риска от ошибки оценивания. В результате расчетов установлено, что применение такой методики возможно при объёме выборки в количестве двух-трех элементов.

Обсуждение и заключение. Предложенная методика явилась следствием анализа результатов более 20 проведённых обследовательских работ по оценке прочностных возможностей действующих металлических конструкций. На основе примененного метода неразрушающего контроля одномоментно определялись предел текучести, временное сопротивление разрыву, относительное удлинение и твердость. В статье приведены данные для значений временного сопротивления разрыву. Следует отметить, что даже при условии длительности одного измерения в 20–30 сек. в некоторых случаях на обследование крупных сооружений (например, мостов) требовалось значительное время, иногда измеряемое неделями. Выполненный расчет по предложенной методике, объединившей опытную и доопытную информацию об одной из прочностных характеристик стали, временном сопротивлении разрыву, показал высокую эффективность применения такого подхода и возможность дальнейшего его применения при обследовательских работах.

Ключевые слова: механические характеристики, временное сопротивление разрыву, неразрушающий контроль, байесовское оценивание, оптимальный объем выборки при испытаниях

Благодарности. Автор выражает глубокую признательность и благодарность А.Н. Бескопыльному и А.А. Веремеенко, принимавшим вместе с автором участие в обследовании металлоконструкций.

Для цитирования. Вернези Н.Л. Определение оптимального объема элементов строительных и машиностроительных конструкций при неразрушающем контроле их прочности. *Безопасность техногенных и природных систем.* 2024;8(4):29–38. https://doi.org/10.23947/2541-9129-2024-8-4-29-38

Introduction. The article discusses the problem of surveying steel structures prior to their repair or reconstruction. The issue arises due to several factors, including the impossibility of cutting out samples for standard tests from the existing structures, the need to ensure sufficient accuracy of the results of non-destructive testing, the impossibility of conducting non-destructive testing in all studied places of the structure due to the design features of the object, high cost and high complexity of the examination of large structures (for example, steel bridges). For this reason, it is necessary to develop an approach to the examination of structures that will ensure the accuracy of the results while minimizing the amount of work. This can be achieved by using previously obtained information about the characteristics of the metal of the structure.

When developing such an approach, three important questions need to be answered:

– how do the properties of the metal change during the operation of the structure;

– how should information be obtained;

– how to supplement it with known experimental information and minimize the amount of survey work.

The answers to these questions are extremely important, as it is known that under the influence of various factors (temperature or force in the form of cyclic loads), changes in the strength characteristics of a metal may occur.

The literature offers different interpretations of the first question (how the properties of metal change during the operation of the structure). V.I. Bryushko in [1] indicates an increase in strength characteristics and a decrease in ductility of steels 20, 15X5M, 19G. In [2] G.N. Nikiforchin, O.T. Tsirulnik, O.I. Zvirko, M.I. Gredil, V.A. Voloshin provide information about an increase in strength characteristics during the first 20 years of operation of a steel 17G pipe, and a steady decrease in strength and ductility over the next 10 years. In their work of I.V. Gorynin and B.T. Timofeeva [3] note the stability of mechanical characteristics of the metal in nuclear power structures and 17G1C pipe steel over 25–40 years of operation. The author of work [4] V.V. Kiselev draws attention to the fact that the nature of changes in the strength and plastic characteristics of steels mainly depends on the temperature influence and loading parameters, primarily cyclic. As a result, it is not entirely correct to focus on the values of the characteristics of the source material specified in the technical documentation. Moreover, such documentation may simply be lost over a long period of operation. Therefore, in order to obtain an objective assessment of changes in material characteristics, it is necessary to periodically or continuously monitor the condition of structures. Today, this practice is extremely rare.

The solution to the problem of obtaining information about the current design, especially if monitoring is taken into account, is exclusively related to non-destructive testing. Currently, non-destructive testing of structures uses methods of qualitative assessment of the state of metal based on the use of ultrasound, acoustic emission, radiation flaw detection for metal [5, 6], welded joints [7, 8] or in hard-to-reach places [9]. These techniques allow us to determine the presence of defects in metal, but they do not provide a quantitative measure of the material's ability to resist external forces.

There are techniques and portable devices available to assess the hardness of materials. One method for determining mechanical characteristics involves constructing stretching diagrams based on indentation results, such as by using an indenter [10]. The article [11] considers the issue of evaluating the mechanical characteristics of plastic materials by the ball indentation method based on the application of a finite element model. In [12], the problem of indentation of plastic materials with ball indenters is considered using numerical modeling. The sensitivity of the numerical results to the elasticity of the indenter is investigated. However, the instrumentation used in these methods is often cumbersome and is only used in laboratory settings, making it impractical for survey work.

Often, the controlled sites within a structure that need to be monitored are difficult to reach, and therefore, it is essential to have a tool that enables you to minimize the number of samples collected during survey work. At present, the range of techniques that allow for the joint processing of prior and experimental data is rather limited. In fact, there are three main categories: methods for assigning weights to prior and experimental information in posterior estimates, methods for extending past data into the future, and methods based on Bayesian procedures.

The authors of the article, V.N. Arsenev and P.V. Labetskii, [13] note that the issue of selecting a criterion for determining the significance coefficient of a priori information remains unsolved.

Bayesian procedures make it possible to reduce the a posteriori variance of the random variable under study by combining experimental and pre-experimental information. Experimental information can be expressed, for example, in the knowledge about the type of distribution of a random variable or one of its parameters.

Techniques based on the use of Bayesian procedures are widely applied today. These techniques are used to describe a systematic approach to decision-making, based on a large number of examples developed by the authors of the work [14]. The authors of the article [15] apply Bayesian analysis to assess economic uncertainty in investor behavior prediction. It is noted in [16], that the use of Bayesian parametric models for assessing survival in medicine is not inferior to traditional approaches, but requires less parameter tuning and increases the possibilities of statistical conclusions and forecasts. In [17], a methodology for developing a classifier of common dental diseases based on Bayesian statistical procedures is proposed.

In general, it is worth noting that methods of non-destructive testing, as well as methods of accounting for a priori information, have been highlighted and described in detail by many authors. However, it is obvious that the development of a methodological approach to solving the problem of minimizing the sample size of the examined elements has not been fully worked out, especially with regard to the method based on the synthesis of non-destructive testing of mechanical characteristics by indentation and Bayesian accounting of a priori information.

It is therefore essential to develop systems for monitoring the condition of metal structures based on non-destructive testing of mechanical characteristics by the indentation method. At the same time, in order to reduce material and time costs, such monitoring should be carried out using the possibilities of taking into account additional information about other similar objects.

The aim of this article is to substantiate the methodology proposed by the author, which combines the use of the original non-destructive testing method with the Bayesian approach for calculating the minimum necessary volume of examined elements, carried out on a specific example.

Materials and Methods. By order of a construction company, the metal pipe sheet piling structures were inspected during the construction of a building at 51 Gorsovetskaya Street in Rostov-on-Don. Most of the pipe structures had already been put in the ground, while a small number that had not been put yet had to be inspected to assess their mechanical properties. At the same time, it was important to use the minimum number necessary from the standpoint of minimizing the error in the results of such an inspection.

For this purpose, additional experimental data was used on the strength of 11 low-carbon steel pipe elements obtained by non-destructive testing during the construction of a building at 23 Suvorova Street in Rostov-on-Don, Additionally, we used a Bayesian estimate of the optimal number of elements required for this experimental examination of pipe elements of a similar strength class.

The article describes an original method of non-destructive testing, developed with the participation of the author, which allows you to simultaneously obtain values of temporary tear resistance, yield strength, hardness and elongation at a local site of any operated metal structure. The method is especially effective when examining metal of the same strength class of similar machine structural elements (sections of a tower crane), for example, when it is necessary to conduct an examination of the condition of a lifting crane[1], that has served its service life, or here are doubts about the deformations. At the same time, it is often very difficult to inspect the elements of a metal structure, even by non-destructive methods, due to technical difficulties in accessing certain areas. Therefore, the question arises about how to minimize sample size while maximizing information content based on a priori knowledge.

The non-destructive testing method used is based on the impact insertion of a conical indenter into the tested metal [18]. This method is implemented in the “Strength” system, which include a spring-loaded impact mechanism with an induction sensor for recording the speed of movement of the indenter, an analog-to-digital converter and a laptop. The velocity graph obtained during impact is differentiated and integrated to plot acceleration and displacement graphs, respectively. The extreme values of the three graphs represent an image of the metal. Previously conducted experiments with various grades of steel allowed us to establish and enter into a computer the correlations between standard yield strength and temporary tear resistance, hardness, elongation, on the one hand, and maximum and minimum values of velocity and acceleration, the depth of indenter insertion, on the other. Measurement using the repeatedly tested “Strength” system is possible for a section of an element with a diameter greater than 3 centimeters. The total error of the instrument is ±4%.

With the help of the “Strength” system, dozens of structures were examined according to orders from manufacturing enterprises. These included booms, running wheels, frames of construction and road vehicles, various construction metal structures of stadium stands, roof trusses, power transmission poles, bridges, pipes, etc. [19]. In three-dimensional structures with a large number of similar elements, it is recommended, in accordance, for example, with SP 13–102–2003[2], to examine at least 10% of these elements from their total number. This can amount to several dozen elements for a building structure, determining a significant amount of labor and cost for the work performed.

When examining, for example, a lifting crane boom, which may have up to 100 or more identical parts, the volume of the sample that is acceptable is also important.

However, when it is difficult to take even a few measurements in hard-to-reach areas, the issue of reducing the number of elements examined becomes relevant.

To address this issue, we apply the Bayesian method, which takes into account a priori information.

Let us assume that it is necessary to obtain information about the mechanical properties of the metal in the structure that has been operating for a long time (for diagnosis, monitoring or subsequent reconstruction in conditions of limited access to controlled elements of the same type) when the examination is carried out by non-destructive testing. Additional experimental data is used to justify the required sample size of n surveyed elements of the same type. In this case, we have average value $\sigma_{\text{вт cp}}$ of the measured value of the characteristic, variance S^2 of its experimental values and a priori information about this characteristic of the metal of a similar strength class.

In the pre-experimental (a priori) knowledge of distribution $\sigma_в$, there is parameter μ expressing the mathematical expectation of the value of tensile strength $\sigma_в$. From previous experience, density $H(\mu)$ of the distribution of this parameter is known. Let $(\sigma_{\text{вт}} \mid \mu)$ be the density of the distribution of values $\sigma_{\text{вт}}$ obtained as a result of this measurement, provided that mathematical expectation $\sigma_{\text{вт}}$ is μ. Then a posteriori density $K(\mu \mid \sigma_{\text{вт}})$ of the distribution of parameter μ of the measured random variable of characteristic $\sigma_в$, in accordance with Bayes' theorem, will be expressed as follows:

$$K(\mu \mid \sigma_{\text{вт}}) \sim H(\mu)\, g(\sigma_{\text{вт}} \mid \mu), \tag{1}$$

where $K(\mu \mid \sigma_{\text{вт}})$ — density of the a posteriori distribution of parameter μ, synthesizing experimental and a priori information, provided that experimental values $\sigma_{\text{вт}}$ are realized. In the expression for this density, parameter μ will be understood as the mathematical expectation of the value of tensile strength $\sigma_в$ after the implementation of the measured current values $\sigma_{\text{вт}}$.

The main condition for practical application of formula (1) is the conjugacy of distribution densities $H(\mu)$ and $g(\sigma_{\text{вт}} \mid \mu)$ (i.e., the possibility of obtaining a convenient result).

The densities of two normally distributed random variables are best conjugated. However, numerous studies have found that the distribution of mechanical characteristics is most reliably described by Weibull's law, since it has a distribution shift parameter or a minimum characteristic value hat is not in the sample but in the general population. This inconvenience can be eliminated if we take as $\sigma_{\text{вт}}$ not the instantaneous, but its average value $\sigma_{\text{вт\_cp}}$. Then in

[1] RD 10–112–2–09. *General Purpose Boom Cranes and Lifting Cranes, Part 2.* (In Russ.) URL: https://meganorm.ru/Data2/1/4293828/4293828984.pdf (accessed: 15.05.2024).

[2] SP 13–102–2003. *Rules for Inspection of Load-Bearing Building Structures of Buildings and Structures.* (In Russ.) URL: https://docs.cntd.ru/document/1200034118 (accessed: 15.05.2024).

accordance with central limit theorem $H(\mu)$ and $g(\sigma_{\text{вт\_ср}} \mid \mu)$ can be assumed to be normally distributed, and the a posteriori distribution density of parameter μ is expressed as:

$$P\left(\mu \mid \sigma_{\text{вт\_ср}}, S\right) \sim P\left(\mu\right) \cdot g\left(\sigma_{\text{вт\_ср}} \mid \mu, S\right), \tag{2}$$

where $\sigma_{\text{вт\_ср}}$ — not current, but average values of measured experimental value $\sigma_{\text{вт}}$, and μ, S — their mathematical expectation and standard deviation, respectively.

In this case, $P(\mu \mid \sigma_{\text{вт\_ср}}, S)$ will also have a normal form, and the a posteriori estimate of variance $D[\mu]$ will take the form [20]:

$$D\left[\mu\right] = \frac{\dfrac{S_a^2 S_t^2}{n}}{S_a^2 + \dfrac{S_t^2}{n}}, \tag{3}$$

where S^2_a — respectively, the standard deviations of the average value of a random measured value from μ and μ from μ_a; μ_a — mathematical expectation μ; n — required number of experimental data or a sufficient number of experimental S^2_t measurements from the condition of minimal risk from estimation error. Therefore

$$n = \frac{S_t^2\left(S_a^2 - D\left[\mu\right]\right)}{S_a^2 \cdot D\left[\mu\right]}. \tag{4}$$

Let us note that in formula S^2_t and S^2_a, have a priori information, the a posteriori information is expressed in a posteriori variance $D[\mu]$ and the number of necessary experimental measurements n.

The work investigated the material of tube steel, which was intended for the construction of sheet pile screen for a construction pit.

Research Results. The procedure proposed above was based on the use of similar information about the mechanical properties of sheet pile pipes obtained during the examination of similar steel piles-pipes of the screen. During the initial examination, it was found that the tensile resistance of a sheet pile screen material was 418 MPa at 51 Gorsovetskaya Street.

The average value of the tensile strength of the metal of the batch of pipes examined earlier (at 23 Suvorov Street) was 405 MPa, which indicated that both batches of pipes belonged to approximately the same strength class. This information was used as a priori. Table 1 shows the values of tensile strength of the metal of the 11 pipes previously examined, ranked in ascending order.

Table 1

Values of tensile strength obtained by measurement on 11 pipes, MPa

393	399	402	408	417
394	399	402	408	418
394	399	402	409	418
394	399	402	411	418
395	400	403	411	419
396	400	403	411	420
396	400	404	412	420
396	400	405	412	421
396	400	405	412	425
396	400	405	412	426
396	400	405	412	426
396	400	405	412	427
397	400	406	413	427
397	401	406	413	430
397	401	406	414	430
397	401	407	414	435
398	401	407	415	436
398	401	407	416	436
398	402	407	416	
398	402	407	416	

Figure 1 shows the frequency of $n_{зн}$ values of tensile strength with standard deviation $S\sigma_в$ = 11.3 MPa and dispersion $S^2\sigma_в$ = 110 MPa^2.

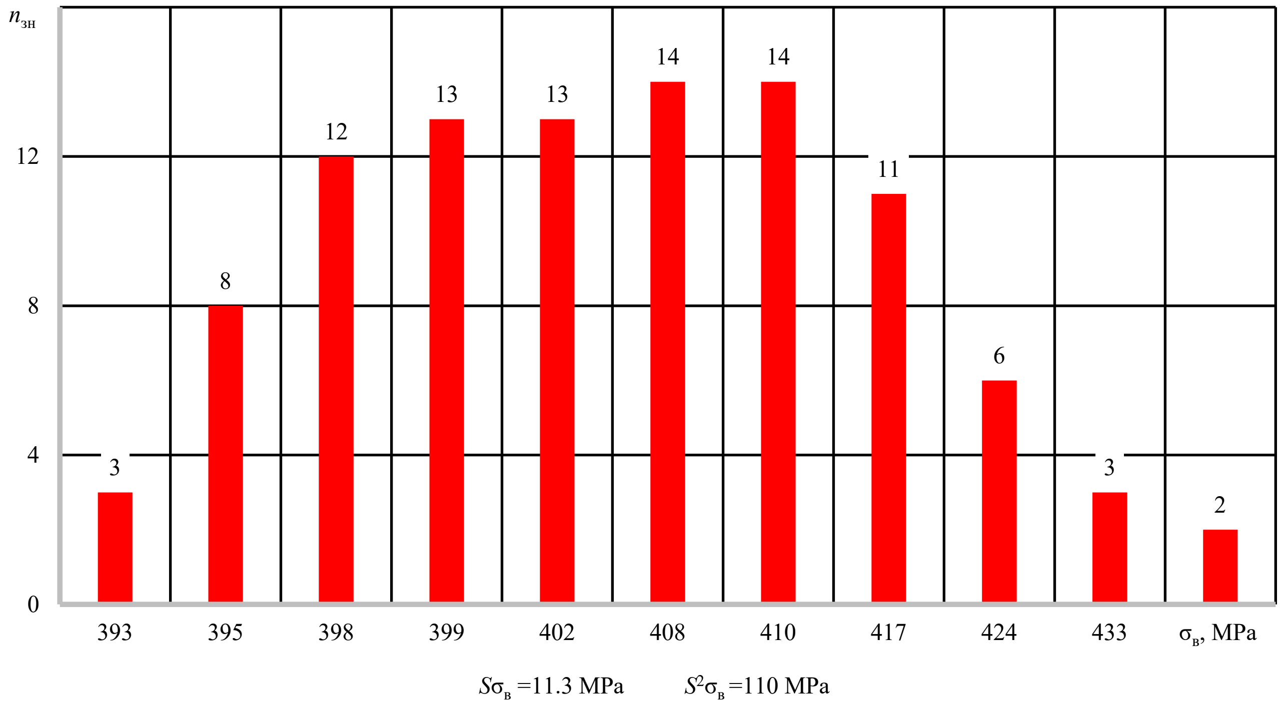

Fig. 1. Distribution of tensile strength values of metal pile pipes of sheet pile screen at Suvorov Street, 23 in Rostov-on-Don

Average values of tensile strength $\sigma_{Bср\_тр}$ for each of $m_{тр}$ pipes are shown in Figure 2 and Figure 3 — their distribution with average value $\sigma_{Bср}$ = 405 MPa, standard deviation $S\sigma_в$ = 3.6 MPa and dispersion $S^2\sigma_в$ = 14 MPa^2.

To calculate a sufficient sample size using formula (4), a posteriori variance $D[\mu]$ is determined as follows. For St3 steel of strength classes C255–C275, from which the pipe is made, a range of possible values of tensile strength[3] from 380 to 400 MPa is provided, i.e. based on the rule of three sigma of a normally distributed random variable, the permissible range of 20 MPa approximately corresponds to six standard deviations

Then a posteriori standard deviation will be expressed as (20/6) = 3.33 (MPa).

Since the reasoning concerns the average values of tensile strength, we can use the ratio of a priori standard deviations of current (110 MPa) and average (14 MPa) values of tensile strength, assuming that their ratio in the a posteriori estimate will remain approximately the same.

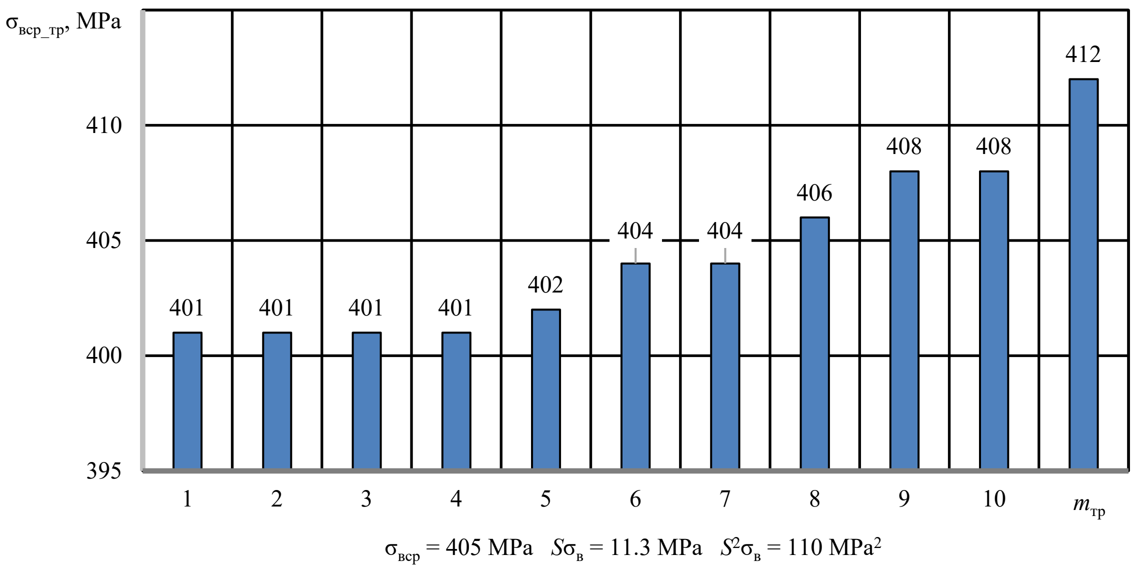

Fig. 2. Average values of tensile strength of metal of 11 pile pipes of sheet pile screen at Suvorov Street, 23 in Rostov-on-Don

[3] GOST 27772–88. *Rolled Products for Structural Steel Constructions. General Specifications*. (In Russ.) URL: https://docs.cntd.ru/document/1200003192 (accessed: 15.05.2024).

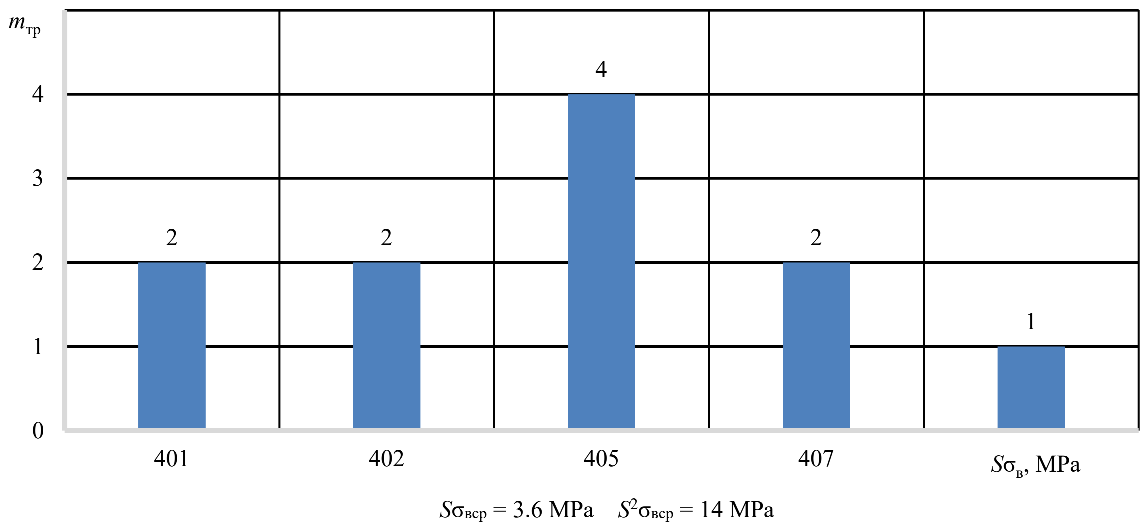

Fig. 3. Distribution of pipes with average value σ_{Bcp} = 405 MPa, standard deviation $S\sigma_B$ = 3.6 MPa and dispersion $S^2\sigma_B$ = 14 MPa^2

Thus, a posteriori variance of the average value of tensile strength can be determined:

$$D[\mu] = \frac{11 \cdot 14}{110} = \frac{11}{7.86} = 1.4 \text{ MPa}^2.$$

A priori variance of the average value of tensile strength:

$$S^2_t = S^2\sigma_{Bcp} = 14 \text{ MPa}.$$

The a priori variance of parameter μ of the distribution of the average value of tensile strength S^2_a is also assumed under the assumption that the ratio of S^2_t to S^2_a will remain the same (7.86). As a result of our research, we have determined the minimum number of elements that need to be examined — two or three pipe piles.

$$S_a^2 = \frac{14}{7.86} = 1.78 \text{ MPa},$$

$$n = \frac{S_t^2\left(S_a^2 - D[\mu]\right)}{S_a^2 \cdot D[\mu]} = \frac{14(1.78 - 1.4)}{1.78 \cdot 1.4} = 2.13.$$

Discussion and Conclusion. When solving the problem of minimizing the sample size for an experimental batch of pipe piles, a novel method of non-destructive testing based on indentation was employed. At the same time, mechanical characteristics obtained during the previous examination of 11 similar pile pipes were used as prior information. Due to the limited number of pile pipes available in the experimental batch for inspection, the use of Bayesian techniques made it possible to reduce the required sample size significantly to three, while minimizing the risk of error in the assessment.

The steels considered in the article for pipe manufacturing belong to the strength class KP 245. According to GOST 54157–10[4] they have a yield strength of 245 MPa and a temporary tensile strength of 412 MPa. These steels are mainly made from 3sp and 3ps steel. The same steels are widely used in the manufacturing of machine-building structures in lifting cranes, in the frames of tractors, trailers, semi-trailers, etc. For these structures, the approach described in the article also applies and is feasible. Thus, the use of a priori information based on Bayesian procedures for non-destructive testing of mechanical characteristics of low-carbon steels used in construction and machine-building structures allows us to justify the minimum required number of elements of the object of inspection, significantly reduce the volume, time, labor intensity, and cost of work.

[4] GOST 54157–10. *Profile Steel Pipes for Metal Constructions. Specifications.* (In Russ.) URL: https://docs.cntd.ru/document/1200084959 (accessed: 15.05.2024).

References

1. Bryushko VI. *Assessment of Metal Condition of Main and Technological Pipelines.* Author's abstract. Tolyatti; 2006. 19 p. (In Russ.)

2. Nikiforchin GN, Tsirul'nik OT, Zvirko OI, Gredil' MI, Voloshin VA. Degradation of the Physical and Mechanical Properties of Steels in Long-Run Gas Pipelines. *Industrial Laboratory. Diagnostics of Materials.* 2013;79(9):48–55. (In Russ.)

3. Gorynin IV, Timofeev BT. Degradation of Properties of Structural Materials at Long Time Influence of Operational Temperatures. *Voprosy Materialovedeniya.* 2011;1(65):41–59. (In Russ.)

4. Kiselev VV. Influence of High Temperatures on the Strength Properties of Metal Structures. *NovaInfo*. 2018;(82):9–12. (In Russ.) URL: https://novainfo.ru/article/14859 (accessed: 15.05.2024).

5. Pullin R, Holford KM, Lark RJ, Eaton MJ. Acoustic Emission Monitoring of Bridge Structures in the Field and Laboratory. *Journal of Acoustic Emission.* 2008;26:172–181. URL: https://www.ndt.net/article/ewgae2008/papers/136.pdf (accessed: 15.05.2024).

6. Anastasopoulos AA, Kourousis DA, Cole PT. Acoustic Emission Inspection of Spherical Metallic Pressure Vessels. In: *The 2nd International Conference on Technical Inspection and NDT.* Tehran, Iran: 2008. URL: http://www.ndt.net/article/tindt2008/papers/177.pdf (accessed: 15.05.2024).

7. Gongtian Shen, Zhanwen Wu. Study on Spectrum of Acoustic Emission Signals of Bridge Crane. *Insight - Non-Destructive Testing and Condition Monitoring.* 2010;52(3):144–148. URL: http://www.ndt.net/article/ecndt2010/reports/1_07_08.pdf (accessed: 15.05.2024).

8. Aljets D, Chong A, Wilcox S, Holford K. Acoustic Emission Source Location in Plate-Like Structures using a Closely Arranged Triangular Sensor Array. In: *Proceedings of the 29th European Conference on Acoustic Emission Testing EWGAE.* Vienna, September; 2010. P. 85–98.

9. Rhys P, Baxter M, Eaton M, Holford K, Evans S. Novel Acoustic Emission Source Location. *Journal of Acoustic Emission.* 2007;(25):194–214.

10. Rong Chen, Xiao Yang Li, Lin Lin Zhang, Xiang Yu Wang. Numerical Simulation of Spherical Indentation Method to Identify Metal Material Properties. *Advanced Materials Research.* 2015;(1119):779–782. http://doi.org/10.4028/www.scientific.net/AMR.1119.779

11. Syngellakis S, Habbab H, Mellor BG. Finite Element Simulation of Spherical Indentation Experiments. *International Journal of Computational Methods and Experimental Measurements.* 2018;6(4):749–763. http://doi.org/10.2495/CMEM-V6-N4-749-763

12. Matyunin VM, Marchenkov AYu, Karimbekov MA, Demidov AN, Volkov PV, Abusaif N, et al. Express Evaluation of Welded Joints Cool Resistance. *IOP Conference Series: Materials Science and Engineering.* 2020;759:012016. http://doi.org/10.1088/1757-899X/759/1/012016

13. Arseniev VN, Labetsky PV. A Method of Posterior Estimation of Characteristics of Flying Vehicle Control System. *Journal of Instrument Engineering.* 2014;57(10):23–28. (In Russ.) URL: https://pribor.ifmo.ru/en/article/10855/metod_aposteriornogo_ocenivaniya_harakteristik_sistemy_upravleniya_letatelnogo_apparata_.htm (accessed: 15.05.2024).

14. Kjærulff UB, Madsen AL. Bayesian. *Networks and Influence Diagrams: A Guide to Construction and Analysis.* Latest edition. New York: Springer VS; 2013. 382 p.

15. Boubekeur Baba, Güven Sevil. Bayesian Analysis of Time-Varying Interactions between Stock Returns and Foreign Equity Flows. *Financial Innovation.* 2021;7:51. https://doi.org/10.1186/s40854-021-00267-9

16. Paolucci I, Yuan-Mao Lin, Silva JAM, Brock KK, Odisio BC. Bayesian Parametric Models for Survival Prediction in Medical Applications. *BMC Medical Research Methodology.* 2023;23:250. https://doi.org/10.1186/s12874-023-02059-4

17. Chattopadhyay S, Davis RM, Menezes DD, Singh G, Acharya RU, Tamura T. Application of Bayesian Classifier for the Diagnosis of Dental Pain. *Journal of Medical Systems.* 2012;36:1425–1439. https://doi.org/10.1007/s10916-010-9604-y

18. Belen'kii DM, Vernezi NL, Cherpakov AV. Changes in the mechanical properties of butt welded joints in elastoplastic deformation. Welding International. 2004;18:213–215. https://doi.org/10.1533/wint.2004.3268

19. Vernezi NL. Variation Coefficient of Metal Yield Strength in New and Long-Used Building Structures. *Safety of Technogenic and Natural Systems.* 2023;7(3):44–54. (In Russ.) https://doi.org/10.23947/2541-9129-2023-7-3-44-54

20. Vernezi NL. Method of an Assessment of Durability of Metal in the Nondestructive Way with Use of Aprioristic Information. *Engineering journal of Don.* 2013;3(26):133. (In Russ.) URL: http://www.ivdon.ru/ru/magazine/archive/n3y2013/1898 (accessed: 15.05.2024).

About the Author:

Nikos L. Vernezi, Cand. Sci. (Eng.), Associate Professor of the Transport Systems and Logistics Department, Don State Technical University (1, Gagarin Sq., Rostov-on-Don, 344003, Russian Federation), SPIN-code, ORCID, vernezin@mail.ru

Conflict of Interest Statement: **the author does not have any conflict of interest.**

The author has read and approved the final version of manuscript.

Об авторе:

Никос Леонидович Вернези, кандидат технических наук, доцент кафедры эксплуатации транспортных систем и логистики Донского государственного технического университета (344003, Российская Федерация, г. Ростов-на-Дону, пл. Гагарина, 1), SPIN-код, ORCID, vernezin@mail.ru

Конфликт интересов: **автор заявляет об отсутствии конфликта интересов.**

Автор прочитал и одобрил окончательный вариант рукописи.

Received / Поступила в редакцию 20.09.2024
Revised / Поступила после рецензирования 04.10.2024
Accepted / Принята к публикации 15.10.2024

MACHINE BUILDING
МАШИНОСТРОЕНИЕ

UDC 62-192
https://doi.org/10.23947/2541-9129-2024-8-4-39-46

Original Theoretical Research

Fisher-Tippet Law Truncated Form for Loading Modeling of Machinery Structures

Anatoly A. Kotesov
Don State Technical University, Rostov-on-Don, Russian Federation
✉ a.kotesov@yandex.ru

EDN: OXXQDQ

Abstract

Introduction. Statistical data are used as a basis for assessing the reliability of engineering structures. However, incomplete data or inaccurate modeling of random variables may lead to an overestimation of reliability indicators. In practice, laws with infinitely decreasing or increasing distribution functions of an exponential family are usually used to model random variables characterizing the bearing capacity, load, and resource of engineering structures. To improve the accuracy of modeling of random variables, truncated forms of distribution laws are often used. These forms allow us to consider the random variable within a specified interval, excluding impossible values. Several studies have suggested using the Fisher-Tippett law with three parameters for modeling random variables related to the loading of engineering structures. The advantage of this law is that it limits the range of the random variable on the right side, but the left side of the distribution function decreases indefinitely, which is not ideal for load characteristics. To improve the accuracy of predicting random variables that characterize the load, it would be helpful to have a left-sided restriction using the Fisher-Tippett law. Currently, there are no descriptions of truncated forms of the distribution law in scientific literature. This article will explore the justification and development of a three-parameter truncated form of the Fisher-Tippett law and its use in calculation methods. The goal is to create a left-sided truncated version of the Fisher-Tippett distribution with three parameters to model random variables within a specific range.

Materials and Methods. The article provides a detailed description of the history of the Fisher-Tippet law, including its three-parameter form, and justifies the need for obtaining its truncated form.

Results. As a result of the research, a truncated form of the Fisher-Tippet three-parameter law in differential and integral forms was obtained and substantiated. The findings included graphs and calculations that demonstrated the normalization of a random variable within a given range.

Discussion and Conclusion. The conclusion was drawn about the advantages and disadvantages of the truncated form of the Fisher-Tippet law. The possibility of its practical application in the schematization of random loading processes under operating conditions and testing of machine elements and structures to assess fatigue life and determine fatigue resistance characteristics was established. The direction of further research is related to the practical use of the truncated form, particularly with the need to develop a method for evaluating the parameters of the truncated distribution and verifying the consistency of the proposed model.

Keywords: random variable, distribution law, truncated form, loading, reliability

Acknowledgements. The author would like to express his gratitude to the reviewers for their critical assessment of the submitted materials and their suggestions for improvement. These comments have contributed significantly to the enhancement of the quality of the presentation of the research results presented in this paper.

For citation. Kotesov AA. Fisher-Tippet Law Truncated Form for Loading Modeling of Machinery Structures. *Safety of Technogenic and Natural Systems.* 2024;8(4):39–46. https://doi.org/10.23947/2541-9129-2024-8-4-39-46

Оригинальное теоретическое исследование

Усеченная форма закона Фишера-Типпета для моделирования нагруженности машиностроительных конструкций

А.А. Котесов

Донской государственный технический университет, г. Ростов-на-Дону, Российская Федерация

✉ a.kotesov@yandex.ru

Аннотация

Введение. Статистические данные служат основой для оценки показателей надежности машиностроительных конструкций. Неполнота таких данных или неточность при моделировании случайных величин могут стать причиной завышенной оценки при определении показателей надежности. На практике для моделирования случайных величин, характеризующих несущую способность, нагруженность, ресурс машиностроительных конструкций, обычно применяют законы с бесконечно убывающими или возрастающими функциями распределения экспоненциального семейства. Для повышения точности при моделировании случайных величин часто используют усеченные формы законов распределения, которые позволяют рассматривать случайную величину в заданном интервале, исключая тем самым область невозможных значений. В ряде работ для моделирования случайных величин, характеризующих нагруженность машиностроительных конструкций, предлагается использовать закон Фишера-Типпета с тремя параметрами. Преимуществом данного закона является параметр, ограничивающий область определения рассматриваемой случайной величины справа, но при этом левая часть фунции распределения бесконечно убывает, что не совсем корректно для характеристик нагруженности. Поэтому для повышения точности моледирования случайных величин, характеризующих нагруженность, законом Фишера-Типпета целесообразно иметь ограничение слева. В настоящий момент в научной литературе не представлено описание усеченных форм для закона распределения, поэтому в предлагаемой статье будут рассмотрены обоснование и получение усеченной формы закона Фишера-Типпета с тремя параметрами и последующее использование ее в расчетных методиках. В связи с этим цель автора — получение левосторонней усеченной формы закона Фишера-Типпета с тремя параметрами для моделирования случайных величин в заданном интервале.

Материалы и методы. В статье подробно описана история получения, представлено описание и отличительные особенности закона Фишера-Типпета с тремя параметрами, а также обоснована необходимость получения его усеченной формы.

Результаты исследования. В результате исследования обоснована и получена усеченная форма закона Фишера-Типпета с тремя параметрами в дифференциальном и интегральном виде. Представлены результаты вычислений и графики функций, подтверждающие нормировку случайной величины в заданном интервале.

Обсуждение и заключение. Сделан вывод о преимуществах и недостатках усеченной формы закона Фишера-Типпета. Определена возможность практического применения усеченного закона при схематизации случайных процессов нагружения, возникающих в условиях эксплуатации или испытаний элементов машин и конструкций для оценки усталостной долговечности и определения характеристик сопротивления усталости. Направление дальнейших исследований связывается с практическим применением усеченной формы, в частности с необходимостью разработки методики для оценки параметров усеченного закона и проверки согласия предложенной модели.

Ключевые слова: случайная величина, закон распределения, усеченная форма, нагруженность, надежность

Благодарности. Автор выражает благодарность рецензентам, чья критическая оценка представленных материалов и предложения по их совершенствованию способствовали значительному повышению качества изложения результатов исследования, представленных в настоящей статье.

Для цитирования. Котесов А.А. Усеченная форма закона Фишера-Типпета для моделирования нагруженности машиностроительных конструкций. *Безопасность техногенных и природных систем.* 2024;8(4):39–46. https://doi.org/10.23947/2541-9129-2024-8-4-39-46

Introduction. Ensuring the reliability of mechanical engineering structures remains a crucial task at the present time. Failure of load-bearing elements in these structures during operation can lead to dangerous situations and economic losses. Consequently, the issues of determining reliability indicators, as well as the development of methods for a more accurate and reliable assessment of these indicators, as well as related research, are undoubtedly important and relevant.

In particular, the works of Professor V.E. Kas'yanov [1] emphasize that a reliable car is not necessarily expensive or more expensive than a less reliable one. Low reliability can be caused by various factors. One possible cause of sudden failures is the imperfection of calculation methods and the incompleteness of statistical data used to assess reliability indicators [2].

In practice, the laws of distribution of an exponential family with infinitely decreasing distribution functions are usually used to model random variables characterizing the bearing capacity, load, and resource of machine-building structures. This is described in detail in the works of V.V. Moskvichev and M.A. Kovalev [3], I.A. Panachev and I.V. Kuznetsov [4], G.Sh. Khazanovich and D.S. Apryshkin [5]. To increase accuracy, truncated forms of distribution laws are usually used, which allow us to consider a random variable in a given interval, focusing on available statistical data to determine the appropriate boundaries. V.E. Kas'yanov, L.P. Shchulkin [6], D.B. Demchenko [7], A.A. Kotesova [8] have proposed using the Fisher-Tippett law with three parameters for modeling random variables characterizing the loading of machine-building structures. The advantage of this law is the parameter that limits the area of definition of the random variable in question on the right, but at the same time the left part of the distribution function decreases infinitely, which is not entirely correct for load characteristics. Therefore, in order to increase the accuracy of modeling random variables characterizing the load, it is advisable to have a restriction on the left by the Fisher-Tippett law. Truncated forms for the most commonly applied laws are known and used in computational methods[1]. However, there is currently no description of a truncated Fisher-Tipet law in scientific literature. Therefore, this article addresses the issue of substantiating and obtaining a truncated form of the Fisher-Tippett law with three parameters and its subsequent use in calculation methods.

Materials and Methods. When modeling random variables, the Gaussian distribution (normal law) is most often used, and this is largely justified [9]. The limits of determining random variables in this model are set by the interval (–∞; ∞), which is not entirely correct for the characteristics of strength, load, and resources. Therefore, for modeling such random variables in the works of V.E. Kas'yanov, it is proposed to use the Weibull model with three parameters, which differs from the Gaussian model and the two-parameter Weibull in that it sets a slightly different interval for a random variable [c; ∞), where c is the shift parameter that determines the minimum value of a random variable, i.e. it has a restriction on the left.

The density function of the distribution of Weibull's law with three parameters defines the expression:

$$f\left(x\,|\,a,b,c\right)=\frac{b}{a}\left(\frac{x-c}{a}\right)^{b-1}e^{-\left(\frac{x-c}{a}\right)^{b}}, \tag{1}$$

where x — value of a random variable; a, b, c — parameters of scale, shape and shift of the distribution, respectively.

It is also proposed to use one of the three limiting forms of distributions attributed to type III by R. Fisher and K. Tippett to model the load characteristics. The distributions of Gumbel and Frechet were assigned to the first and second types, respectively [10].

The density function of the distribution of the third type defines the following expression:

$$f\left(x\,|\,k\right)=k\left(-x\right)^{k-1}e^{-\left(-x\right)^{k}}, \tag{2}$$

where x — value of a random variable; k — shape parameter.

It is obvious that this distribution is similar to the one-parameter Weibull distribution, which is also a special case of the generalized distribution of extreme values [11], only oriented to minimum values. By specifying the notation and adding additional parameters to expression (2) by analogy with the three-parameter Weibull's law, namely scale parameter — a and shift parameter (position) — c, we obtain the following expression for the distribution density function:

$$f\left(x\,|\,a,b,c\right)=\frac{b}{a}\left(\frac{c-x}{a}\right)^{b-1}e^{-\left(\frac{c-x}{a}\right)^{b}}, \tag{3}$$

where x — value of a random variable; a, b, c — the parameters of scale, shape and shift of the distribution, respectively.

Integrating expression (3) with respect to x, we obtain the distribution function of the law:

$$F\left(x\right)=\int f\left(x\,|\,a,b,c\right)dx,$$

$$F\left(x\right)=e^{-\left(\frac{c-x}{a}\right)^{b}}. \tag{4}$$

The resulting expression is proposed to be called the Fisher-Tippett law with three parameters, which, unlike the Weibull law, has a restriction on the right and defines the domain of determination of a random variable in the interval (–∞;c].

[1] RTM 24.090.25-76 *Lifting cranes. Calculation of the probability of failure-free operation of the elements.* (In Russ.) URL: https://gostrf.com/normadata/1/4293827/4293827795.htm (accessed: 15.05.2024).

As you can see, the Fisher-Tippett law with three parameters does not have a restriction on the left. The assumption of this model, given by the interval (–∞;0], may contradict the physical meaning of the random variables under consideration. In particular, the interval [0;c] will be more correct for load characteristics. Therefore, it is necessary to define the left-hand truncated form of the Fisher-Tippett law.

To solve this problem, it is proposed to use an approach similar to the approach considered in [12] and [13] to obtain a right-sided truncated Weibull law.

Research Results. To obtain the left-hand truncated form of the Fisher-Tippett law, it is necessary to set a condition under which all values of random variable x will be greater than a certain predetermined value t, which, in turn, will determine the truncation point of the law on the left, i.e. $x \in [t;c]$. Let us suppose that X_t ($t \geq 0$) denotes a left-truncated random variable distributed according to the Fisher–Tippett law, such that $F_t = c - x \mid c - x \geq t$, where $x \in W(a, b)$, a, $b > 0$ and $c > t$. Since $t \geq 0$, the value of the integral of the distribution density function f (x) in the interval [t;c] will be less than in the interval [–∞;c]:

$$\int_t^c f\left(x \mid a,b,c\right) dx < \int_{-\infty}^c f\left(x \mid a,b,c\right) dx = 1.$$

Therefore, to obtain a truncated form, it is necessary to redistribute the random variable in the interval [–∞;t] by determining the normalizing coefficient dependent on t:

$$K_{[t;c]} \cdot \int_t^c f\left(x \mid a,b,c\right) dx = \int_{-\infty}^c f\left(x \mid a,b,c\right) dx,$$

$$K_{[t;c]} \cdot \int_t^c f\left(x \mid a,b,c\right) dx = 1,$$

$$K_{[t;c]} = \frac{1}{\int_t^c f\left(x \mid a,b,c\right) dx},$$

$$K_{[t;c]} = \frac{1}{F(c) - F(t)},$$

where $F(c)$ and $F(t)$ — distribution function of the Fisher-Tippett law with three parameters, respectively, for $x = c$ and $x = t$.

Therefore, the truncated distribution function will be determined by the following expression:

$$f_{[t;c]}(x \mid a,b,c) = K_{[t;c]} \cdot f\left(x \mid a,b,c\right),$$

$$f_{[t;c]}(x \mid a,b,c) = \frac{f\left(x \mid a,b,c\right)}{F(x=c) - F(x=t)},$$

since $F(c) = 1$, we get:

$$f_{[t;c]}(x \mid a,b,c) = \frac{f\left(x \mid a,b,c\right)}{1 - F(t)}.$$

As a result, we obtain a distribution density function for the left-hand truncated form of the Fisher-Tippett law with three parameters in the range [t;c]:

$$f_{[t;c]}(x \mid a,b,c) = \frac{\frac{b}{a}\left(\frac{c-x}{a}\right)^{b-1} e^{-\left(\frac{c-x}{a}\right)^b}}{1 - e^{-\left(\frac{c-t}{a}\right)^b}}, \tag{5}$$

where x — value of a random variable; a, b, c — parameters of scale, shape and shift of the distribution, respectively; t — truncation point of the distribution (the minimum possible value of a random variable).

Obviously, taking $t = 0$, we get the following expression for the interval $[0;c]$:

$$f_{[0;c]}(x\,|\,a,b,c)=\frac{\dfrac{b}{a}\left(\dfrac{c-x}{a}\right)^{b-1}e^{-\left(\frac{c-x}{a}\right)^{b}}}{1-e^{-\left(\frac{c}{a}\right)^{b}}}. \tag{6}$$

In order to demonstrate the result obtained, the distribution parameters ($a = 10$; $b = 2.5$; $c = 15$) are arbitrarily set, graphs of the distribution density functions of initial (3) and truncated form (6) of the Fisher-Tippett law are constructed (Fig. 1). According to the specified parameters, certain integrals from the initial density function are calculated (3) and density functions of the truncated form (6) in the intervals $(–\infty;c]$, $(–\infty;0]$, $[0;c]$ are calculated. The calculations were performed in the Mathcad 14.0.0.163 software package with an acceptable convergence $1\cdot10^{-5}$. Table 1 presents the calculation results.

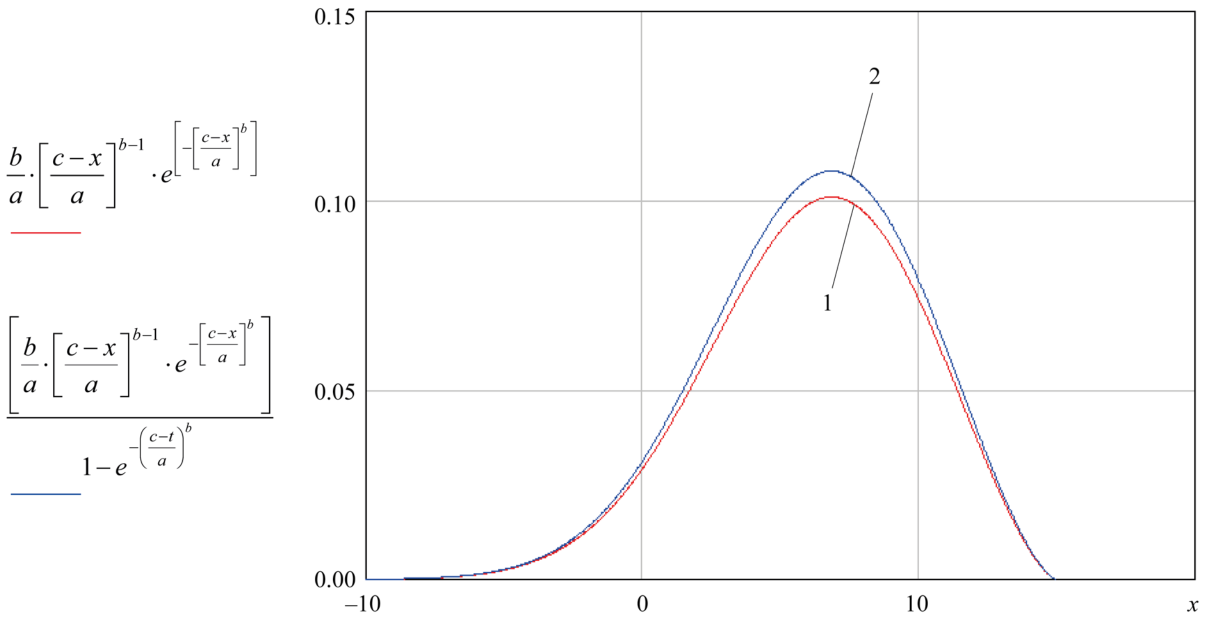

Fig. 1. Graphs of density distribution of the Fisher-Tippett law with three parameters ($a = 10$; $b = 2.5$; $c = 15$):
1 — initial density function; 2 — density function of the truncated law

Table 1

The results of calculating certain integrals from the density functions of the initial and truncated forms of the Fisher-Tippett law

Interval of a random variable	Limits of integration		Integration function and variable	
	lower	upper	$f\,(x\,|\,a,b,c)\,dx$	$f_{[0;c]}\,(x\,|\,a,b,c)\,dx$
$(–\infty;c]$	$–\infty$	c	0.99999999997581260	1.06788096063614480
$(–\infty;0]$	$–\infty$	0	0.06356603700150229	0.06788096066197107
$[0;c]$	0	c	0.93643395954036040	0.99999999631045600

The graphs of the functions in Figure 1 and the results of the numerical solution presented in Table 1 allow us to conclude that the analytically obtained distribution density function for the left-hand truncated form of the Fisher-Tippett law with three parameters (6) is correct and normalizes a random variable in the range $[0;c]$:

$$\int_0^c f_{[0;c]}\left(x\,|\,a,b,c\right)dx=1.$$

But at the same time, the function retains the definition area to the left of the truncation point, i.e. in the interval (–∞;0], which must be taken into account when using the truncated form of the law in calculation methods:

$$\int_{-\infty}^{0} f_{[0;c]}(x \mid a,b,c)\,dx + \int_{0}^{c} f_{[0;c]}(x \mid a,b,c)\,dx = \int_{-\infty}^{c} f_{[0;c]}(x \mid a,b,c)\,dx > 1.$$

To obtain the distribution function of the truncated Fisher-Tippett law, we integrate expression (5):

$$F_{[t;c]}(x) = \int f_{[t;c]}(x \mid a,b,c)\,dx,$$

$$F_{[t;c]}(x) = \frac{e^{-\left(\frac{c-x}{a}\right)^{b}}}{1-e^{-\left(\frac{c-t}{a}\right)^{b}}}. \qquad (7)$$

Graphs of initial (4) and truncated (7) distribution functions are shown in Figure 2.

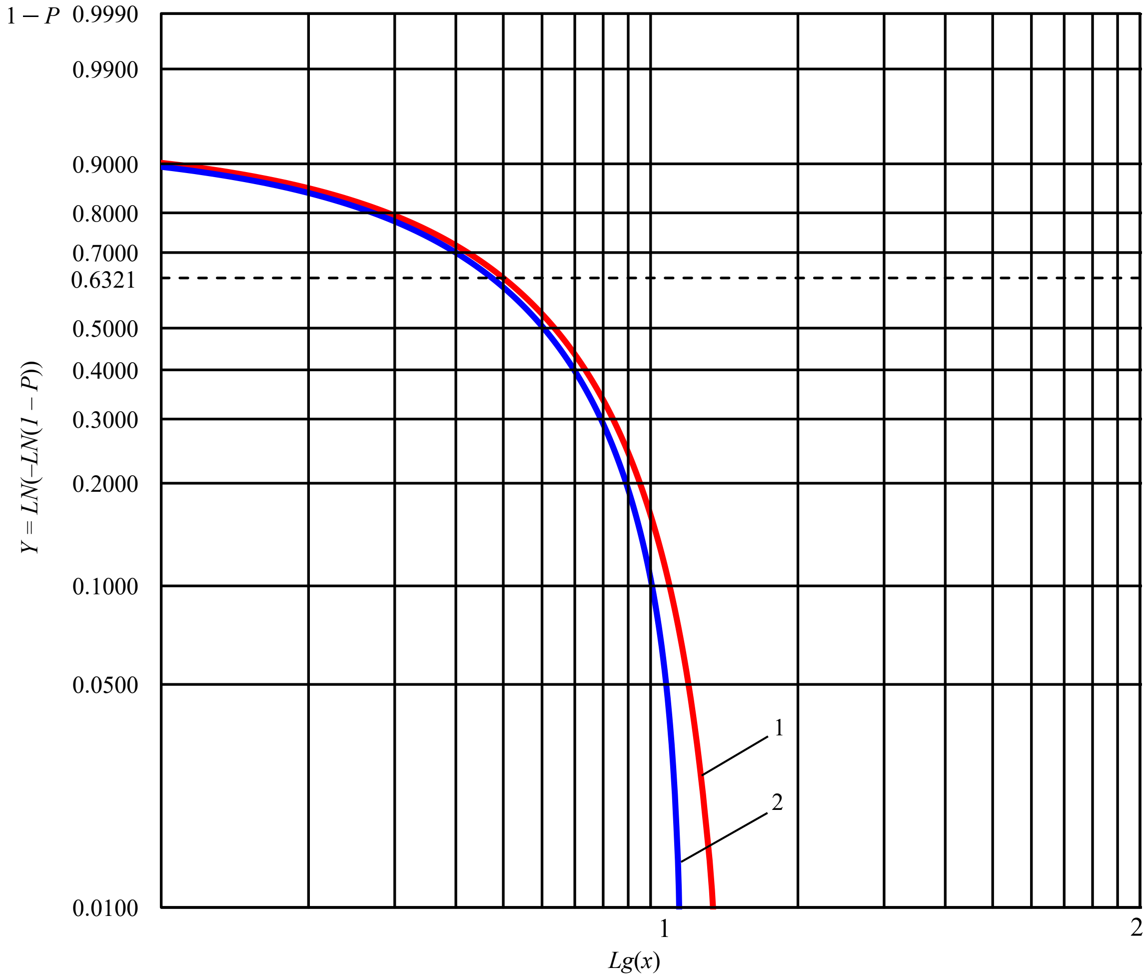

Fig. 2. Graphs of distribution functions of the Fisher-Tippett law with three parameters:
1 — original form; 2 — truncated form (t = 0); P — probability; x — random variable

From expression (7) we get the inverse function:

$$F^{-1}_{[t;c]}(x) = c - a\sqrt[b]{-ln\left(F_{[t;c]}(x)\cdot\left(1-e^{-\left(\frac{c-t}{a}\right)^{b}}\right)\right)}. \qquad (8)$$

Discussion and Conclusion. Thus, a left-sided truncated form of the Fisher-Tippett law with three parameters has been obtained, which can be used to schematize random loading processes that occur under operating conditions or tests of machine elements and structures according to GOST 25.101[2]. The use of the truncated form of the law makes it possible to

[2] GOST 25.101-83 *Strength calculation and testing. Representation of random loading of machine elements and structures and statistical evaluation of results.* (In Russ.) URL: https://docs.cntd.ru/document/1200012857 (accessed: 15.05.2024).

limit the interval of a random variable and exclude the area of impossible values to the left of the truncation point, which makes it possible to increase accuracy when using in computational methods for assessing the fatigue life of elements of mechanical engineering structures according to criteria for accumulation of fatigue damage, modeling the loading process during fatigue tests and calculating the characteristics of fatigue resistance. The calculation results shows that the distribution density function of the truncated law is correct and normalizes a random variable in a given interval, but at the same time retains the area of determination to the left of the truncation point, which is a disadvantage of the resulting model. Therefore, for the adequate application of the truncated law in calculation methods, it is necessary to introduce an appropriate restriction. The subject of future research is practical application of the truncated law, in particular, for statistical data processing, it is necessary to determine the methodology for estimating the parameters of the truncated law and determining confidence intervals. This includes obtaining expressions for estimating mathematical expectation and variance, as well as consider the possibility of using existing criteria of agreement.

References

1. Kasyanov VE. A Methodof Ensuringthe Absolute Reliability of Parts and Machines and Calculating the Increase of their Prices. *Engineering journal of Don*. 2016;1(40):19. (In Russ.)

2. Trukhanov VM. Prediction of the Life of Details, Units, Mechanisms, and the Devices in General at the Design Stage. *Journal of Machinery Manufacture and Reliability*. 2013;3:38–42. (In Russ.)

3. Moskvichev VV, Kovalev MA. Assessment of Operational Reliability Indicators of Mine Hydraulic Excavators. *Journal of Siberian Federal University. Engineering & Technologies.* 2020;13(6):745–756. (In Russ.) http://doi.org/10.17516/1999-494X-0263

4. Panachev IA, Kuznetsov IV. Substantiation of the Loading of Elements of Metal Structures of Heavy-Duty Dump Trucks during the Transportation of Rock Mass in the Kuzbass Sections. In: *Proceedings of the International Scientific and practical Conference "New Approaches to the Development of the Coal Industry"*. Кемерово; 2013. P. 61–64. (In Russ.)

5. Khazanovich GS, Apryshkin DS. Assessment of Load of Load-Bearing Elements of the Passenger Elevator Based on Regular Monitoring Results. *Safety of Technogenic and Natural Systems.* 2020;(1):32–42. (In Russ.) http://doi.org/10.23947/2541-9129-2020-1-32-42

6. Kasyanov VE, Schulkin LP. Determination of the Maximum Loading of Parts with the Help of Modeling. *Science Review*. 2014;10(3):671–674. (In Russ.)

7. Demchenko DB, Kasyanov VE. Optimization Method for Static Calculation of Construction Designs with the Use of Probabilistic Laws with Restrictions. *Engineering journal of Don*. 2013;2(25):84. (In Russ.)

8. Kotesov AA, Kasyanov VE, Kotesova AA. Model for Ensuring the Reliability of Metal Structures of Lifting Cranes during Their Service Period. *Vestnik Rostovskogo Gosudarstvennogo Universiteta Putey Soobshcheniya.* 2020;4(80):30–39. (In Russ.) http://doi.org/10.46973/0201-727X_2020_4_30

9. Horrace WC. Moments of the Truncated Normal Distribution. *Journal of Productivity Analysis.* 2015;43:133–138. https://doi.org/10.1007/s11123-013-0381-8

10. Fisher RA, Tippet LHC. Limiting Forms of the Frequency Distribution of the Longest of Smallest Member of Sample. *Mathematical Proceedings of the Cambridge Philosophical Society.* 1928;24(2),180–190. https://doi.org/10.1017/S0305004100015681

11. Bashir Ahmed Albashir Abdulali, Mohd Aftar Abu Bakar, Kamarulzaman Ibrahim, Noratiqah Mohd Ariff. Extreme Value Distributions: An Overview of Estimation and Simulation. *Journal of Probability and Statistics.* 2022:5449751. https://doi.org/10.1155/2022/5449751

12. Salman Abbas, Muhammad Farooq, Jumanah Ahmed Darwish, Saman Hanif Shahbaz, Muhammad Qaiser Shahbaz. Truncated Weibull–Exponential Distribution: Methods and Applications. *Scientific Reports.* 2023;13:20849. https://doi.org/10.1038/s41598-023-48288-x

13. Crénin F. Truncated Weibull Distribution Functions and Moments. *Journal of Productivity Analysis.* 2015;43:133–138. http://dx.doi.org/10.2139/ssrn.2690255

About the Author:

Anatoly A. Kotesov, Cand. Sci. (Eng.), Associate Professor of the Department of Operation of Transport Systems and Logistics, Don State Technical University (1, Gagarin Sq., Rostov-on-Don, 344003, Russian Federation), SPIN-code, ORCID, ScopusID, ResearcherID, a.kotesov@yandex.ru

Conflict of Interest Statement: **the author does not have any conflict of interest.**

The author has read and approved the final version of manuscript.

Об авторе:

Анатолий Анатольевич Котесов, кандидат технических наук, доцент кафедры эксплуатации транспортных систем и логистики Донского государственного технического университета (344003, Российская Федерация, г. Ростов-на-Дону, пл. Гагарина, 1), SPIN-код, ORCID, ScopusID, ResearcherID, a.kotesov@yandex.ru

***Конфликт интересов*: автор заявляет об отсутствии конфликта интересов.**

Автор прочитал и одобрил окончательный вариант рукописи.

Received / Поступила в редакцию 14.08.2024
Revised / Поступила после рецензирования 10.09.2024
Accepted / Принята к публикации 17.09.2024

CHEMICAL TECHNOLOGIES, MATERIALS SCIENCES, METALLURGY
ХИМИЧЕСКИЕ ТЕХНОЛОГИИ, НАУКИ О МАТЕРИАЛАХ, МЕТАЛЛУРГИЯ

Check for updates

UDC 621.793

Original Empirical Research

https://doi.org/10.23947/2541-9129-2024-8-4-47-53

Microarc Molybdenum Steel Saturation Using Ammonium Molybdate

EDN: AFQAPG

Makar S. Stepanov ✉, **Yuriy M. Dombrovskii**

Don State Technical University, Rostov-on-Don, Russian Federation

✉ stepanovms@yandex.ru

Abstract

Introduction. One of the most significant challenges in modern materials science is increasing the reliability and durability of tools and machine parts. To address this issue, it is essential to develop high-hardness coatings with enhanced properties. Typically, high-energy techniques are employed for this purpose, but they require complex and costly equipment, limiting their widespread use. Therefore, problem of creating such coatings remains a significant challenge. An effective and affordable approach to creating these coatings on steel products is microarc surface alloying from a coating pre-applied to the surface of the hardened products. The aim of the work was to assess the potential of diffusion molybdenum saturation for creating such coatings. Ammonium molybdate was used as the diffusant agent.

Materials and Methods. To achieve the aim of this study, we used thermodynamic analysis of chemical reactions that can occur within the temperature range of the microarc heating process. For each reaction, we calculated the change in standard Gibbs energy, which allowed us to determine the feasibility and range of occurrence. An experimental study of the microarc molybdenum saturation process was conducted using ammonium molybdate on steel 20 samples using a laboratory setup. The surface current density was set at 0.53 A/cm², and the duration of the process was 6 minutes.

Results. The Gibbs free energy changes for chemical reactions that can occur during the thermal decomposition of ammonium molybdate have been calculated. An experimental study has shown the formation of a molybdenum coating, and the concentration of molybdenum in the diffusion layer has been determined. On the surface of the samples, carbides Mo_2C and Fe_3Mo_3C have been found. The dependence of the coating depth on the content of diffusant in the coating and its thickness has been determined.

Discussion and Conclusion. Thermodynamic analysis has shown that atomic molybdenum can be formed through direct reduction or with the intermediate formation of molybdenum dioxide. The research has confirmed the formation of a diffusion coating on steel after microarc saturation with molybdenum, and the depth of this coating depends on the amount of diffusant in the coating and its thickness. These findings will be used to develop technological processes for microarc molybdenum plating of steel products.

Keywords: microarc surface alloying, diffusion molybdenum saturation, formation of a high-hardness coating

Acknowledgements. The authors would like to thank the Editorial team and the reviewers for their attention and valuable recommendations, which made it possible to improve the quality of the paper.

For citation. Stepanov MS, Dombrovskii YuM. Microarc Molybdenum Steel Saturation Using Ammonium Molybdate. *Safety of Technogenic and Natural Systems.* 2024;8(4):47–53. https://doi.org/10.23947/2541-9129-2024-8-4-47-53

Оригинальное эмпирическое исследование

Микродуговое молибденирование стали с использованием молибдата аммония

М.С. Степанов ✉, Ю.М. Домбровский
Донской государственный технический университет, г. Ростов-на-Дону, Российская Федерация
✉ stepanovms@yandex.ru

Аннотация

Введение. Одной из актуальных проблем современного материаловедения является повышение надежности и долговечности инструмента и деталей машин. Для ее решения целесообразно создание высокотвердых покрытий с повышенными эксплуатационными характеристиками. Как правило, для этого используется высокоэнергетическое воздействие на материал. Однако оно требует использования сложного и дорогостоящего оборудования и не получило широкого распространения. Поэтому в настоящее время проблема создания таких покрытий остается актуальной. Эффективным и недорогим методом создания таких покрытий на стальных изделиях является микродуговое поверхностное легирование из обмазки, предварительно наносимой на поверхность упрочняемых изделий. Целью работы являлась оценка возможности создания таких покрытий с помощью диффузионного молибденирования с использованием молибдата аммония в качестве источника диффузанта.

Материалы и методы. Для достижения цели исследования использовали термодинамический анализ химических реакций, протекание которых возможно в температурном диапазоне процесса микродугового нагрева. Для каждой реакции рассчитывали изменение стандартной энергии Гиббса, что позволило определить возможность и диапазон их протекания. Экспериментальное исследование процесса микродугового молибденирования с использованием молибдата аммония выполнено с использованием лабораторной установки на образцах из стали 20; поверхностная плотность тока составляла 0,53 А/см^2; продолжительность процесса — 6 минут.

Результаты исследования. Рассчитаны зависимости изменения свободной энергии Гиббса для химических реакций, протекание которых возможно при термическом разложении молибдата аммония. Экспериментально установлено формирование молибденированного покрытия и определена концентрация молибдена в диффузионном слое. На поверхности образцов обнаружены карбиды Mo_2C и Fe_3Mo_3C. Определена зависимость глубины покрытия от содержания диффузанта в обмазке и ее толщины.

Обсуждение и заключение. Анализ полученных уравнений показал возможность образования атомарного молибдена прямым восстановлением или через промежуточное образование диоксида. Результаты экспериментальных исследований подтвердили образование диффузионного покрытия на стали после микродугового насыщения молибденом. Глубина такого покрытия зависит от содержания диффузанта в обмазке и ее толщины. Полученные результаты могут быть использованы при разработке технологических процессов микродугового молибденирования стальных изделий.

Ключевые слова: микродуговое поверхностное легирование, диффузионное насыщение молибденом, формирование высокотвердого покрытия

Благодарности. Авторы благодарят сотру дников редакции и рецензентов за внимание, проявленное к публикации и ценные замечания, которые позволили улучшить ее содержание.

Для цитирования. Степанов М.С., Домбровский Ю.М. Микродуговое молибденирование стали с использованием молибдата аммония. *Безопасность техногенных и природных систем.* 2024;8(4):47–53. https://doi.org/10.23947/2541-9129-2024-8-4-47-53

Introduction. The formation of high-hardness coatings on steel products is one of the most important tasks of materials science [1]. Therefore, methods for obtaining coatings due to a highly concentrated energy flow to the material have been proposed, including laser treatment [2], plasma heating [3], electro-chemical thermal treatment [4], heating in an electrolyte [5], microarc oxidation [6], ion plasma treatment [7], electric spark alloying [8], and combinations of these techniques [9]. However, these methods are not widely used due to high energy consumption and the need to use complex and expensive equipment. Therefore, the problem of creating reinforcing coatings on steel products remains relevant.

An effective method of surface hardening is microarc alloying. In this process, the products are placed in a metal container filled with carbon powder, and an electric current is passed through the container. Microarc discharges occur between the product and the powder medium, which results in diffusion saturation of the steel surface with carbon and an alloying element [10]. This method accelerates diffusion processes and significantly reduces the duration of saturation compared to other methods. It also does not require complex and energy-intense equipment [11]. Microarc alloying can be used to create carbide coatings. The source of alloying elements is a coating applied to the treated surface [12]. Diffusion coatings can also be created by saturating the surface with molybdenum. For this purpose, inexpensive and widely available compounds can be used. For example, an inexpensive and complex microelement fertilizer — ammonium molybdate $(NH_4)_2MoO_4$ can be used. However, the possibility of using it in the composition of a coating can only be determined through thermodynamic analysis.

The aim of the study was to investigate the potential and conditions for using ammonium molybdate for surface molybdenum plating of steel.

Materials and Methods. To achieve the aim of the study, we used a thermodynamic analysis method. According to this method, the change in free energy of a chemical reaction was represented as the sum of enthalpies of formation of substances obtained as a result of reaction, minus the sum of the enthalpy of formation of the initial substances [13]. The possibility of a reaction was determined in the temperature range at which the Gibbs energy change had a negative value. This took into account the dependence of heat capacity on temperature [14]:

$$C_P = a_1 + b_1 \cdot T + d_1 \cdot T^{-2}. \quad (1)$$

Gibbs energy ΔG_T^0 was calculated as:

$$\frac{\Delta G_T^0}{T} = \frac{\Delta H_{298}^0}{T} - \Delta S_{298}^0 - \left(M_0 \Delta a + M_1 \Delta b + M_{-2} \Delta d \right), \quad (1)$$

where Δa, Δb, Δd — algebraic sums of coefficients a_1, b_1 and d_1 in formula (1); M_0, M_1 and M_2 — integral functions [13].

Table 1 presents the initial data [15] for calculations.

Table 1

Initial data for thermodynamic calculations

Substance	$-\Delta H^0_{298}$, kJ/mol	S^0_{298}, J/molK	C_{p298}, J/molK	$C_p = a_1 + b_1T + d_1T^{-2}$, J/mol		
				a	$b \cdot 10^3$	$d \cdot 10^{-5}$
C	0.000	5.744	8.540	17.170	4.270	–8.790
CO	110.600	197.680	29.130	28.430	4.100	–0.460
CO_2	393.777	213.820	37.140	44.170	9.040	–8.540
H_2	0.000	130.520	28.830	27.300	3.270	0.500
H_2O	241.990	188.850	33.599	30.020	10.720	0.330
CH_4	74.850	186.190	35.710	14.320	74.660	–17.430
Mo	0.000	28.600	24.100	21.670	6.950	–
MoO_2	589.100	46.280	55.980	67.800	12.600	–13.000
MoO_3	745.200	77.740	75.020	56.900	56.500	–
NH_3	45.940	192.660	35.630	29.800	25.480	–1.670
N_2	0.000	199.900	29.100	27.880	4.270	–
NO_2	33.500	240.200	37.500	42.160	9.550	–6.990

To experimentally verify the calculation results, microarc alloying of cylindrical steel samples with a diameter of 12 mm and a length of 35 mm was performed. An electrically conductive gel with the addition of ammonium molybdate powder was used to make the coating.

Microarc alloying was performed according to method [10], surface electric current density was 0.53 A/cm^2, heating duration was 6 minutes. After processing, the samples were sanded and polished according to the standard procedure, followed by etching with Rzheshotarsky reagent. A Neophot-21 microscope, an ARL X'TRA-435 diffractometer in Cu-Kα radiation, and a ZEISS CrossBeam 340 electron microscope with an Oxford Instruments X-max 80 microanalyzer were used for metallographic studies.

Research Results. When ammonium molybdate was heated, a reaction occurred:

$$(NH_4)_2MoO_4 = MoO_3 + H_2O + 2NH_3$$

During thermal decomposition of coal powder, gaseous substances were released [16], which could be reducing agents of atomic molybdenum according to schemes $MoO_3 \rightarrow Mo$ or $MoO_3 \rightarrow MoO_2 \rightarrow Mo$.

Chemical reactions and calculation results according to the above-described method are presented in Table 2. For each reaction, dependence ΔG_T^0 was calculated, the possibility (Yes/No) and the temperature range of the reaction during microarc heating were determined.

Table 2

Calculation results and the possibility of chemical reactions in the process of microarc heating

No.	Reaction	Dependence ΔG_T^0	Possibility of reaction
1	$MoO_3+3C=Mo+3CO$	383.100 – 0.490·T	Yes, > 509°C
2	$2MoO_3+3C=2Mo+3CO_2$	130.600 – 0.230·T	Yes, > 295°C
3	$MoO_3+C=MoO_2+CO$	33.500 – 0.147·T	Yes, the entire range
4	$2MoO_3+C=2MoO_2+CO_2$	–41.550 – 0.061·T	Yes, the entire range
5	$MoO_3+3CO=Mo+3CO_2$	–103.550 + 0.008·T	No
6	$MoO_3+CO=MoO_2+CO_2$	–134.760 + 0.026·T	No
7	$MoO_3+3H_2=Mo+3H_2O$	–24,830.000 – 61.180·T	Yes, the entire range
8	$4MoO_3+3CH_4=4Mo+3CO_2+6H_2O$	463,800.000 – 903.200·T	Yes, > 240°C
9	$4MoO_3+CH_4=4MoO_2+CO_2+2H_2O$	–221,800.000 – 238.200 T	Yes, the entire range
10	$3MoO_3+CH_4=3MoO_2+CO+2H_2O$	–86,300.000 – 263.800 T	Yes, the entire range
11	$7MoO_3+2NH_3=7MoO_2+2NO_2+3H_2O$	–258,000.000 + 554.200·T	Yes, < 190°C
12	$3MoO_3+2NH_3 \rightarrow 3MoO_2+N_2+3H_2O$	–446,900 + 143.800·T	Yes, the entire range
13	$MoO_2 + C = Mo + CO_2$	181.070 – 0.169 T	Yes, > 799°C
14	$MoO_2 + 2C = Mo + 2CO$	350.500 – 0.353 T	Yes, > 720°C
15	$MoO_2 + 2CO = Mo + 2CO_2$	76.050 – 0.094 T	Yes, > 536°C
16	$MoO_2 + 2H_2 = Mo + 2H_2O$	77,612.000 – 56.472 T	Yes, > 1,100°C

Thus, thermodynamic analysis confirmed the possibility of using ammonium molybdate as part of the coating during molybdenum plating. Reactions 1, 2, 7, 8 provided direct reduction, reactions 3, 4, 9, 10, 11, 12 — reduction with an intermediate stage of dioxide formation and further reactions 13, 14, 15, 16.

To experimentally verify the results obtained, microarc surface alloying of the samples was performed using a coating containing ammonium molybdate. The analysis of the samples confirmed the formation of a layer of α-solid molybdenum solution on their surface, followed by a zone with high carbon content and then the initial structure (Fig. 1).

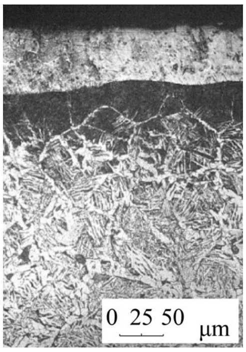

Fig. 1. Microstructure of the surface of steel 20 after saturation with molybdenum

Molybdenum content in steel by layer depth is shown in Figure 2.

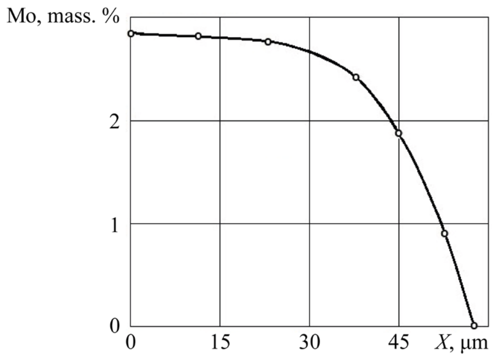

Fig. 2. Mo distribution by diffusion layer depth.
The content of the diffusant powder in the coating — 50%, its thickness — 1.0 mm

https://bps-journal.ru

The formation of Mo_2C and Fe_3Mo_3C carbides on the surface of the samples was established by X-ray phase analysis (Fig. 3).

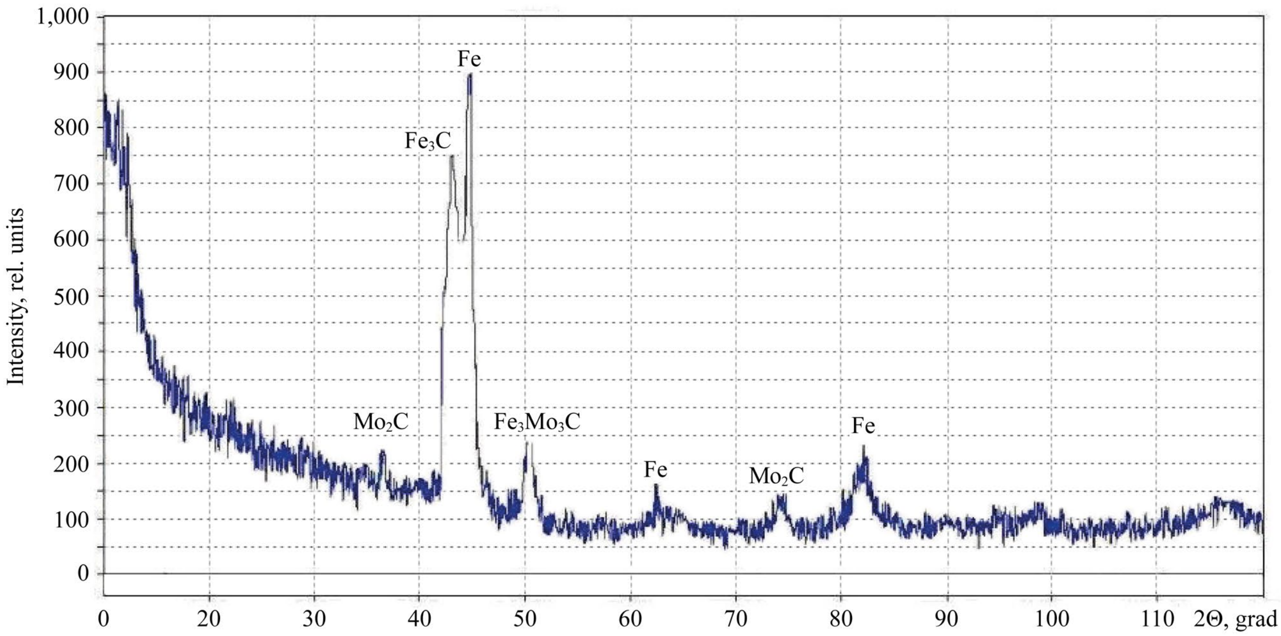

Fig. 3. X-ray diffractogram of the surface

Figure 4 shows the dependence of the coating thickness on the amount of diffusant powder in the coating.

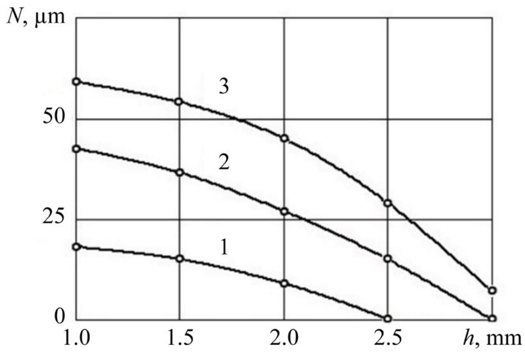

Fig. 4. Dependence of depth H of the diffusion layer on thickness h of the coating layer and the content of the diffusant powder: dependencies 1, 2, 3 correspond to 10; 30; 50 (vol. %)

To achieve the highest coverage, the diffusant content in the coating should be 50 vol. %, and the thickness of the coating layer on the treated surface should be 1 mm.

Discussion and Conclusion. The calculation results shows that a coating consisting of ammonium molybdate powder and a binder can be used for the process of microarc molybdenum plating of steel. As a result of microarc saturation, a molybdenum coating is formed, consisting of an α-solid solution of molybdenum with inclusions of carbides, then a carbonized zone is located, passing into the initial structure. The thickness of the coating is determined by the content of the diffusant in the coating and its thickness. The largest coating thickness (50–55 µm) was obtained at a diffusant content of 50 vol. % and coating thickness of 1 mm. The results of the study are planned to be used in the development of technological processes for microarc molybdenum plating of steel products.

References

1. Mittemeijer EJ, Somers MAJ. (eds). *Thermochemical Surface Engineering of Steels.* Woodhead Publishing; 2015. 827 p.

2. Liexin Wu, Li Meng, Yueyue Wang, Shuhuan Zhang, Wuxia Bai, Taoyuan Ouyang, et al. Effects of Laser Surface Modification on the Adhesion Strength and Fracture Mechanism of Electroless-Plated Coatings. *Surface and Coatings Technology*. 2022;429:127927. https://doi.org/10.1016/j.surfcoat.2021.127927

3. Zhen Huang, Zi-Xin Guo, Lei Liu, Yuan-Yuan Guo, Jun Chen, Ze Zhang, et al. Structure and Corrosion Behavior of Ultra-Thick Nitrided Layer Produced by Plasma Nitriding of Austenitic Stainless Steel. *Surface and Coatings Technology.* 2021;405:126689. https://doi.org/10.1016/j.surfcoat.2020.126689

4. Czerwinski F. Thermochemical Treatment of Metals. In book: *Heat Treatment – Conventional and Novel Applications.* London: InTechOpen; 2012. 422 p. https://doi.org/10.5772/51566

5. Belkin PN, Kusmanov SA. Plasma Electrolytic Carburising of Metals and Alloys. *Surface Engineering and Applied Electrochemistry.* 2021;57(1):19–50. https://doi.org/10.3103/S1068375521010038

6. Venugopal A, Rajiv Panda, Sushant Manwatkar, Sreekumar K, Rama Krishna L, Sundararajan G. Effect of Microarc Oxidation Treatment on Localized Corrosion Behavior of AA7075 Aluminum Alloy in 3.5% NaCl Solution. *Transactions of Nonferrous Metals Society of China.* 2012;22(3):700–710. https://doi.org/10.1016/S1003-6326(11)61234-X

7. Nie X, Tsotsos C, Wilson A, Yerokhin AL, Leyland A, Matthews A. Characteristics of a Plasma Electrolytic Nitrocarburising Treatment for Stainless Steels. *Surface and Coatings Technology.* 2001;139(2–3):135–142. https://doi.org/10.1016/S0257-8972(01)01025-8

8. Wang RJ, Qian YY, Liu J. Structural and Interfacial Analysis of WC92–Co8 Coating Deposited on Titanium Alloy by Electrospark Deposition. *Applied Surface Science.* 2024;228(1–4):405–409. https://doi.org/10.1016/j.apsusc.2004.01.043

9. Aleksandrov VA, Petrova LG, Sergeeva AS, Aleksandrov VD, Akhmetzhanova EU. Combined Plasma Methods of Chemical and Thermal Treatment to Create Modified Coatings on the Instrument. *STIN.* 2019;(3):13–16. (In Russ.)

10. Stepanov MS, Dombrovskii YuM, Davidyan LV. Structure, Phase Composition, Mechanical Properties and Wear Resistance of Steel after Microarc Boriding and Vanadation. *Izvestiya. Ferrous Metallurgy.* 2019;62(6):446–451. (In Russ.) https://doi.org/10.17073/0368-0797-2019-6-446-451

11. Stepanov MS, Dombrovskiy YuM. Deposition of Carbide-Type Coatings during Micro-Arc Thermodiffusion Tungstening of Steel. *Material Science.* 2018;(1):20–25. (In Russ.)

12. Stepanov M.S., Dombrovskii Yu.M., Pustovoit V.N. Diffusion Saturation of Carbon Steel under Microarc Heating. *Metal Science and Heat Treatment.* 2017;59(1–2):55–59. https://doi.org/10.1007/s11041-017-0102-4

13. Ponomarev SV, Mishchenko S, Divin A, Vertogradskii V, Churikov A. *Theoretical and Practical Foundations of Thermophysical Measurements.* Ponomarev SV. (ed.). Moscow: FIZMATLIT; 2008. 408 p. (In Russ.)

14. Isaev SI, Kozhinov IA, Kofanov VI, Leontev AI, Mironov BM, Nikitin VM, et al. *The Theory of Heat and Mass Transfer.* Leontev AI (ed.). Moscow: Publishing House of Bauman Moscow State Technical University; 2018. 462 p. (In Russ.)

15. Lidin RA (ed.), Molochko VA, Andreeva LL. *Constants of Inorganic Substances: Reference Book.* 3d ed., ster. Moscow: Drofa; 2006. 685 p. (In Russ.)

16. Gyulmaliev AM, Golovin G., Gladun TG. *Theoretical Foundations of Coal Chemistry.* Moscow: MSUH; 2003. 556 p. (In Russ.)

About the Authors:

Makar S. Stepanov, Dr.Sci. (Eng.), Professor of the Quality Management Department, Don State Technical University (1, Gagarin Sq., Rostov-on-Don, 344003, Russian Federation), SPIN-code, ORCID, ScopusID, ResearcherID, stepanovms@yandex.ru

Yuriy M. Dombrovskii, Dr.Sci. (Eng.), Professor of the Materials Science and Technologies of Metals Department, Don State Technical University (1, Gagarin Sq., Rostov-on-Don, 344003, Russian Federation), SPIN-code, ORCID, ScopusID, yurimd@mail.ru

Claimed Contributorship:

MS Stepanov: collection of initial data for thermodynamic calculations, carrying out thermodynamic calculations, analysis of the results obtained.

YuM Dombrovsky: experimental studies, determination of technological parameters of the surface alloying process, analysis of the results obtained.

Conflict of Interest Statement: **the authors do not have any conflict of interest.**

All authors have read and approved the final manuscript.

Об авторах:

Макар Степанович Степанов, доктор технических наук, профессор кафедры управления качеством Донского государственного технического университета (344003, Российская Федерация, г. Ростов-на-Дону, пл. Гагарина, 1), SPIN-код, ORCID, ScopusID, ResearcherID, stepanovms@yandex.ru

Юрий Маркович Домбровский, доктор технических наук, профессор кафедры материаловедения и технологии металлов Донского государственного технического университета (344003, Российская Федерация, г. Ростов-на-Дону, пл. Гагарина, 1), SPIN-код, ORCID, ScopusID, yurimd@mail.ru

Заявленный вклад соавторов:

М.С. Степанов: сбор исходных данных для термодинамических расчетов, проведение термодинамических расчетов, анализ полученных результатов.

Ю.М. Домбровский: экспериментальные исследования, определение технологических параметров процесса поверхностного легирования, анализ полученных результатов.

Конфликт интересов: **авторы заявляют об отсутствии конфликта интересов.**

Все авторы прочитали и одобрили окончательный вариант рукописи.

Received / Поступила в редакцию 29.08.2024
Revised / Поступила после рецензирования 16.09.2024
Accepted / Принята к публикации 25.09.2024

CHEMICAL TECHNOLOGIES, MATERIALS SCIENCES, METALLURGY
ХИМИЧЕСКИЕ ТЕХНОЛОГИИ, НАУКИ О МАТЕРИАЛАХ, МЕТАЛЛУРГИЯ

Check for updates

UDC 669.1:66.04

Original Empirical Research

https://doi.org/10.23947/2541-9129-2024-8-4-54-61

Formation of Residual Stress Diagram after Quenching in a Magnetic Field

Viktor N. Pustovoit, Yuri V. Dolgachev ✉

Don State Technical University, Rostov-on-Don, Russia

✉ yuridol@mail.ru

EDN: AKVGXS

Abstract

Introduction. After hardening, a product has residual stresses: structural and thermal. The magnitude of the total stresses in the finished part determines its crack resistance under the influence of operational loads. Quenching in a constant magnetic field affects the process of martensite nucleation, and the kinetics of martensite transformation, as well as the processes of martensite decomposition. However, there is currently no data available on how these changes in structure affect the stress diagram in a heat-treated product. The aim of this study was to investigate the influence of a constant magnetic field during hardening of iron-carbon alloys on the stress distribution across the cross-sectional area of parts.

Materials and Methods. The studies were conducted on samples of technical iron, steel 45, and ferritic malleable cast iron. Cylindrical samples with a diameter of 16 mm and ring samples with an outer diameter of 20 and 55 mm were used. The samples were heated in an electric furnace or an induction heating lamp generator LZ-13, and quenched in water or mineral oil. A constant magnetic field with strength of 768 to 1600 kA/m during hardening was created in the bore of a FL-1 electromagnet. Residual stresses were determined using the original method developed by V.A. Blinovskii based on measuring bending deformations in hollow bodies of revolution.

Results. The change in temperature on the surface, in the core, and the temperature difference across the cross-section of a cylindrical sample during cooling in water with and without a magnetic field was obtained. The distribution of stresses over the cross-section after quenching with and without a field for industrial iron in still water was studied. The stress distribution over the cross-section was studied after quenching in a field and without a field in calm water, as well as during spray cooling of steel 45 and ferritic ductile cast iron at different rates.

Discussion and Conclusion. The obtained calculated and experimental data allowed us to evaluate possible changes in the residual stress diagrams under the influence of a magnetic field after quenching with volumetric and surface heating. A study of the kinetics of cooling in water under the influence of a magnetic field showed that the temperature difference across the cross-section remained practically unchanged, but there was a decrease in the cooling capacity of the water, which contributed to a reduction in the level of thermal stress. Hardening in a magnetic field led to a reduction of residual stresses in iron-carbon alloys. The change in the distribution of total residual stresses during magnetic tempering was due to a change in their structural component. The magnetic field influenced the distribution of structural, thermal and total residual stresses. The reason for the observed effects was the change in the structural state of steel and cast iron and the cooling ability of water-based quenching liquids under the influence of a magnetic field. The reduction of the level of residual stresses during heat treatment in a magnetic field reduced the likelihood of brittle fracture and cracking, led to a decrease in deformation and warping of hardened steels, and created favorable conditions for the operation of parts under conditions of alternating loads and abrasive friction.

Keywords: hardening, steel, cast iron, residual stresses, magnetic field, structural stresses, thermal stresses

Acknowledgements. The authors would like to express their gratitude to the Editorial team of the Journal for their valuable comments and to the staff of the Department of Materials Science and Technology of Metals at Don State Technical University, particularly Head of the Department M.S. Egorov, Professor Yu.M. Dombrovsky and Associate Professor S.A. Grishin, for their assistance in obtaining and reviewing the results.

For citation. Pustovoit VN, Dolgachev YuV. Formation of Residual Stress Diagram after Quenching in a Magnetic Field. *Safety of Technogenic and Natural Systems.* 2024;8(4):54–61. https://doi.org/10.23947/2541-9129-2024-8-4-54-61

Оригинальное эмпирическое исследование

Формирование эпюры остаточных напряжений после закалки в магнитном поле

В.Н. Пустовойт, **Ю.В. Долгачев**

Донской государственный технический университет, г. Ростов-на-Дону, Российская Федерация

yuridol@mail.ru

Аннотация

Введение. После закалки в изделии имеются остаточные напряжения: структурные и тепловые. Величина суммарных напряжений в готовой детали определяет её трещиностойкость под действием эксплуатационных нагрузок. Закалка в постоянном магнитном поле оказывает влияние на процесс зарождения мартенсита, кинетику мартенситного превращения, а также процессы распада мартенсита. В настоящее время отсутствуют данные о том, как указанные изменения в структуре влияют на эпюру напряжений в термически обработанном изделии. Цель работы — исследование влияния постоянного магнитного поля при закалке железоуглеродистых сплавов на распределение напряжений по сечению деталей.

Материалы и методы. Исследования проводили на образцах технического железа, стали 45 и ферритного ковкого чугуна. Применялись цилиндрические образцы диаметром 16 мм и кольцевые образцы с наружным диаметром 20 и 55 мм. Образцы нагревали в электропечи или индукционным нагревом токами высокой частоты от лампового генератора ЛЗ-13. Закалку проводили в воде или минеральном масле. Постоянное магнитное поле напряжённостью от 768 до 1600 кА/м при закалке создавалось в зазоре электромагнита ФЛ-1. Определение остаточных напряжений осуществлялось по оригинальной методике В.А. Блиновского, основанной на измерении деформации изгиба в полых телах вращения.

Результаты исследования. Получено изменение температуры на поверхности, в сердцевине и перепад температур по сечению цилиндрического образца при охлаждении в воде без поля и в магнитном поле. Изучено распределение напряжений по сечению после закалки в поле и без поля технического железа в спокойной воде. Исследовано распределение напряжений по сечению после закалки в поле и без поля в спокойной воде, а также при спреерном охлаждении с различной скоростью стали 45 и ферритного ковкого чугуна.

Обсуждение и заключение. Полученные расчетные и экспериментальные данные позволили оценить возможные изменения под действием магнитного поля эпюр остаточных напряжений после завалки с объемным и поверхностным нагревом. Исследование кинетики охлаждения в воде под действием магнитного поля показало, что перепад температуры по сечению оставался практически неизменным, но наблюдалось снижение охлаждающей способности воды, что способствовало снижению уровня тепловых напряжений. Закалка в магнитном поле способствовала снижению остаточных напряжений в железоуглеродистых сплавах. Изменение распределения суммарных остаточных напряжений при магнитном отпуске обусловлено изменением их структурной составляющей. Магнитное поле оказывает влияние на распределение структурных, тепловых и суммарных остаточных напряжений. Причиной наблюдаемых эффектов является изменение под действием магнитного поля структурного состояния стали и чугуна и охлаждающей способности закалочных жидкостей на водной основе. Снижение уровня остаточных напряжений при термической обработке в магнитном поле уменьшает вероятность хрупкого разрушения и трещинообразования, приводит к снижению деформаций и коробления закаленных сталей, создает благоприятные условия для работы деталей в условиях знакопеременных нагрузок и абразивного трения.

Ключевые слова: закалка, сталь, чугун, остаточные напряжения, магнитное поле, структурные напряжения, тепловые напряжения

Благодарности. Авторы благодарят редакцию журнала за ценные замечания и сотрудников кафедры «Материаловедение и технологии металлов» ДГТУ: заведующего кафедрой М.С. Егорова, профессора Ю.М. Домбровского и доцента С.А. Гришина за помощь в получении и обсуждении результатов

Для цитирования. Пустовойт В.Н., Долгачев Ю.В. Формирование эпюры остаточных напряжений после закалки в магнитном поле. *Безопасность техногенных и природных систем.* 2024;8(4):54–61. https://doi.org/10.23947/2541-9129-2024-8-4-54-61

Introduction. Residual stresses after quenching are usually divided into two main categories: structural [1, 2] and thermal [3, 4]. Thermal stresses arise from the simultaneous influence of two factors: changes in the specific volume of the metal with temperature and the presence of a temperature gradient in the product undergoing heat treatment. Structural stresses are caused by dilation effects from phase transitions, especially when phase transformations occur inhomogeneously throughout the volume of a part. Thus, the resulting stresses in a processed product are formed through the addition of structural and thermal stress. It is known [5, 6], that the main factor determining the magnitude of stress after quenching is the moment when the sign of thermal stresses changes relative to the moment when structural stresses occur. The appearance of structural stresses prior to changing the sign of thermal stresses leads to an increase in the resulting stresses in the product. Accordingly, the occurrence of structural stresses before the sign of thermal stresses changes lowers the total stresses. The magnitude of the total stresses in a finished part determines the reliability of machine-building products during operation [7, 8]. The influence of a constant magnetic field during quenching of steels and cast irons is manifested through the process of martensite nucleation, changes in the kinetics of martensite transformation, as well as changes in tempering processes occurring directly during quench cooling. It is currently unknown how a magnetic field affects the residual stress in a heat-treated product. The aim of this work is to investigate the influence of a constant magnetic field during iron-carbon alloy quenching on the stress distribution over the section of parts.

Materials and Methods. In this work, samples of technical iron, steel 45, and ferritic ductile iron were studied. Cylindrical samples with a diameter of 16 mm and annular samples with outer diameters of 20 and 55 mm were used. The samples were heated in an electric furnace or by induction heating using high-frequency currents from a lamp generator LZ-13. During quenching, a constant magnetic field with strengths ranging from 768 to 1,600 kA/m was created in the FL-1 bore of the electromagnet.

The determination of residual stresses was carried out according to the original methodology developed by V.A. Blinovskii [9]. This technique is based on measuring bending deformation in hollow rotational bodies. It provided for cutting out an annular sector from a sample and measuring the resulting diameter changes. The resulting deformation curve served as the initial input for calculating residual stresses using a computer.

Research Results and Discussion. When quenching steel, the temperature gradient, which caused inhomogeneous changes in specific volume over the cross-section of the part, influenced the formation of a residual stress diagram. With a significant temperature difference between the surface and the core at the time of martensitic transformation (such as during through-quenching with water cooling after heating in a furnace), compressive tangential and axial stresses developed on the surface of a solid cylinder. Conversely, quenching in oil, where the temperature difference between core and surface was minimal at the time of martensitic transformation, resulted in tensile stresses on the surface. In this case, the stress diagram developed in the following manner. Rapid cooling of the surface caused volume reduction, but a higher temperature persisted within, counteracting volume decrease and leading to tensile stress in the outer layer. At the same time, plastic deformation of the outer layers was possible up to temperatures $T_{упр}$(~500–550°C). With further cooling, plasticity decreased, σ_T increased and only elastic deformations remained possible, which led to an increase in tensile stresses. Their growth continued until the cooling of inner layers, which shifted the maxima of tensile stresses to the center and slightly reduced surface tensile stresses. With a sufficient heating depth (almost more than 2 mm), the reduction in the volume of central layers led not only to the complete elimination of initial tensile stresses, but also to the appearance of compressive stresses on the surface, which persisted after the end of cooling.

When surface layers were cooled to point $M_н$, the quenching process led to an increase in volume. At the same time, inner layers that did not undergo hardening prevented this increase, which formed tensile stresses in the inner layers and compressions in the surface layers. As the quenching front moved away from the surface, the compressive stresses decreased and their maximum shifted to the center. As a result, after quenching, the stresses on the surface might have a different sign (although they might remain unchanged). The magnitude of compressive stresses in the surface layer increased with decreasing depth of the hardened layer.

Figure 1 shows the results of the study on the kinetics of cooling in water of a 16 mm diameter sample made of armco-iron. As can be seen, when a magnetic field was applied, the temperature drop across the cross-section of the samples remained almost unchanged, however, time dependence Δt shifted towards longer cooling durations. This was due to a decrease in the cooling capacity of water in a magnetic field [10, 11] and contributed to more intense stress relaxation by plastic deformation, as a result of which a decrease in the level of thermal stresses was observed (Fig. 2). Consequently, a magnetic field during quenching affected the formation of both structural and thermal components of residual stresses.

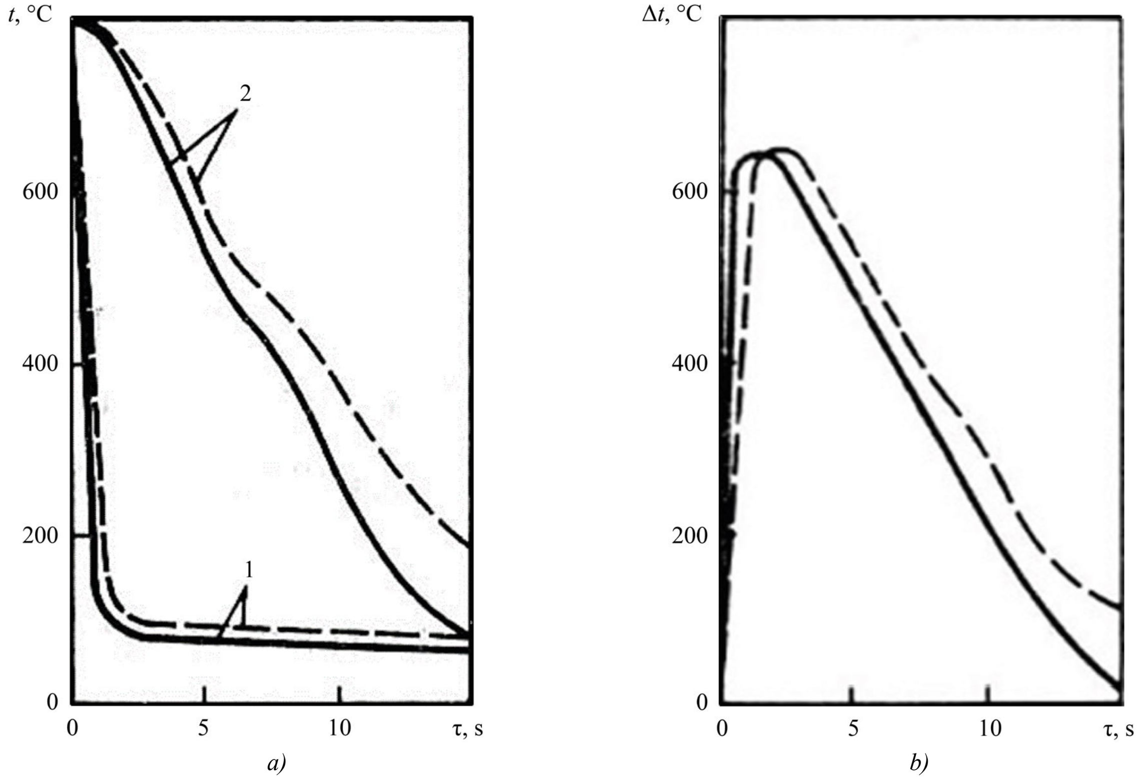

Fig. 1. Temperature changes in a cylindrical sample during cooling in water:
solid line — without a field; dashed line — in a magnetic field with a strength of 1.6 MA/m;
a — on surface 1 and in core 2; *b* — difference in cross section

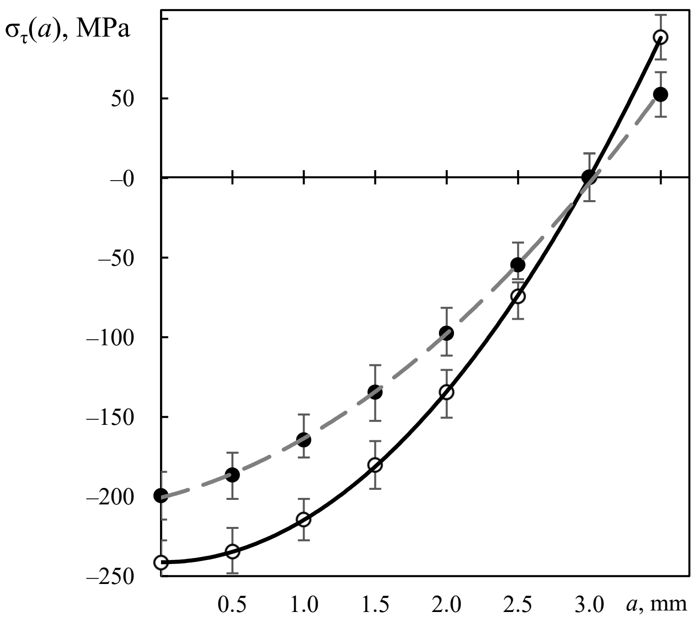

Fig. 2. Stress distribution over the cross section after quenching of technical iron from 800°C in calm water:
solid line — without a field; dashed line — in a magnetic field with a strength of 1.4 MA/m

To assess the effect of the magnetic field on the distribution of total residual stresses in hardened and tempered alloys, the experiments were conducted, the results of which are shown in Figure 3. After the usual hardening of annular samples with an outer diameter of 20 mm, tensile stresses were observed on the surface. This was explained by the small temperature difference between the periphery and the center during martensitic transformation. Therefore, their structural component had a predominant effect on the distribution of total residual stresses. Quenching in a magnetic field helped to reduce residual stresses in alloys with both negative (steel 45) and positive (ferritic ductile iron) changes in the volumetric effect of martensitic transformation. This indicated that the main reason for the reduction of residual stresses was their intense relaxation under the action of a magnetic field. An increase in the degree of martensite decay under the influence of a magnetic field [12] caused an increase in this effect.

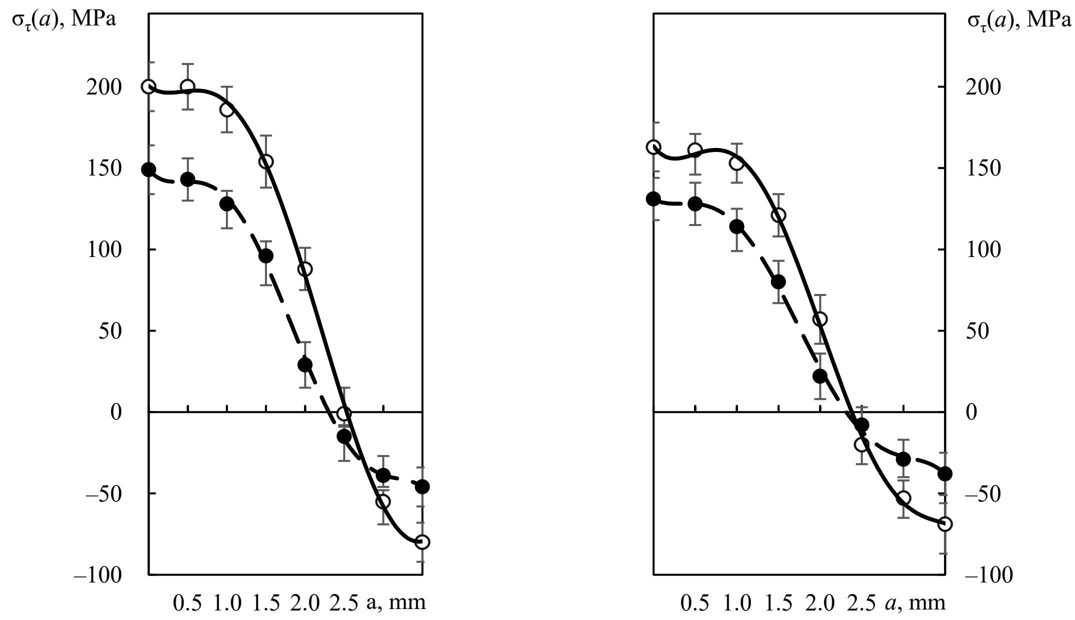

a) *b)*

Fig. 3. Stress distribution over the cross section after quenching from 1000°C in calm water, solid line — without a field; dashed line — in a magnetic field with a strength of 1.4 MA/m; *a* — steel 45; *b* — ferritic ductile iron

Similar patterns were observed during spray cooling with water of annular samples with a diameter of 55 mm (Fig. 4). The difference was in the fact that exposure to a magnetic field caused a decrease in surface compressive stresses due to the prevailing influence of the thermal component of residual stresses on the total stress diagram.

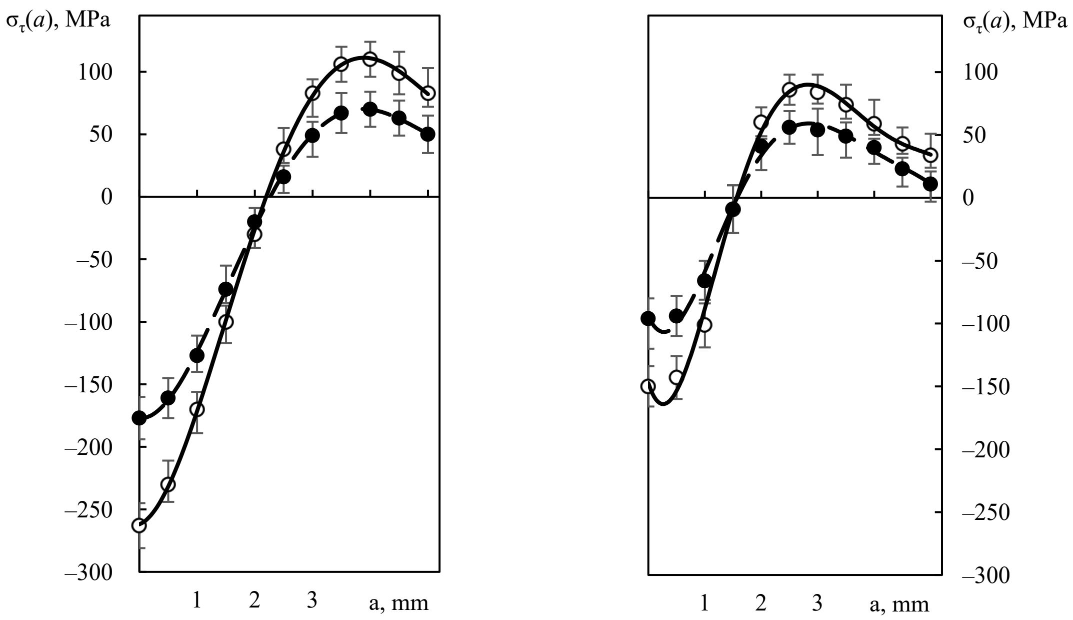

a) *b)*

Fig. 4. Stress distribution after quenching from 1000°C with spray cooling with water υ = 2 m/s: solid line — without a field; dashed line — in a magnetic field with a strength of 768 kA/m; *a* — steel 45; *b* — ferritic ductile iron

An increase in the velocity of water flow through the sprayer to υ = 10 m/s led to an increase in the magnitude of surface compressive stresses during conventional quenching. At such a flow rate, the cooling capacity and the degree of "quenching" stress relaxation under the influence of a magnetic field changed slightly. Therefore, the observed changes were mainly due to a structural factor: an increase in the degree of breakdown of martensite in steel 45 and an increase in the amount of martensite in ductile iron.

Table 1

The effect of cooling in a magnetic field after heating in a furnace on the level of residual stresses

Parameters	Carbon-free alloys		Medium-carbon alloys		High-carbon alloys	
	Cooling medium					
	Water	Oil	Water	Oil	Water	Oil
Stresses on the surface of a solid cylinder after conventional cooling	Compressive	Compressive, but less than when cooled in water	Compressive	Tensile	Compressive	Tensile
Change in stresses on the surface of a solid cylinder after cooling in a magnetic field as a result of: reducing the cooling capacity of quenching liquids	Decrease in compression	–	Decrease in compression	–	Decrease in compression	–
increase in the amount of martensite	–	–	–	–	Increase in compression	Increase in tension
increase in the decay processes of martensite (“in statu nascendi”)	–	–	Decrease in compression	Decrease in tension	Decrease in compression	Decrease in tension

Table 2

The effect of cooling in a magnetic field after induction (surface) heating on the level of residual stresses

Parameters	Carbon-free alloys		Medium-carbon alloys		High-carbon alloys	
	Depth of the hardened layer					
	low	high	low	high	low	high
Stresses on the surface of a solid cylinder after conventional cooling	Tensile	Compressive	Compressive		Compressive	
Change in stresses on the surface of a solid cylinder after cooling in a magnetic field as a result of: reducing the cooling capacity of quenching liquids	Decrease in tension	Decrease in compression	Decrease in compression		Decrease in compression	
increase in the amount of martensite	–	–	–		Increase in compression	
increase in the decay processes of martensite («in statu nascendi»)	–	–	Decrease in compression		Decrease in compression	

Discussion and Conclusion. The calculated and experimental data made it possible to estimate the possible changes in the residual stress diagrams under the influence of a magnetic field after quenching with volumetric (Table 1) and surface heating (Table 2). The change in the distribution of total residual stresses during magnetic release was due to a change in their structural component.

Thus, the magnetic field affects the distribution of structural (during quenching and tempering), thermal (during quenching) and total residual stresses. The reason for the observed effects is the change in the structural state of steel and cast iron and the cooling capacity of water-based quenching liquids under the influence of a magnetic field. An increase in the phenomena of martensite decay causes a decrease, and an increase in the completeness of martensite transformation causes an increase in the level of structural stresses. A decrease in the cooling capacity of water-based quenching liquids leads to a decrease in residual stresses as a result of intensive relaxation by plastic deformation. The enhancement of relaxation processes under the influence of a magnetic field in most cases is the main factor in changing the residual stress diagram. In turn, reducing the level of residual stresses during heat treatment in a magnetic field can reduce the likelihood of brittle fracture and cracking, as well as deformations and warping in hardened steels. This creates favorable conditions for the performance of parts under alternating loads and abrasive friction.

References

1. Samuel A, Prabhu KN. Residual Stress and Distortion during Quench Hardening of Steels: A Review. *Journal of Materials Engineering and Performance.* 2022;31(7):5161–5188. https://doi.org/10.1007/s11665-022-06667-x

2. Villa M, Niessen F, Somers MAJ. In Situ Investigation of the Evolution of Lattice Strain and Stresses in Austenite and Martensite During Quenching and Tempering of Steel. *Metallurgical and Materials Transactions A.* 2018;49:28–40. https://doi.org/10.1007/s11661-017-4387-0

3. Ali Tabatabaeian, Ahmad Reza Ghasemi, Mahmood M. Shokrieh, Bahareh Marzbanrad, Mohammad Baraheni, Mohammad Fotouhi. Residual Stress in Engineering Materials: A Review *Advanced Engineering Materials.* 2022;24(3):2100786. https://doi.org/10.1002/adem.202100786

4. Bhadeshia HKDH, Honeycombe RWK. *Steels: Structure, Properties, and Design.* Elsevier; 2024. 550 p. URL: https://books.google.ru/books?id=U9PKEAAAQBAJ&hl=ru&lr= (accessed: 20.08.2024).

5. Gvozdev AE, Zhuravlev GM, Kuzovleva OV. *Fundamentals of the Formation of State of High Deformation Capability of Metal Systems.* Monograph. Tula: Tula State University; 2018. 382 p. (In Russ.)

6. Bhadeshia HKDH, Honeycombe RWK. *Steels: Microstructure and Properties*. Butterworth-Heinemann; 2017. 488 p. URL: https://books.google.ru/books?id=4Rt5CgAAQBAJ&hl=ru (accessed: 20.08.2024).

7. Kasyanov VE, Demchenko DB, Kosenko EE, Teplyakova SV. Method of Machine Reliability Optimization Using Integral Indicator. *Safety of Technogenic and Natural Systems.* 2020;(1):23–31. (In Russ.) https://doi.org/10.23947/2541-9129-2020-1-23-31

8. Vernezi NL. Variation Coefficient of Metal Yield Strength in New and Long-Used Building Structures. *Safety of Technogenic and Natural Systems.* 2023;(3):44–54. (In Russ.) https://doi.org/10.23947/2541-9129-2023-7-3-44-54

9. Blinovskii VA. *Investigation of Transformations, Structural Features and Residual Stresses during Quenching and Tempering of Iron-Carbon Alloys in a Magnetic Field.* Author's abstract. Rostov-on-Don: Rostov-on-Don Institute of Agricultural Engineering; 1978. 28 p. (In Russ.)

10. Pustovoit VN. Cooling Capacity of Quenching Liquids in Magnetic Field. *Metal Science and Heat Treatment.* 1978;20(2):131–133. https://doi.org/10.1007/BF00670306

11. Youkai Wang, Huinan Wei, Zhuangwen Li. Effect of Magnetic Field on the Physical Properties of Water. *Results in Physics.* 2018;8:262–267. https://doi.org/10.1016/j.rinp.2017.12.022

12. Pustovoit V.N., Dolgachev Yu., Dombrovskii Yu.M. Use of the Superplasticity Phenomenon of Steel for "Internal" Magnetic Correcting a Product. *Solid State Phenomena.* 2017;265:745–749. https://doi.org/10.4028/www.scientific.net/SSP.265.745

About the Authors:

Viktor N. Pustovoit, Dr. Sci. (Eng.), Professor of the Materials Science and Technologies of Metals Department, Don State Technical University, (1, Gagarin Sq., Rostov-on-Don, 344003, Russian Federation), SPIN-code, ORCID, ScopusID, ResearcherID, pustovoyt45@gmail.com

Yuri V. Dolgachev, Cand. Sci. (Eng.), Associate Professor of the Materials Science and Technologies of Metals Department, Don State Technical University, (1, Gagarin Sq., Rostov-on-Don, 344003, Russian Federation), SPIN-code, ORCID, ScopusID, ResearcherID, yuridol@mail.ru

Claimed Contributorship:

VN Pustovoit: formulation of the basic concept, goals and objectives of the research, academic advising, revision of the text, correction of the conclusions.

YuV Dolgachev: obtaining experimental data, calculations, analysis of the research results, preparation of the text, formulation of the conclusions.

***Conflict of Interest Statement:* the authors do not have any conflict of interest.**

All authors have read and approved the final version of manuscript.

Об авторах:

Виктор Николаевич Пустовойт, доктор технических наук, профессор, профессор кафедры материаловедения и технологии металлов Донского государственного технического университета (344003, Российская Федерация, г. Ростов-на-Дону, пл. Гагарина, 1), SPIN-код, ORCID, ScopusID, ResearcherID, pustovoyt45@gmail.com

Юрий Вячиславович Долгачев, кандидат технических наук, доцент кафедры материаловедения и технологии металлов Донского государственного технического университета (344003, Российская Федерация, г. Ростов-на-Дону, пл. Гагарина, 1), SPIN-код, ORCID, ResearcherID, ScopusID, yuridol@mail.ru

Заявленный вклад авторов:

В.Н. Пустовойт: формирование основной концепции, цели и задач исследования, научное руководство, доработка текста, корректировка выводов.

Ю.В. Долгачев: получение экспериментальных данных, расчеты, анализ результатов исследований, подготовка текста, формулирование выводов.

Конфликт интересов. **авторы заявляют об отсутствии конфликта интересов.**

Все авторы прочитали и одобрили окончательный вариант рукописи.

Received / Поступила в редакцию 22.08.2024
Revised / Поступила после рецензирования 17.09.2024
Accepted / Принята к публикации 21.09.2024

CHEMICAL TECHNOLOGIES, MATERIALS SCIENCES, METALLURGY ХИМИЧЕСКИЕ ТЕХНОЛОГИИ, НАУКИ О МАТЕРИАЛАХ, МЕТАЛЛУРГИЯ

Check for updates

UDC 621.785: 669.14.018.29
https://doi.org/10.23947/2541-9129-2024-8-4-62-71

Original Empirical Research

Morphology and Properties of the Laser-Irradiated Composition "Chrome Coating — Copper Substrate"

EDN: APWCZN

Galina I. Brover[1] ✉, **Elena E. Shcherbakova**[1], **Elena B. Borisenko**[2]
[1] Don State Technical University, Rostov-on-Don, Russian Federation
[2] Osipyan Institute of Solid State Physics RAS, Chernogolovka, Russian Federation
✉ brover@mail.ru

Abstract

Introduction. During pulsed laser processing and modification of the surface of non-ferrous alloys and coatings based on them, several still unresolved issues arise. In particular, the extreme thermal deformation conditions of laser processing are not linked to the peculiarities of structure formation and formation of properties in irradiated "coating — copper substrate" compositions. A metal physical analysis of the possibility and reasons for increasing the adhesion strength of coatings to a metal (copper) substrate during high-speed laser processing is insufficiently substantiated and evidence-based. To make a reasonable choice of technological parameters for the surface hardening mode of non-ferrous alloy products, as well as for obtaining high-quality workable composite layers on their surface, it is necessary to solve the above issues and tasks. The aim of this article is to determine the possibility and conditions for increasing the adhesion strength of a chrome coating to a copper substrate under laser irradiation of the composition.

Materials and Methods. Metal physical studies in the work were carried out on samples of non-ferrous alloys of the Cu–Zn system with a chrome electrochemical coating with a thickness of 20 µm. The "copper substrate — chrome coating" composition was irradiated at a Kvant-16 installation with a radiation power density of 70–250 MW/m^2. Metallographic structural analysis, scanning probe microscopy, and durometric studies were used in the work.

Results. It has been calculated that the dynamic and thermal stresses arising in the laser-irradiated compositions "chrome coating — copper substrate" were about 320 MPa. Metal physical studies revealed that, in extreme thermal deformation conditions of laser treatment, the effect of contact melting was manifested at the boundary of the coating with the copper base. Dynamic recrystallization occurred in the surface layers of the irradiated L62 copper alloy, resulting in the formation of grains with a size of 4.5–5.0 µm on the surface of the alloy with an initial grain size of 25 µm.

Discussion and Conclusion. It has been found that the adhesion strength of a chrome coating to a copper alloy substrate increased laser irradiation at a radiation power density of 150 MW/m^2. This was due to the formation of a transition region 2–4 µm deep in the contact zone with a structure consisting of sections of mutually insoluble solid solutions based on chromium and copper. Based on the analysis of the copper —chromium state diagram and the model of the temperature field under laser irradiation of the chromium coating, it was suggested that contact melting occurred in the transition zone from the coating to the copper substrate. It was shown that thermostrictive stresses, the calculated quantitative values of which were about 320 MPa, had an initiating effect on the observed processes of structure formation in the laser irradiation zones. It was found that such a level of stresses arising in copper alloys under laser irradiation was sufficient for plastic deformation and dynamic recrystallization of the metal and contributed to the formation of a fine-grained structure (4.5–5.0 µm) with an initial grain size of 25 µm. An analysis of the results of studies of irradiated compositions "coating — copper substrate" allowed us to conclude that they expanded the technological capabilities of the laser method of hardening materials and ensure guaranteed high performance of irradiated products with coatings.

Keywords: copper alloys, coatings, laser irradiation, structure, properties

Acknowledgements. The authors would like to express their gratitude to the reviewers for their critical assessment of the submitted materials and their suggestions that improved the quality of the article.

For citation. Brover GI, Shcherbakova EE, Borisenko EB. Morphology and Properties of the Laser-Irradiated Composition "Chrome Coating — Copper Substrate". *Safety of Technogenic and Natural Systems.* 2024;8(4):62–71. https://doi.org/10.23947/2541-9129-2024-8-4-62-71

Оригинальное эмпирическое исследование

Морфология и свойства лазернооблученной композиции «хромовое покрытие — медная подложка»

Г.И. Бровер[1], **Е.Е. Щербакова**[1], **Е.Б. Борисенко**[2]

[1] Донской государственный технический университет, г. Ростов-на-Дону, Российская Федерация

[2] Институт физики твердого тела имени Ю.А. Осипьяна Российской академии наук, г. Черноголовка, Российская Федерация

✉ brover@mail.ru

Аннотация

Введение. При проведении импульсной лазерной обработки и модифицирования поверхности цветных сплавов и покрытий на их основе возникает ряд до сих пор не решенных проблем. В частности, не увязаны экстремальные термодеформационные условия лазерной обработки с особенностями структурообразования и формирования свойств в облученных композициях «покрытие — медная подложка». Недостаточно аргументированно обоснован и доказательно проведен металлофизический анализ возможности и причин повышения прочности сцепления покрытий с металлической (медной) подложкой при высокоскоростной лазерной обработке. Для обоснованного выбора технологических параметров режима поверхностного упрочнения изделий из цветных сплавов, а также для получения на их поверхности качественных работоспособных композиционных слоев требуется решение приведенных выше вопросов и задач. Целью данной статьи явилось определение возможности и условий повышения прочности сцепления хромового покрытия с медной подложкой при лазерном облучении композиции.

Материалы и методы. Металлофизические исследования в работе проводились на образцах цветных сплавов системы Cu–Zn с хромовым электрохимическим покрытием толщиной 20 мкм. Композиция «медная подложка — хромовое покрытие» облучалась на установке «Квант-16» с плотностью мощности излучения 70–250 МВт/м^2. В работе использовались металлографический структурный анализ, сканирующая зондовая микроскопия, дюрометрические исследования.

Результаты исследования. Расчетным путем установлено, что возникающие в лазернооблученных композициях «хромовое покрытие — медная подложка» динамические и термические напряжения составляют около 320 МПа. Металлофизическими исследованиями обнаружено, что в экстремальных термодеформационных условиях лазерной обработки на границе покрытия с медной основой проявляется эффект контактного плавления. В поверхностных облученных слоях медного сплава Л62 обнаружен эффект динамической рекристаллизации. Это выражается в формировании на поверхности сплава с исходным размером зерна 25 мкм мелких зерен размером 4,5–5,0 мкм.

Обсуждение и заключение. Установлено, что прочность сцепления хромового покрытия с подложкой из медных сплавов повышает лазерное облучение с плотностью мощности излучения 150 МВт/м^2. Это происходит за счет формирования в зоне контакта переходной области глубиной 2–4 мкм со структурой, состоящей из участков взаимно нерастворимых твердых растворов на основе хрома и меди. На основании анализа диаграммы состояния «медь — хром» и модели температурного поля при лазерном облучении хромового покрытия высказано предположение о протекании в переходной зоне от покрытия к медной подложке контактного плавления. Показано, что инициирующее влияние на наблюдаемые процессы структурообразования в зонах лазерного облучения оказывают термострикционные напряжения, расчетные количественные значения которых составили около 320 МПа. Установлено, что такой уровень возникающих в медных сплавах при лазерном облучении напряжений достаточен для пластической деформации и динамической рекристаллизации металла и способствует формированию мелкозернистой структуры (4,5–5,0 мкм) при исходном размере зерен 25 мкм. Анализ результатов исследований облученных композиций «покрытие — медная подложка» позволил сделать вывод, что они расширяют технологические возможности лазерного метода упрочнения материалов и позволяют гарантированно обеспечивать высокую работоспособность облученных изделий с покрытиями.

Ключевые слова: медные сплавы, покрытия, лазерное облучение, структура, свойства

Благодарности. Авторы выражают благодарность рецензентам, чья критическая оценка представленных материалов и высказанные предложения по их усовершенствованию способствовали значительному повышению качества настоящей статьи.

Для цитирования. Бровер Г.И., Щербакова Е.Е., Борисенко Е.Б. Морфология и свойства лазернооблученной композиции «хромовое покрытие — медная подложка». *Безопасность техногенных и природных систем*. 2024;8(4):62–71. https://doi.org/10.23947/2541-9129-2024-8-4-62-71

Introduction. In the work of G.V. Lomaev and E.V. Kharanzhevskii, "Hardening Surface Treatment Using High-Speed Laser Overcrystallization" [1], and in some other studies [2, 3], it has been shown that during laser irradiation, high temperature gradients, thermostrictive stresses of various origins appear in the surface layers of the hardened material, the relaxation of which leads to local plastic deformation, as well as the phenomena of dynamic return, polygonization, and recrystallization of metal in irradiated zones. The possibility to achieve a sufficiently high defect density in a crystalline structure and the desired level of mechanical properties in the surface layers is of practical significance [4].

It should be noted that during pulsed laser treatment [5], hardening [6] and modification [7] of the surface of non-ferrous alloys, in particular, copper alloys, several problems arise [8]. For example, the extreme thermal deformation conditions of pulsed laser treatment are not linked to the peculiarities of structure formation and formation of properties in irradiated "coating — copper substrate" compositions [8]. The reasons for increasing the adhesion strength of coatings to a metal (copper) substrate during high-speed laser processing have not been sufficiently substantiated [9].

The solution of the above-mentioned problems is of significant importance, as it allows for the reasonable assignment of technological modes of surface hardening and microalloying for copper alloy products. This, in turn, contributes to the creation of high-quality, workable composite surface layers on copper parts, thus creating conditions for trouble-free operation of irradiated components in mechanisms located in difficult-to-repair areas. In this regard, the aim of this article is to obtain, analyze, and quantify the results of metal physical studies, as well as to assess the degree of influence of pulsed laser treatment on the formation of structure and properties of the irradiated "chrome coating — copper substrate" composition.

Materials and Methods. Metal physical studies were conducted on samples of non-ferrous alloys of the Cu–Zn system with a chrome electrochemical coating with a thickness of 20 µm. The "copper substrate — chrome coating" composition was irradiated at a Kvant-16 installation with a radiation power density of 70–250 MW/m^2.

Metallographic structural analysis, scanning probe microscopy, and durometric studies were performed. MIM-7 and Neophot-21 microscopes were used for the metallographic analysis. Microhardness measurements were conducted on the PMT-3 device with an indenter load of 0.49 N.

The adhesive properties of the coatings were determined based on indirect experiments to measure the microhardness of the coatings under different indentation loads. Traces of destruction or peeling of the coatings from the surface of the copper substrate, as observed on the cross-section of the coating–substrate composition, were considered a criterion for insufficient adhesion strength.

Research Results. As a result of metallographic and durometric studies, we found that laser treatment improved the adhesion strength between the chrome coating and the copper substrate (Fig. 1). This conclusion was based on the fact that there was no chipping of the coating when the microhardness tester indenter was pressed into it, that is, when a load was applied.

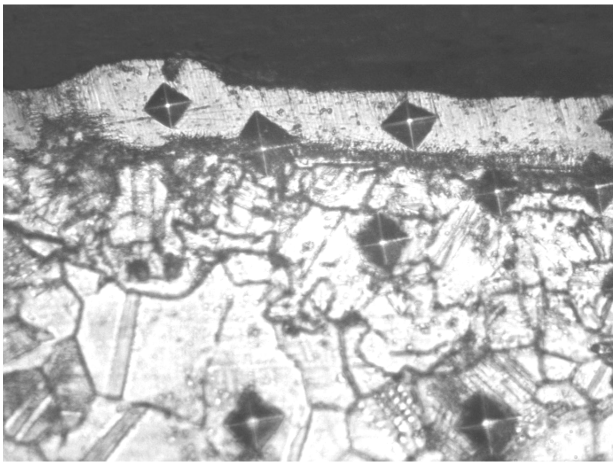

Fig. 1. Structure of the chrome coating on the copper alloy (brass L62)
with impressions from the microhardness tester indenter

At the same time, as can be seen in Figure 2, in the transition zone at the boundary between the chrome coating and the copper substrate, that is, at a depth of 20 µm, after laser treatment, there were clearly visible local areas of solid solutions, apparently based on chromium and copper, penetrating each other at a distance of 2–4 µm.

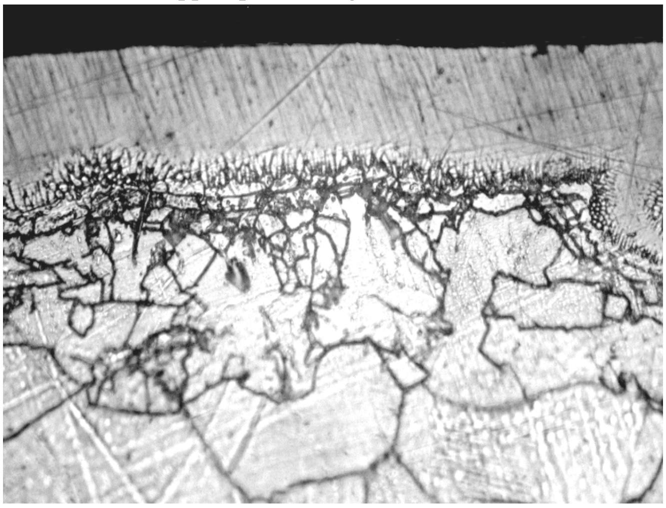

Fig. 2. Microstructure of the contact zone of the chrome coating with brass after laser irradiation

To study the features of the structure formation at the boundary of the coating and the substrate, an analysis of the state diagram of the Cr–Cu system was conducted [10]. It was noted that at a temperature of 1767°C, monotectic equilibrium was observed; the liquid phase was stratified to form two liquids of different chemical composition. It could be assumed that the observed in Figure 2 structure of the contact zone of the coating and the substrate was also formed from a state melted by laser exposure, that is, an immiscibility region of copper and chromium in the liquid state was formed in the transition zone, in which two solid solutions based on Cu and Cr were fixed after high-speed crystallization. But the quantitative analysis of the temperature field carried out using the Mathcad software package during laser irradiation of the chrome coating [11] excluded the possibility of reaching melting temperatures at the depth of the coating, that is, at a depth of 20 µm (Fig. 3).

The “chrome coating — copper substrate” composition was exposed to radiation with a power density of 150 MW/m^2. These energy conditions did not lead to evaporation of the coating and to the formation of “craters” on the surface. Thermal calculations, which are shown in Figure 3, allowed us to determine that a temperature of 900–1000°C was achieved in the transition zone. However, this temperature was not high enough for melting, and no formation of two solid solutions based on the components of the “chrome coating – copper substrate” composition was observed during the study. The possible cause of the described effect requires a separate discussion.

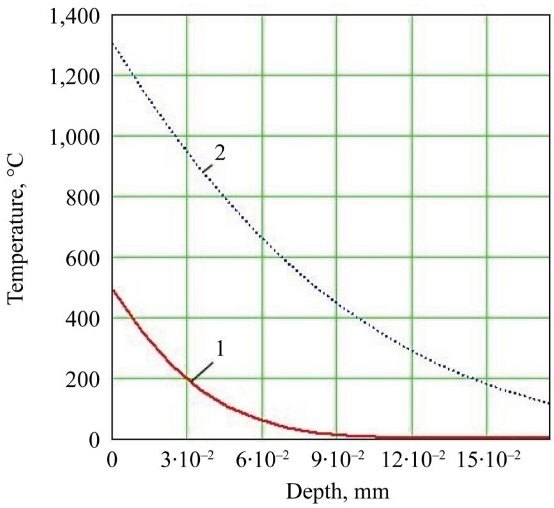

Fig. 3. Temperature distribution over the depth of the chrome coating at the heating stage
(1 — the beginning of the laser pulse; 2 — he end of the pulse)

Layers of copper alloy at a depth of 5–10 µm were subjected to melting and subsequent high-speed crystallization. A feature of the structure of the fused surface layer of brass, as shown by the results of studies on a scanning probe microscope (SPM), was a homogeneous dispersed structure consisting of solid solution dendrites with a cross section of up to 25 nm (Fig. 4) and with a sufficiently high hardness of about 1 GPa.

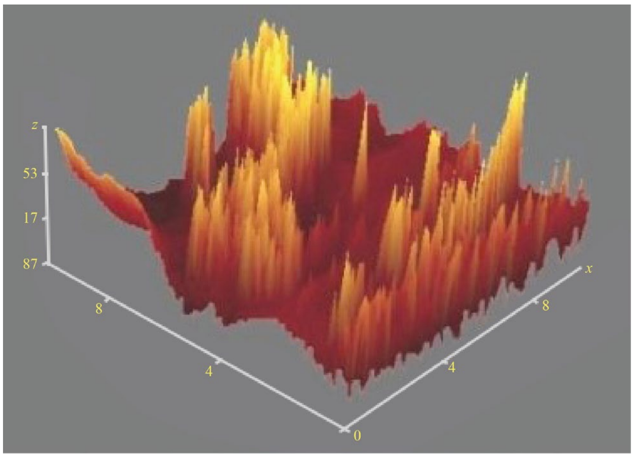

Fig. 4. Scanned image of the surface of the L62 copper alloy (SPM)

Under the influence of heating alone, the recorded structural transformations could not occur during the laser pulse action (10^{-3} s). However, thermostrictive stresses appeared to have made a significant contribution to the acceleration of structure formation processes.

In order to determine the level of stresses and local plastic deformations in the irradiated zones of alloys, quantitative estimates were made using “model” single-component copper samples. As shown above, the melting point was not reached in the contact zone of the coating and the substrate, therefore, the irradiation of uncoated copper samples was carried out in a mode that did not lead to melting of the surface (with a radiation power density of 100 MW/m^2). After laser irradiation, as can be seen in Figure 5 *a*, sliding lines appear on the pre-polished surfaces of copper samples, that is, traces of local plastic deformation of the metal.

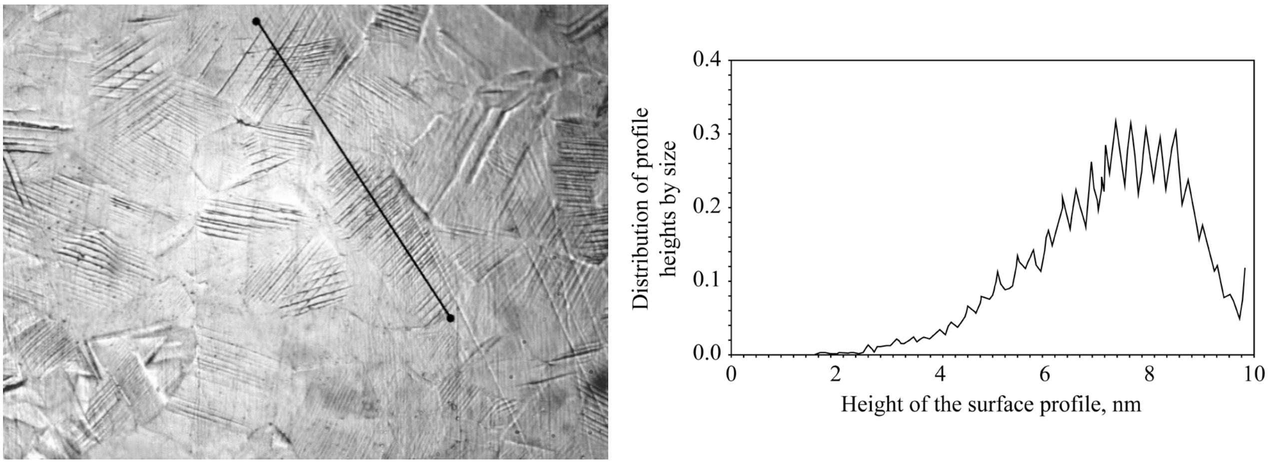

a) *b)*

Fig. 5. Microstructure and height distribution of the emerging surface relief on copper after laser irradiation:
a — sliding lines; *b* — height distribution of the surface relief

It should be noted that the sliding lines are formed due to the movement of dislocations in the areas of the metal that have been irradiated [12]. Due to the appearance of different numbers of dislocations on the irradiated surface, a relief with varying heights of the surface profile was created [13] (shear steps h in Fig. 6).

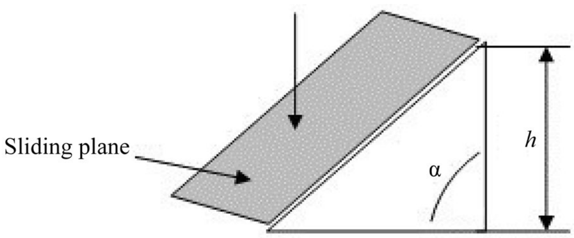

Fig. 6. Diagram of the shear step on sliding lines [14]

The analysis of the pattern of the sliding lines and the relief of the irradiated surface was carried out using the computer image processing program Gwiddion. As can be seen in Figure 5 *b*, the average height of the profile of the irradiated surface of the copper sample, and therefore the height of shear site *h*, was 6.5–8.5 nm. Based on the results of measurements of this height, it was possible to judge the degree of plastic deformation achieved during metal processing and the level of stresses causing it.

Considering that during plastic deformation, the height of step *h* was proportional to value *nb*, where *n* — number of dislocations that have come to the surface, and *b* — Burgers vector of the irradiated material, we can write:

$$nb = h. \tag{1}$$

To simplify the calculation of shear stresses, it was assumed that the elastic deformation preceding slid in the crystal could be defined as *t*/*G*, where t — applied stress; *G* — shear modulus of the material. It was also taken into account that elastic deformation during sliding could relax in an area with a diameter of 2*L*, where *L* — length of the dislocation slip lines.

Assuming the complete transition of elastic deformation ($2L\tau/G$) to plastic deformation equal to the value *nb*, we obtain [14]:

$$\tau = h\left(\frac{G}{2L}\right).$$

By calculation, we determine shear stress (τ), causing plastic deformation using expressions (1), (2) and, taking $L = 10^{-3}$ mm, from expression [15]:

where *h* — height of the shear site, during laser processing was 6.5–8.5 nm; *G* — shear modulus, for copper $G = 4.3 \times 10^4$ MPa; *L* — length of the dislocation slip lines, we assume $L = 10^{-3}$ mm.

Shear stresses amounted to approximately 320 MPa, which exceeded the conditional yield strength of copper (40–80 MPa) and led to plastic deformation of the surface layers of the irradiated metal.

The work also assessed the degree of local residual plastic deformation, which ranged from 5 to 9% in the case of laser treatment of copper.

Possible structural processes in the laser irradiation zones of the "coating – metal substrate" composition, in particular, in a copper substrate, were studied in detail using the Mathcad program. A temperature field was constructed that spread along the depth after irradiation of the surface of the brass sample (Fig. 7).

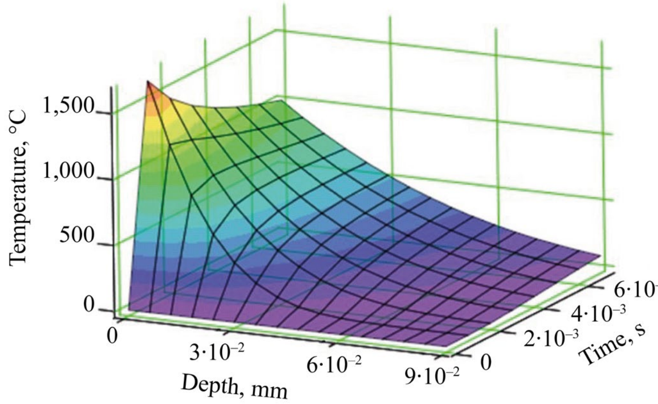

Fig. 7. Temperature field in a copper alloy during laser irradiation of the surface

As can be seen in Figure 7, at a depth of 15 μm, the temperature dropped to 800°C. At this temperature, in the thermal deformation conditions of pulsed processing, despite the extremely short time of thermal exposure to laser radiation, there was a possibility of dynamic stress relaxation effects accompanying the process of high-speed laser irradiation, that is, processes of polygonization and recrystallization in irradiated zones on copper alloys are possible. The consequences of recrystallization of irradiated brass L62 are shown in Figure 8 *a* in the form of grinding of grains of solid solution.

A similar recrystallization process was observed in a brass substrate under a chrome coating after laser irradiation. It was found that in the presence of a coating, the metal grain was larger than on an uncoated copper sample. Apparently, recrystallization in this case reached the stage of collective recrystallization. It can be concluded that there was a lower level of residual stresses and a decrease in the risk of cracking in the composition during laser irradiation.

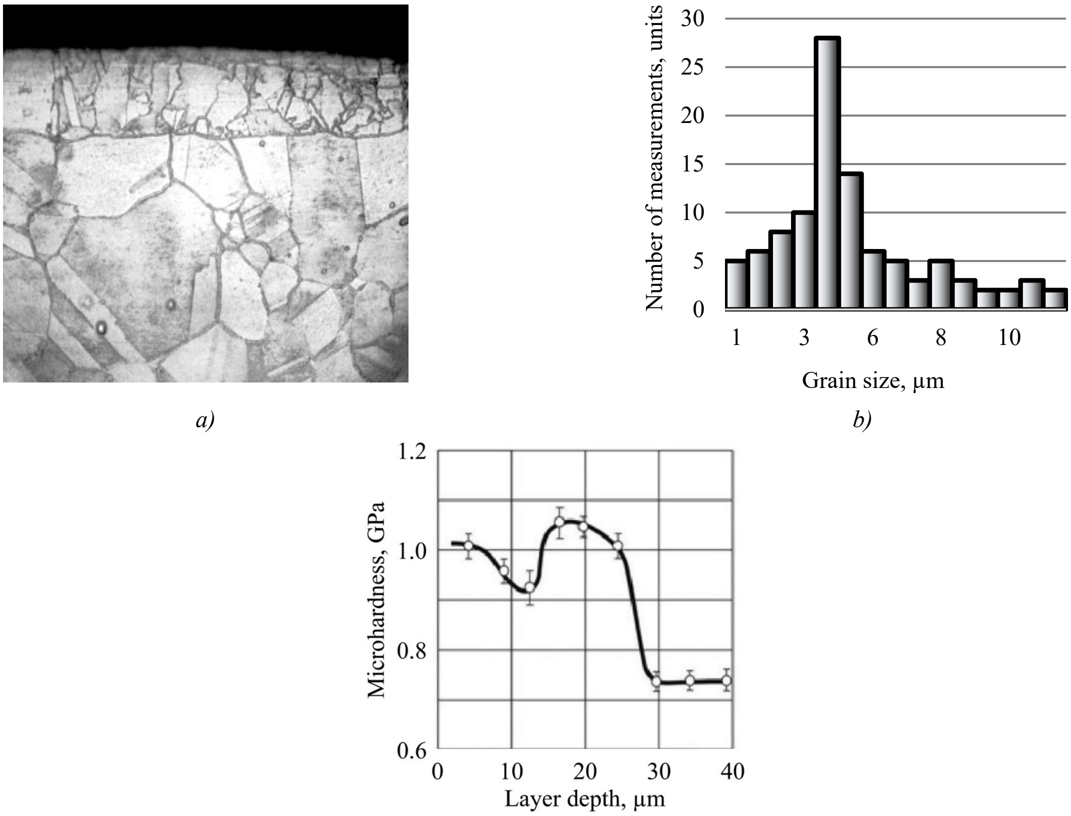

c)

Fig. 8. Microstructure, histogram of size distribution of the subgrains and hardness distribution over the depth of the irradiated zone on the L62 copper alloy: *a* — microstructure; *b* — size distribution of the subgrains; *c* — hardness distribution over the depth of the alloy L62

The average size of the recrystallized grains, as shown in Figure 8 *b*, was 4–5 µm with an initial grain size of 25 µm. At the same time, the highest hardness was achieved in the considered area of the irradiated spot on brass (Fig. 8 *c*).

Discussion and Conclusion. The increase in the adhesion properties of the "chrome coating — copper substrate" composition after laser treatment can be indirectly assessed through the results of durometric tests. It is notable that when the microhardness tester indenter was introduced into the coating, its peeling from the copper matrix was not observed, whereas immediately after application the coating had insufficiently high adhesion strength to the metal (copper) substrate.

The adhesion effects in the irradiated composition are positively influenced by grain grinding, i.e. recrystallization, in a copper substrate, as well as local structural ensembles formed in the transition zone at the boundary of the coating and the substrate from sections of solid solutions based on chromium and copper.

The observed processes of structure formation under the action of an "instantaneous" heat source are possible only under conditions of joint action of high temperatures and stresses on the irradiated composition.

To evaluate the parameters of these thermal power factors and determine the degree of their influence on the formation of structure and properties of irradiated materials, first of all, an analysis of the state diagram of the Cr–Cu system has been conducted. It showed that the observed structural transformations can occur if the contact zone between the chrome coating and copper substrate melts, that is, if the temperature is heated to 1767°C. At this temperature, according to the diagram, the formation of two liquids is observed, that is, in the transition zone between the coating and the substrate, an immiscibility region of copper and chromium in the liquid state should be formed, and after high-speed crystallization, two solid solutions based on Cu and Cr should result. The quantitative analysis of the temperature field, conducted using the Mathcad software package, during laser irradiation of the chrome coating, excluded the possibility of reaching melting temperatures at a depth of 20–30 µm, which is the depth of the contact zone studied in the composition. On the other hand, an analysis of structural processes in the laser irradiation zone of a copper brass sample has showed that melting and subsequent rapid crystallization of copper occur at a depth of 5–10 µm. Scanning probe microscope studies have confirmed that the surface fused layer of the copper sample has a dispersed structure and a sufficiently high hardness of approximately 1 GPa.

The most significant aspect is that the structure of the thin fused layer on the copper alloy is similar to the structure of sections of a copper-based solid solution in the contact area between the copper substrate and the chrome coating. This indirectly confirms that in the transition zone from the coating to the copper substrate, despite heating to temperatures below the melting point, a liquid phase was still present. It can be assumed that contact melting occurs at the studied boundary under extreme thermal deformation conditions of laser treatment, leading to the described structure formation and, as a result, to an increase in the adhesive properties of the "chrome coating — copper substrate" composition.

It should be noted that the results obtained are primarily related to the extreme temperature and force conditions of laser irradiation. Significant temperature gradients combined with high laser processing speeds lead to the formation of high levels of thermostrictive stresses and local plastic deformations in the irradiated areas of alloys. To confirm their existence and perform a quantitative assessment of the values they achieve, as well as for the purity of the experiment, research was conducted not only on copper alloys, but also on single-component copper samples [11]. After laser irradiation, sliding lines appeared on the pre-polished surfaces of the copper samples, indicating traces of local plastic deformation of the metal. The analysis of patterns of sliding lines and relief of the irradiated surface made it possible to determine that the average height of the surface profile of the irradiated copper sample, and, consequently, the height of the shear site was 6.5–8.5 nm.

Based on the measurements of this height and the calculations made, it was found that the shear stresses were approximately 320 MPa. These values were higher than the conditional yield strength of copper (40–80 MPa), which led to plastic deformation of the surface layers of the irradiated metal, which ranged from 5 to 9% [3].

It should be noted that the actual values of stresses and plastic deformation that arise during the action of a powerful thermal shock of a laser pulse on local metal sites will undoubtedly have much higher values.

Thermal deformation effects appearing in the areas of laser irradiation of alloys, despite the extremely short laser pulse time (10^{-3} s), lead to stress relaxation not only to local plastic deformation, but also to dynamic polygonization and recrystallization of the structure in the surface layers of metals.

As shown by the results of quantitative assessment of temperatures in the irradiated copper substrate, at a layer depth of 15 µm, the temperature drops to 800°C, that is, the zone of laser treatment of a copper sample in a solid state begins. It can be concluded that at this temperature, under the thermal deformation conditions of laser irradiation, despite the extremely short time of thermal exposure, it becomes possible to manifest dynamic polygonization and recrystallization in irradiated areas on copper. As a result, the copper grain is crushed from the initial size of 25 µm to 4–5 µm in the recrystallized metal. The evidence of dispersion of the structure of the surface irradiated layers of the alloy is the results of durometric analysis, which indicate that the highest hardness is achieved in the recrystallized zone.

The described recrystallization process leads to an increase in the crack resistance of the irradiated "chrome coating – copper substrate" compositions. This is due to the removal of stresses that appear in the coating during its application and high-speed laser processing, which reduces the likelihood of brittle destruction of the composition.

Thus, it was found that laser treatment with a radiation power density of 150 MW/m2 contributes to an increase in the adhesion strength of the chrome coating to a metal (copper) substrate due to the formation of a transition layer of specific morphology at the boundary of the coating and the base material, as well as due to recrystallization processes in the surface layers of the copper alloy.

An analysis of the results of studies of irradiated "coating – copper substrate" compositions has allowed us to conclude that they expand the technological capabilities of laser method of hardening materials and ensure guaranteed high performance of products with irradiated coatings.

References

1. Lomaev GV, Kharanzhevskii EV. Hardening Surface Treatment Using High-Speed Laser Overcrystallization. *Metallovedenie i termicheskaya obrabotka metallov*. 2002;3:27–32. (In Russ.)

2. Kumar H, Bhaduri GA, Manikandan SGK, Kamaraj M, Shiva S. Effect of Laser Surface Processing on the Microstructure Evolution and Multiscale Properties of Atmospheric Plasma Sprayed High-Entropy Alloys Coating. *Journal of Thermal Spray Technology*. 2023;32:831–850. https://doi.org/10.1007/s11666-022-01491-0

3. Brover GI, Shcherbakova EE. Morphology and Properties of Chemical Coatings on Steels after Extreme Thermal Laser Radiation Effects. *Metallurgist*. 2023;66:1105–1113. https://doi.org/10.1007/s11015-023-01423-5

4. Brover AV. Adaptation of Structures of Steel Laser Hardening Zones to Friction Conditions. *Vestnik of Don State Technical University*. 2020;20(1):87-92. https://doi.org/10.23947/1992-5980-2020-20-1-87-92

5. Decheng Kong, Chaofang Dong, Xiaoqing Ni, Liang Zhang, Cheng Man, Guoliang Zhu, et al. Effect of TiC Content on the Mechanical and Corrosion Properties of Inconel 718 Alloy Fabricated by a High-Throughput Dual-Feed

Laser Metal Deposition System. *Journal of Alloys and Compounds*. 2019;803:637-648. https://doi.org/10.1016/j.jallcom.2019.06.317

6. Soumya Sobhan Dash, Daolun Chen. A Review on Processing–Microstructure–Property Relationships of Al-Si Alloys: Recent Advances in Deformation Behavior. *Metals*. 2023;13(3):609. https://doi.org/10.3390/met13030609

7. Xu Yang, Yang Qi, Wenqi Zhang, Yilong Wang, Haihong Zhu. Laser Powder Bed Fusion of C18150 Copper Alloy with Excellent Comprehensive Properties. *Materials Science and Engineering: A*. 2023;862:144512. https://doi.org/10.1016/j.msea.2022.144512

8. Xiangpeng Tang, Xiaohong Chen, Fujia Sun, Lei Li, Ping Liu, Honglei Zhou, et al. A Study on the Mechanical and Electrical Properties of High-Strength CuCrZr Alloy Fabricated Using Laser Powder Bed Fusion. *Journal of Alloys and Compounds*, 2022;924:166627. https://doi.org/10.1016/j.jallcom.2022.166627

9. Platl J, Rainer DBSc, Leitner H, Turk C, Galbusera FMSc, Ali Gökhan Demir, et al. Potential Causes for Cracking of a Laser Powder Bed Fused Carbon-free FeCoMo Alloy. *BHM Berg- und Hüttenmännische Monatshefte*. 2022;167:325–331. https://doi.org/10.1007/s00501-022-01238-y

10. Lyakishev NP. *Diagrams of the State of Double Metal Systems.* Moscow: Mashinostroenie; 1996–2000. 350 p. (In Russ.)

11. Sambit Sahoo, Rajat Mishra, Nishkarsh Srivastava, Amit Arora. FEM Simulation of Pulsed Laser Welding of High-Carbon Alloy Steel: Using Different Heat Source Models. *Transactions of the Indian Institute of Metals.* 2023;66:1005–1013. https://doi.org/10.1007/s12666-023-03008-x

12. Matyunin VM, Kudryakov OV, Varavka VN, Marchenkov AYu. Micromechanics of Small Deformations in Metal Alloys under Laser Irradiation. *Industrial Laboratory. Diagnostics of Materials*. 2022;88(10):66-72. https://doi.org/10.26896/1028-6861-2022-88-10-66-72 (In Russ.)

13. Pustovoit VN, Dombrovskii YuM, Dolgachev YuV. Structural Identification of the Phenomenon of "White Zone". *Metal Science and Heat Treatment*. 2017;59:3–7. https://doi.org/10.1007/s11041-017-0092-2

14. Frolov VA, Yakivyuk OV, Frolov VF, Voroshilov DS. The Study of the Structure of Cast and Deformed Semifinished Products from Aluminum Alloys Doped with Scandium Economically. In: *Materials of the XVIII International Scientific and Technical Ural School-Seminar of Metal Scientists — Young Researches*. Yekaterinburg: UrFU; 2017. P. 627–631. (In Russ.)

15. Smitlz KDzh. *Metals: Reference Book.* Moscow: Metallurgiya; 1980. 448 p. (In Russ.)

About the Authors:

Galina I. Brover, Dr. Sci. (Eng.), Professor of the Materials Science and Technology of Metals Department, Don State Technical University (1, Gagarin Sq., Rostov-on-Don, 344003, Russian Federation), SPIN-code, ORCID, ScopusID, brover@mail.ru

Elena E. Shcherbakova, Cand. Sci. (Eng.), Associate Professor of the Materials Science and Technology of Metals Department, Don State Technical University (1, Gagarin Sq., Rostov-on-Don, 344003, Russian Federation), SPIN-code, ORCID, ResearcherID, ScopusID, sherbakovaee@mail.ru

Elena B. Borisenko, Leading Researcher at the Laboratory of Physical and Chemical Bases of Crystallization, Osipyan Institute of Solid State Physics RAS (2, Academician Osipyan Str., Chernogolovka, Moscow region, 142432, Russian Federation), SPIN-code, borisenko@issp.ac.ru, tnura@mail.ru

Claimed Contributorship:

GI Brover: problem statement, choice of research methods and techniques, planning of experiments, participation in conducting metal physical research and in discussing their results.

EE Shcherbakova: critical review of literature sources on the research topic, participation in conducting metal physical experiments and in discussing their results.

EB Borisenko: participation in conducting metal physical experiments and in discussing their results.

Conflict of Interest Statement: **the authors declare no conflict of interest.**

All authors have read and approved the final manuscript.

Об авторах:

Галина Ивановна Бровер, доктор технических наук, профессор кафедры материаловедения и технологии металлов Донского государственного технического университета (344003, Российская Федерация, г. Ростов-на-Дону, пл. Гагарина, 1), SPIN-код, ORCID, ScopusID, brover@mail.ru

Елена Евгеньевна Щербакова, кандидат технических наук, доцент кафедры материаловедения и технологии металлов Донского государственного технического университета (344003, Российская Федерация, г. Ростов-на-Дону, пл. Гагарина, 1), SPIN-код, ORCID, ResearcherID, ScopusID, sherbakovaee@mail.ru

Елена Борисовна Борисенко, ведущий научный сотрудник лаборатории физико-химических основ кристаллизации Института физики твердого тела имени Ю.А. Осипьяна РАН (142432, Российская Федерация, Московская обл., г. Черноголовка, ул. Академика Осипьяна, 2), SPIN-код, borisenko@issp.ac.ru, tnura@mail.ru

Заявленный вклад авторов:

Г.И. Бровер: постановка задачи, выбор методов и методик исследований, планирование экспериментов, участие в проведении металлофизических исследований и в обсуждении их результатов.

Е.Е. Щербакова: критический обзор литературных источников по теме исследования, участие в проведении металлофизических экспериментов и в обсуждении их результатов.

Е.Б. Борисенко: участие в проведении металлофизических экспериментов и в обсуждении их результатов.

Конфликт интересов: **авторы заявляют об отсутствии конфликта интересов.**

Все авторы прочитали и одобрили окончательный вариант рукописи.

Received / Поступила в редакцию 17.10.2024
Revised / Поступила после рецензирования 11.11.2024
Accepted / Принята к публикации 15.11.2024